

IN THE UNITED STATES PATENT AND TRADEMARK OFFICE

In re Application of: Abbott, *et al.*  
Serial No.: 10/044,899  
Filed: 01/09/2002

Group No.: 1639  
Examiner: Lundgren

**DECLARATION OF DR. NICHOLAS ABBOTT**

EFS WEB-FILED

Assistant Commissioner for Patents  
Washington, D.C. 20231

I, Dr. Nicholas Abbott, state as follows:

1. Currently I am John T. and Magdalen L. Sobota Professor and Chair of the Department of Chemical and Biological Engineering of the University of Wisconsin, Madison. I am an inventor of this application.
2. Paragraph 141 of the application discloses that "In a fourth aspect, the present invention provides a method for detecting an analyte, comprising: (a) contacting with said analyte a recognition moiety for said analyte, wherein said contacting causes at least a portion of a plurality of mesogens proximate to said recognition moiety to detectably switch from a first orientation to a second orientation upon contacting said analyte with said recognition moiety; and (b) detecting said second configuration of said at least a portion of said plurality of mesogens, whereby said analyte is detected.
3. This paragraph accurately describes the invention which is the use of a change in orientation mesogens making up a liquid crystal to detect the interaction of an analyte with a recognition moiety.
4. The Examiner states that "Applicants invention is not adequately described for the full breadth, and is limited to mesogenic liquid crystals encapsulated between two substrates prepared on anisotropic gold hosting an organotypic self-assembled monolayer, and detection using polarized light or optical spectroscopy and transmission." This statement by the Examiner is not scientifically supportable and is inconsistent with the disclosure in the specification and the

scientific literature available at the time the application was filed.

5. The passage cited by the Examiner at page 3 of the Office Action starts with a sentence stating that: "Substrates that are useful in practicing the present invention can be made from practically any physiochemically stable material." It is true, as stated by the Examiner, that the Examples use substrates that comprise anisotropic gold. However, when the scientific literature available at the time the invention was filed is considered, it is apparent that as stated in the specification, any physiologically stable material could be used as a substrate, and that anisotropic gold hosting an organic self assembled monolayer is but one example of a substrate.

6. The following scientific papers demonstrate that a wide variety of such physiochemically stable substrates that orient liquid crystals were known. Some examples include:

Anisotropic fluids. Novel colloidal interactions in anisotropic fluids, Poulin, P; Stark, H; Lubensky, TC, et al. SCIENCE Volume: 275 Issue: 5307 Pages: 1770-1773  
Published: MAR 21 1997 (attached as Tab 1).

Langmuir-Blodgett films of amphiphiles. Investigations on Langmuir-Blodgett films as alignment layers for liquid crystals Chen, J; Vithana, H; Johnson, D, et al.  
MOLECULAR CRYSTALS AND LIQUID CRYSTALS SCIENCE AND  
TECHNOLOGY SECTION A-MOLECULAR CRYSTALS AND LIQUID CRYSTALS  
Volume: 275 Pages: 49-61 Published: 1996 (attached as Tab 2).

Silane-covered glass. OPTICAL 2ND-HARMONIC-GENERATION STUDY OF THE  
INTERACTION OF SILANE-COVERED SURFACES WITH LIQUID-CRYSTAL  
LAYERS. BARMANTLO, M; HOEKSTRA, FR; WILLARD, NP, et al. PHYSICAL  
REVIEW A Volume: 43 Issue: 10 Pages: 5740-5743 Published: MAY 15 1991  
(attached as Tab 3).

Polymeric films. Liquid-crystal alignment of rubbed polyimide films: A microscopic  
investigation Wu, HM; Tang, JH; Luo, Q, et al. APPLIED PHYSICS B-LASERS AND  
OPTICS Volume: 62 Issue: 6 Pages: 613-618 Published: 1996 (attached as Tab 4).

Silanized glass; polymers (PVA, polyimides, polystyrene); inorganic oxides.

ALIGNMENT OF NEMATIC LIQUID-CRYSTALS AND THEIR MIXTURES.

COGNARD, J. MOLECULAR CRYSTALS AND LIQUID CRYSTALS Pages: 1-77

Supplement: 1 Published: 1982 (attached as Tab 5).

7. I further declare that all statement made herein of my own knowledge are true and that all statements made on information and belief are believed to be true; and further that these statements were made with the knowledge that willful false statements and the like so made are punishable by fine or imprisonment, or both, under section 1001 of title 18 of the United States Code, and that such willful false statements may jeopardize the validity of the application or any patent issued thereon.



Dr. Nicholas Abbott

Date: October 21, 2009

# Tab 1

T  
I. 31  
75  
307

AN  
TION FOR THE  
EMENT OF  
SCIENCE

# SCIENCE

21 MARCH 1997

VOL. 275 • PAGES 1705-1844

\$7.00

LW PHARMACY LIBRARY

#026147232# AS 12/12/97 N 5307 71  
PHARMACY LIBRARY  
LW SCHL CHARTER ST  
425 N CHARTER ST  
MADISON WI 53706-1508

89052614971

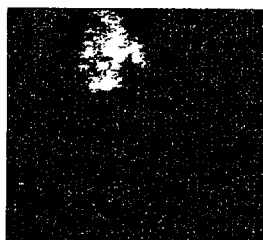
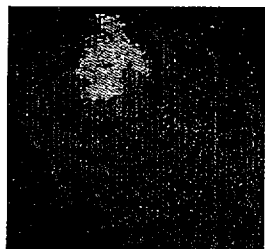


b89052614971a



**1728**

Calling the shots for French science



**1776**

Climate smoke signal

## NEWS & COMMENT

- Who Rules French Science? 1728  
France's Industry-Academe Jobs Agency 1729

- Researchers Vie for Role in Nuclear-Waste Cleanup 1730

- A New Voice for European Scientists? 1731

- Feathered Dino Wins a Few Friends 1731

- U.S. Antarctic Panel Makes Case for Replacement Station 1732

- Mammalian Cloning Debate Heats Up 1733

- ATCC Plant-Virus Collection Threatened 1733

- Staying Off Beaten Track Puts LED Researcher a Step Ahead 1734

## RESEARCH NEWS

- To Catch a WIMP 1736

- Gamma-Ray Source in Distant Universe? 1738

- First Genes Isolated From the Deadly 1918 Flu Virus 1739

- Microbiologists Explore Life's Rich, Hidden Kingdoms 1740

- Subatomic Spin Still in Crisis 1742

- Thanks to a Parasite, Asexual Reproduction Catches On 1743

## PERSPECTIVES

- Protein Prenylation, et cetera: Signal Transduction in Two Dimensions M. H. Gelb 1750

- Nematic Emulsions J. F. Joanny 1751

- $\beta$ -Catenin as Oncogene: The Smoking Gun M. Peifer 1752

- Atomic Parity Violation and the Nuclear Anapole Moment W. C. Haxton 1753

## POLICY FORUM

- Genetic Information and the Workplace: Legislative Approaches and Policy Challenges K. Rothenberg, B. Fuller, M. Rothstein, T. Duster, M. J. E. Kahn, R. Cunningham, B. Fine, K. Hudson, M.-C. King, P. Murphy, G. Sergold, F. Collins 1755

## DEPARTMENTS

- THIS WEEK IN SCIENCE 1713

- EDITORIAL 1719  
Budgetary Foul Weather  
D. Atlas

- LETTERS 1721  
Breast-Screening Brawl: J. Sowinski; H. Hansma; D. B. Kopans • Presidential Chairs in Chile: P. Labarca and R. Latorre; A. Neely • Butterfly Identification: J. A. Hyatt • Bullish About the Bear?: B. Brown

- SCIENCESCOPE 1727

- RANDOM SAMPLES 1745  
Changing Sex Is Hard to Do • NIST Head to Step Down • Designer Pores

- BOOK REVIEWS 1748  
*The Biological Universe*, reviewed by J. N. Tatarewicz • *Electron Correlation in Molecules and Condensed Phases*, S. Das Sarma • Vignettes • Browseings

- PRODUCTS & MATERIALS 1811

## AAAS Board of Directors

Jane Lubchenco  
Retiring President, Chair  
Mildred S. Dresselhaus  
President  
M. R. C. Greenwood  
President-elect

Robert D. Goldman  
Alice S. Huang  
Sheila Jasanoff  
Simon A. Levin  
Marcia C. Linn  
Michael J. Novacek  
Anna C. Roosevelt  
Jean E. Taylor

William T. Golden  
Treasurer  
Richard S. Nicholson  
Executive Officer

SCIENCE (ISSN 0036-8075) is published weekly on Friday, except the last week in December, by the American Association for the Advancement of Science, 1200 New York Avenue, NW, Washington, DC 20005. Periodicals Mail postage (publication No. 484460) paid at Washington, DC, and additional mailing offices. Copyright © 1997 by the American Association for the Advancement of Science. The title SCIENCE is a registered trademark of the AAAS. Domestic individual membership and subscription (51 issues): \$105 (\$58 allocated to subscription). Domestic institutional subscription (51 issues): \$260. Foreign postage extra: Mexico, Caribbean (surface mail) \$55; other countries (air assist delivery) \$90. First class, airmail, student, and emeritus rates on request. Canadian rates with GST available upon request, GST #1254 88122. IPM #1069624. Printed in the U.S.A.

Collage, obtained with a microscope and cross polarizers, of a multiple emulsion of water droplets in larger drops of a nematic liquid crystal. The nematic appears colored, and the water droplets appear darker. The nematic induces novel interactions among the water droplets,

causing them to form linear chains and to lie near the center of the nematic drops (central droplet, 130 micrometers in diameter). See page 1770 and the related Perspective on page 1751. [Image: P. Poulin, H. Stark, T. C. Lubensky, D. A. Weitz, and F. Macera]



## RESEARCH ARTICLE

Measurement of Parity 1759

Nonconservation and an Anapole Moment in Cesium

C. S. Wood, S. C. Bennett, D. Cho, B. P. Masterson, J. L. Roberts, C. E. Tanner, C. E. Wieman

## REPORTS

Giant Friedel Oscillations on the Beryllium(0001) Surface 1764

P. T. Sprunger, L. Petersen, E. W. Plummer, E. Lægsgaard, F. Besenbacher

Probing the Local Effects of Magnetic Impurities on Superconductivity 1767

A. Yazdani, B. A. Jones, C. P. Lutz, M. F. Crommie, D. M. Eigler

Novel Colloidal Interactions in Anisotropic Fluids 1770

P. Poulin, H. Stark, T. C. Lubensky, D. A. Weitz

Direct Radiometric Observations of the Water Vapor Greenhouse Effect Over the Equatorial Pacific Ocean 1773

F. P. J. Valero, W. D. Collins, P. Pilewskie, A. Bucholtz, P. J. Flatau

Direct Radiative Forcing by Smoke from Biomass Burning 1776

P. V. Hobbs, J. S. Reid, R. A. Kotchenruther, R. J. Ferek, R. Weiss

A High-Temperature Electrical Conduction Mechanism in the Lower Mantle Phase (Mg,Fe)<sub>1-x</sub>O 1779

D. P. Dobson, N. C. Richmond, J. P. Brodholt

SNF Cell Cycle Regulator as a Target of the Yeast PKC-MAP Kinase Pathway 1781

K. Madden, Y.-J. Sheu, K. Baetz, B. Andrews, M. Snyder

Constitutive Transcriptional Activation by a  $\beta$ -Catenin-Tcf Complex in APC<sup>-/-</sup> Colon Carcinoma 1784

V. Korinek, N. Barker, P. J. Morin, D. van Wichen, R. de Weger, K. W. Kinzler, B. Vogelstein, H. Clevers

Activation of  $\beta$ -Catenin-Tcf Signaling in Colon Cancer by Mutations in  $\beta$ -Catenin or APC 1787

P. J. Morin, A. B. Sparks, V. Korinek, N. Barker, H. Clevers, B. Vogelstein, K. W. Kinzler

Stabilization of  $\beta$ -Catenin by Genetic Defects in Melanoma Cell Lines 1790

B. Rubinfeld, P. Robbins, M. E. Gamil, I. Albert, E. Porfiri, P. Polakis

Initial Genetic Characterization of the 1918 "Spanish" Influenza Virus 1793

J. K. Taubenberger, A. H. Reid, A. E. Krafft, K. E. Bijwaard, T. G. Fanning

Modulation of Ras and a-Factor Function by Carboxyl-Terminal Proteolysis 1796

V. L. Boyartchuk, M. N. Ashby, J. Rine

Crystal Structure of Protein Farnesyltransferase at 2.25 Angstrom Resolution 1800

H.-W. Park, S. R. Boduluri, J. F. Moomaw, P. J. Casey, L. S. Beese

Reproducibility and Variability in Neural Spike Trains 1805

R. B. de Ruyter van Steveninck, G. D. Lewen, S. P. Strong, R. Koberle, W. Bialek



1750, 1796, & 1800

Protein prenylation

## Indicates accompanying feature

Change of address: allow 4 weeks, giving old and new addresses and 8-digit account number. Postmaster: Send change of address to *Science*, P.O. Box 1811, Danbury, CT 06813-1811. Single copy sales: \$7.00 per issue prepaid includes surface postage; bulk rates on request. Authorization to photocopy material for internal or personal use under circumstances not falling within the fair use provisions of the Copyright Act is granted by AAAS to libraries and other users registered with the Copyright Clearance Center (CCC) Transactional Reporting Service, provided that \$4.00 per article is paid directly to CCC, 222 Rosewood Drive, Danvers, MA 01923. The identification code for *Science* is 0036-8075/93 \$4.00. *Science* is indexed in the *Reader's Guide to Periodical Literature* and in several specialized indexes.

## On the Web

Abstracts will soon be available to registered users of *Science Online* at no cost <http://www.sciencemag.org/>



same Au wire by (i) allowing it to collide with the Nb surface or (ii) performing field emission with it such that there was a significant change in the microscopic configuration of its outermost atoms. The results of these experiments show that the Au tips contribute little to the features in the spectra measured over the narrow range of energies near the Fermi level  $E_F$ , where we are interested in the DOS. Furthermore, our results were insensitive to the value of initial junction impedance (which determines the tip height) over 3.5 decades ( $10^8$  to  $5 \times 10^5$  ohms), except for a constant scaling factor.

8. A. Roy, D. S. Buchanan, D. J. Holmgren, D. M. Ginsberg, *Phys. Rev. B* **31**, 3003 (1985).
9. P. D. Scholten and W. G. Moulton, *ibid.* **15**, 1318 (1977).
10. P. Schlottmann, *ibid.* **13**, 1 (1976).
11. P. G. de Gennes, *Superconductivity in Metals and Alloys* (Addison-Wesley, Reading, MA, 1989).
12. Similar approaches have been used to describe STM measurements near a vortex [(6); J. D. Shore *et al.*, *Phys. Rev. Lett.* **62**, 3089 (1989); F. Gygi and M. Schlüter, *Phys. Rev. B* **41**, 822 (1990)]. For more recent calculations near a vortex, see N. Hayashi, M. Ichioika, K. Machida, *Phys. Rev. Lett.* **77**, 4074 (1996).
13. We have not made a more detailed comparison of the radial dependence between the measurement and the model calculation. Such a comparison would re-

quire us to taken into account the details of the adatom geometry, that is, the fact that at small lateral tip displacements ( $r < 4$  Å), most of the tunneling current is channeled through the impurity site [for example, see N. D. Lang, *Phys. Rev. Lett.* **56**, 1164 (1986)].

14. Our model predicts a local electron-hole asymmetry that oscillates and decays as a function of distance from the impurity. The  $I = 0$  amplitude remains constant, but its contribution decays as a function of  $r$ . Gaussian averaging of the model calculation over typical distances averaged by STM causes a non-oscillatory but decaying asymmetry in the region near the impurity.
15. A. Sakurai, *Prog. Theor. Phys.* **44**, 1472 (1970).
16. Varying the parameters of the calculation, we find that for  $a = 2.5$  Å, we can fit the data using  $U$  ranging from 0 to  $0.15 E_F$ , while allowing  $J$  to vary by 5%. The bound excitation energy, that is, the peak location in the data, is a very sensitive function of  $J$ .
17. M. E. Flatte and J. M. Byers, *Phys. Rev. Lett.*, in press.
18. M. I. Salkola, A. V. Balatsky, J. R. Schrieffer, *Phys. Rev. B*, in press.
19. We thank the authors of (17) and (18) for their interest in our experiment and thank D.-H. Lee, D. J. Scalapino, and M. Tinkham for fruitful discussions.

21 November 1996; accepted 3 February 1997

This material may be protected by Copyright law (Title 17 U.S. Code)

## Novel Colloidal Interactions in Anisotropic Fluids

Philippe Poulin, Holger Stark,\* T. C. Lubensky, D. A. Weitz

Small water droplets dispersed in a nematic liquid crystal exhibit a novel class of colloidal interactions, arising from the orientational elastic energy of the anisotropic host fluid. These interactions include a short-range repulsion and a long-range dipolar attraction, and they lead to the formation of anisotropic chainlike structures by the colloidal particles. The repulsive interaction can lead to novel mechanisms for colloid stabilization.

Dispersions of small particles in a host fluid are a widespread and important state of matter (1); colloidal suspensions are dispersions of solid particles, whereas emulsions are dispersions of liquid droplets coated with a surfactant. They are of considerable technological importance, with applications in everything from paints and coatings to foods and drugs. These are metastable rather than equilibrium systems. Attractive interactions among the particles, which arise, for example, from dispersion forces, can separate the dispersed phase from the host fluid. These forces must be counterbalanced by Coulombic, steric, or other repulsive interactions. The delicate balance between attractive and repulsive colloidal interaction determines the stability and hence usefulness of dispersions.

We report on a novel class of colloidal interactions that arise when the host fluid is anisotropic and provide a comprehensive theoretical framework to understand them.

Department of Physics and Astronomy, University of Pennsylvania, Philadelphia, PA 19104, USA.

\*Present address: Institut für Theoretische und Angewandte Physik, Universität Stuttgart, Pfaffenwaldring 57, D-70550, Stuttgart, Germany.

These interactions have both repulsive and attractive components. We use general theoretical arguments and a variational procedure based on analogies with electrostatics to show how these interactions arise from the orientational elasticity of the host fluid and from topological defects therein induced by the dispersed particles. The nature of these interactions depends on boundary conditions and on the anisotropy direction of the host fluid at particle and other interfaces. Modifications in these boundary conditions can easily be produced through changes in the composition of the surfactant or host fluid, making possible a fine degree of control of colloidal interactions.

We dispersed water droplets 1 to 5  $\mu\text{m}$  in diameter in a nematic liquid crystal (LC) host, pentylcyanobiphenyl (5CB), with a small amount of surfactant added to help stabilize the interface. We also used multiple emulsions, in which the nematic LC host was itself a much larger drop ( $\sim 50$   $\mu\text{m}$  in diameter) in a continuous water phase; this isolated a controlled number of colloidal droplets in the nematic host and allowed us to readily observe their structure. The multiple emulsions were formed with

sodium dodecyl sulfate, a surfactant that is normally ineffective at stabilizing water droplets in oil. Nevertheless, the colloidal water droplets remained stable for several weeks, which suggested that the origin of this stability is the surrounding LC—a hypothesis that was confirmed by the observation that droplets became unstable and coalesced in  $<1$  hour after the LC was heated to the isotropic phase.

We studied these nematic emulsions by observing them between crossed polarizers in a microscope. Between crossed polarizers, an isotropic fluid will appear black, whereas nematic regions will be colored. Thus, the large nematic drops in a multiple emulsion are predominately red in Fig. 1A, whereas the continuous water phase surrounding them is black. Dispersed within virtually all of the nematic drops are smaller colloidal water droplets, which also appear dark in the photo; the number of water droplets tends to increase with the size of the nematic drops. In all cases, the water droplets are constrained at or very near the center of the nematic drops. Moreover, their Brownian motion has completely ceased, an observation that is confirmed by warming the sample to change the nematic into an isotropic fluid, whereupon the Brownian motion of the colloidal droplets is clearly visible in the microscope.

Perhaps the most striking observation in Fig. 1A is the behavior of the colloidal droplets when two or more cohabit the same nematic drop: The colloidal droplets invariably form linear chains. This behavior is driven by the nematic LC—the chains break, and the colloidal droplets disperse immediately upon warming the sample to the isotropic phase. However, although the anisotropic LC must induce an attractive interaction to cause the chaining, it also induces a shorter range repulsive interaction. A section of a chain of droplets under higher magnification (Fig. 1B) shows that the droplets are prevented from approaching too closely, with the separation between droplets being a significant fraction of their diameter.

A clue to the origin of these new interactions comes from close examination of the patterns produced by the nematic host. Nematic drops containing only a single emulsion droplet invariably exhibit a distinctive four-armed star of alternating bright and dark regions that extend throughout the whole nematic drop (Fig. 1C). This pattern is produced by the rotation of the nematic anisotropy axis through a full  $360^\circ$  about the central water droplet and is characteristic of a topological defect called a hedgehog (2). When there is more than one water droplet, there is additional orientational texture between every pair of



droplets. This structure is a distorted four-arm star, which we identify as a hedgehog defect created in the nematic host. The distance between droplets and this host-fluid defect increases with increasing droplet radius. Moreover, there is always one less host defect than there are water droplets.

Colloidal water droplets can also be dispersed in a nematic host confined between parallel plates treated to force molecular alignment parallel to their surfaces. The droplets still form chains, but over time these chains continue to grow into larger and more complicated structures. Exactly one host defect is associated with each water droplet, so each chain has as many extra defects as water droplets rather than one less. We conclude that water droplets create defects in the host fluid that prevent close contact between water droplets and that give rise to a long-range anisotropic attractive interaction between droplets.

To explain these observations, we consider the properties of the unit vector field  $\mathbf{n}(\mathbf{r})$ , called the Frank director, that specifies the direction of local alignment of anisotropic LC molecules (3) at the point  $\mathbf{r} = (x, y, z)$ . Nematics are invariant under the inversion operation  $\mathbf{n}(\mathbf{r}) \rightarrow -\mathbf{n}(\mathbf{r})$ . The energy of long-wavelength, spatially non-uniform distortions of  $\mathbf{n}$  is determined by the Frank free energy ( $F$ ), which in the one-elastic constant approximation is

$$F = \frac{1}{2} \sum_{ij} \int d^3r \nabla_i n_j \nabla_j n_i \quad (1)$$

where the integral is over the volume of the nematic LC;  $i, j = x, y, z$ ;  $n_i$  is the  $i^{\text{th}}$  component of the director, and  $\nabla_i = \partial/\partial x_i$ . The elastic constant  $K$  is of order  $10^{-6}$  dynes in typical nematics. We must also consider topological defects in nematics, an important example of which is a hedgehog: a point defect in which the director sweeps out all directions on the unit sphere as all points on any surface enclosing the defect core are visited. Hedgehogs are characterized by an integer topological charge specifying the number of times the unit sphere is wrapped. These hedgehogs can have different director configurations. The simplest is the radial hedgehog, in which the director  $\mathbf{n}(\mathbf{r}) = (x, y, z)/r$  points radially outward like the electric field of a point charge. Another common configuration is the hyperbolic hedgehog with  $\mathbf{n} = (-x, -y, z)/r$  (Fig. 2A) obtained from the radial hedgehog by rotating all vectors by  $180^\circ$  about the  $z$  axis. These hedgehogs can be characterized by a topological charge of 1. However, the nematic inversion symmetry renders positive and negative charges indistinguishable, so that two unit-charge hedgehog defects can be com-

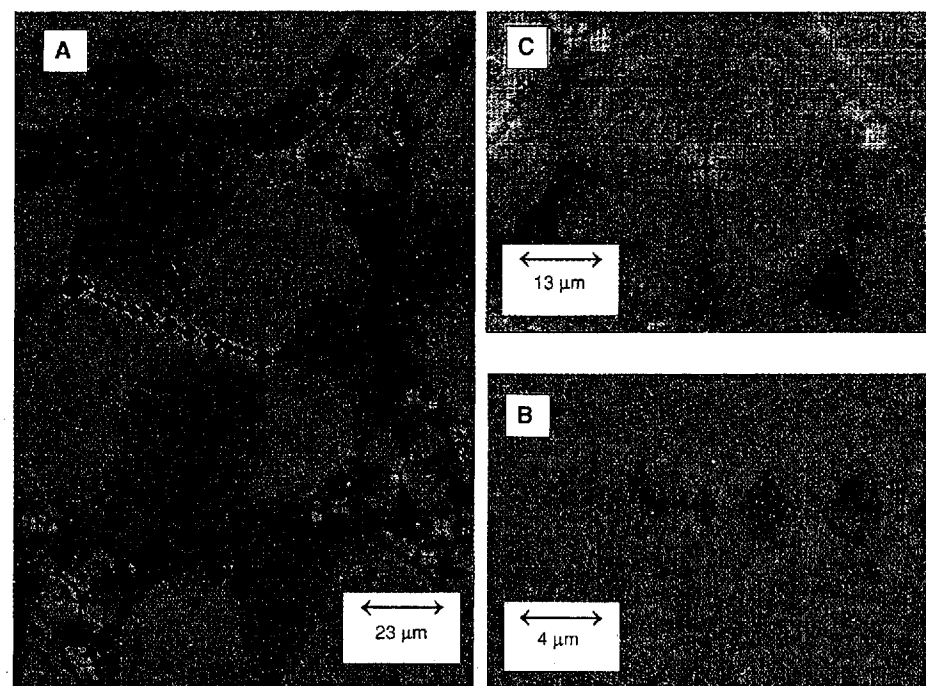
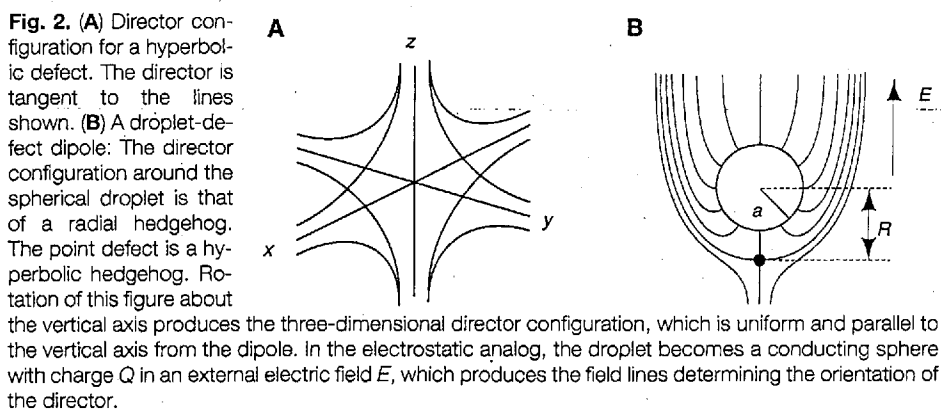


Fig. 1. (A) Microscope image of a nematic multiple emulsion taken under crossed polarizers. (B) A chain of water droplets under high magnification. (C) A nematic drop containing a single water droplet.

bined to give configurations with a total topological charge of either 2 or 0. In addition to hedgehogs, topological line defects called disclinations can also exist in nematics. Although there have been conjectures (4, 5) that a colloidal particle in a nematic will nucleate a disclination ring centered at its equator, we have found no experimental evidence for this for particles of the size we investigate.

Our observations can be qualitatively explained by considering the total topological charge  $Q$  in a nematic, which is determined by boundary conditions on  $\mathbf{n}$ . Parallel boundary conditions at infinity force  $Q$  to be 0, whereas normal or homeotropic boundary conditions on a closed surface with the topology of a sphere force  $Q$  to be 1. Normal boundary conditions at the water droplet surfaces force the creation of a ra-

dial hedgehog at each droplet. Thus, for homeotropic boundary conditions, a single hedgehog in a closed nematic drop with a single water droplet can satisfy both the boundary condition at the water droplet and the requirement  $Q = 1$ . Our observation of a single four-armed texture in single-droplet nematic drops is in accord with this. Each water droplet beyond the first added to the interior of a nematic drop must create orientational structure out of the nematic itself to satisfy the global constraint  $Q = 1$ . Similar considerations apply to each water droplet, including the first, added to a nematic cell with  $Q = 0$ . The simplest (though not the only) way to satisfy this constraint is for each extra water droplet to create a hyperbolic hedgehog in the nematic host (6). The radial droplet hedgehog and the companion host-liquid



hyperbolic hedgehog combine to create a parallel director pattern at infinity (Fig. 2B). All of our experimental observations—including the observation of one host defect per water droplet in the nematic between parallel plates and  $N - 1$  host defects for  $N$  water droplets in a nematic drop—are consistent with this simple scenario.

We can use Eq. 1 to determine the energy  $E_D$  of the droplet-defect dipole as a function of the separation  $R$  between the defect and the droplet center and thereby obtain the equilibrium separation  $R_0$ . Simple dimensional analysis and more detailed calculations (7) show that this energy grows linearly with separation  $R$  for  $R$  much greater than the droplet radius  $a$ . Energy increases as  $R$  approaches  $a$  (Fig. 2B): The director has to change directions from vertical to horizontal in a distance of order  $R - a$  leading to  $\nabla n \sim 1/(R - a)$  in Eq. 1. Beyond a distance of order  $R$  from the sphere, the director is approximately uniform. Thus,  $E_D \sim [K/(R - a)^2][AR^3 - (4\pi/3)a^3]$ , where  $A$  is a number of order unity. This energy is linear in  $R$  at large  $R$ , diverges as  $R$  approaches  $a$ , and has a minimum at some  $R_0 \sim a$ . To obtain a more reliable estimate, we constructed a variational ansatz for the unit vector field,  $\mathbf{n}(\mathbf{r})$ , that is parallel to the  $z$  axis at infinity, that is perpendicular to the surface of the droplet, and that has a companion hyperbolic defect somewhere. A vector field satisfying these conditions can be obtained from the electrostatic problem of a conducting sphere of positive charge  $Q$  in a uniform electric field  $\mathbf{E}_0 = E_0 \mathbf{e}_z$  parallel to the  $z$  axis as shown in Fig. 2. In reduced units with  $\tilde{\mathbf{r}} = \mathbf{r}/a = (\tilde{x}, \tilde{y}, \tilde{z})$ , the solution to this problem for a sphere at the origin yields an electric field  $\mathbf{E}(\mathbf{r})/E_0 = \mathbf{e}_z + \lambda^2 \tilde{\mathbf{r}}/\tilde{r}^3 - \tilde{r}^{-5}(\tilde{r}^2 \mathbf{e}_z - 3\tilde{\mathbf{r}}\tilde{r})$ , where  $\lambda^2 = Q/E_0 a^2$ . This field arises from the external field, the charge on the sphere, and an induced dipole at the center of the sphere. There is no negative electric charge in this problem, but there is a point where the electric field goes to zero (provided  $\lambda^2$  is sufficiently large). The electric field configuration in the vicinity of this point is identical to that of a unit vector field in the vicinity of a hyperbolic hedgehog defect. Thus, a variational ansatz for the director that satisfies all of our conditions is  $\mathbf{n}(\mathbf{r}) = \mathbf{E}(\mathbf{r})/|\mathbf{E}(\mathbf{r})|$ . At distances  $r \gg a$

$$\mathbf{n}(\mathbf{r}) \approx \left( \lambda^2 a^2 \frac{x}{r^3}, \lambda^2 a^2 \frac{y}{r^3}, 1 \right) \quad (2)$$

and  $n_x$  and  $n_y$  are solutions to Laplace's equation as they must be to minimize  $F$ . The zero of the electric field and thus the distance  $R = |\tilde{\mathbf{z}}|a$  to the hyperbolic defect is determined by the solution to  $|\tilde{\mathbf{z}}|^3 - \lambda^2 |\tilde{\mathbf{z}}| + 2 = 0$ . We can therefore use our ansatz for

$\mathbf{n}(\mathbf{r})$  in Eq. 1 to obtain an estimate of  $E_D$  as a function of reduced separation  $\tilde{R} = |\tilde{\mathbf{z}}|$  (Fig. 3A). This energy is linear in  $\tilde{R}$  at large  $\tilde{R}$  and has a minimum of  $13.00\pi Ka$  at  $R_0 = 1.17a$ . The curvature is  $33\pi Ka$  indicating that thermal fluctuations in the reduced separation between droplet and hyperbolic hedgehog is negligible:  $(\delta \tilde{R}_0)^2 \approx kT/33\pi Ka \approx 10^{-5}$ , where  $\delta \tilde{R} = \tilde{R} - \tilde{R}_0$ ,  $k$  is the Boltzmann constant, and  $T$  is the temperature. A well-defined distance,  $R_0$ , separates a colloidal water droplet from its companion defect, and this distance scales with the droplet radius. A host defect between two water droplets, therefore, prevents the water droplets from approaching each other too closely; it provides a repulsive barrier between two water droplets.

To treat long-range attractive interactions between droplets that lead to chaining, we seek a phenomenological free energy (5) describing how the water droplet distorts the director field at distances that are large compared to  $R_0$ . This energy must produce the large- $R$  director field predicted by Eq. 2. The droplet-defect pair has vector symmetry, and we assign it a dipole moment  $\mathbf{p} = (\lambda a)^2 \mathbf{e} \equiv p \mathbf{e}$ , where  $\mathbf{e}$  is the unit vector from the companion defect to the droplet center. From this we can construct a dipole-moment density for a collection of defects at positions  $\mathbf{r}_\alpha$  with respective dipole moments  $\mathbf{p}_\alpha$ :  $\mathbf{P}(\mathbf{r}) = \sum_\alpha \mathbf{p}_\alpha \delta(\mathbf{r} - \mathbf{r}_\alpha)$ . We now seek a free energy that, upon minimization, will lead to Eq. 2 for a single defect located at the origin with  $\mathbf{p}$  pointing in the minus  $z$  direction:

$$F = K \int d^3 r \left[ \frac{1}{2} \sum (\nabla n_i)(\nabla n_i) - 4\pi \mathbf{P}(\mathbf{r}) \cdot \mathbf{n}(\nabla \cdot \mathbf{n}) \right] - \frac{1}{2} A \sum_\alpha [\mathbf{p}_\alpha \cdot \mathbf{n}(\mathbf{r}_\alpha)]^2 \quad (3)$$

The second term in this energy is a flexoelectric term (8), and the last term (with an as-yet-unmeasured coefficient  $A$ ) results from the energetic preference for the dipoles to align either parallel or antiparallel to the director. Minimization of Eq. 3 over  $\mathbf{n}$  for a single defect at the origin [ $\mathbf{P} = p \mathbf{e}_z \delta(\mathbf{r})$ ] for small deviations from linear

equilibrium leads to  $n_i(\mathbf{r}) = p r_i / r^3$  for  $i = x, y$ . This reproduces Eq. 2 for  $p = \lambda^2 a^2$ .

The tendency to form chains can be explained by the effective dipole-dipole interaction predicted by Eq. 3. By calculating the director field at  $\mathbf{r}'$  produced by a dipole moment density at  $\mathbf{r}$ , we can calculate the effective dipole-dipole potential:

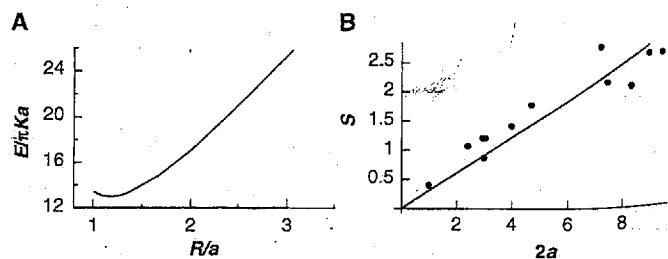
$$U_{\alpha\beta} = 4\pi K p_\alpha^z p_\beta^z \frac{1 - 3\cos^2\theta}{R^3} \quad (4)$$

where  $\theta$  is the angle between  $\mathbf{R} = \mathbf{r}_\beta - \mathbf{r}_\alpha$  and the  $z$  axis.  $p_\alpha^z$  is the component of the dipole moment of defect  $\alpha$  along the  $z$  axis; it can be either positive or negative. This energy is clearly minimized when  $p_\alpha^z$  and  $p_\beta^z$  have the same sign (that is,  $\mathbf{p}_\alpha$  and  $\mathbf{p}_\beta$  point in the same direction) and their separation vector is parallel to the  $z$  axis. This form accounts for the attractive interaction and leads to the formation of chains as seen in experiments. It is similar to configurations seen in other dipole systems such as electrorheological fluids and in magnetic emulsions (9).

The predicted scale for both the dipole-dipole attractive and defect-mediated repulsive interactions should be set by the droplets' diameter; as a consequence, the droplet separation within the chains should scale with  $a$ . To test this hypothesis, we measured the separations between the surfaces of neighboring droplets as their radius increased, and the results are plotted in Fig. 3B. A linear increase was observed. Moreover, the fit to the data (solid line) gives  $S \approx 0.6a$ . This value is in good accord with the expectation that the distance between droplets be somewhat greater than twice the separation  $2(R_0 - a)$  between a droplet and its companion defect.

The model free energy of Eq. 3 also accounts for several other experimental observations. It incorporates a preference for  $\mathbf{p}$  to align along  $\mathbf{n}$ . This was verified by observing single droplets between parallel glass plates treated to force tangential alignment of the director at their surface;  $\mathbf{p}$  is invariably aligned with  $\mathbf{n}$ . In addition, Eq. 3 also predicts that the defects will seek regions with maximum director splay ( $\nabla \cdot \mathbf{n}$ ) and that  $\mathbf{p}$  will prefer to orient antiparallel

Fig. 3. (A) Plot of reduced energy  $E/\pi Ka$  of a droplet-negative hedgehog as a function of reduced separation  $R/a$ . Note the linear dependence at large  $\tilde{R}$  and the minimum at  $R_0 \approx 1.17a$ . (B) Plot of the distance  $d$  between droplet surfaces as a function of their diameter  $2a$ .



to  $n$  when  $\nabla \cdot n$  is positive. A nematic drop with  $Q = 1$  has nonvanishing positive splay everywhere. This splay acts as an external field that establishes minimum energy positions for droplet dipoles and thereby arrests Brownian motion. The minimum energy position of a single droplet is at the center of a nematic drop. A second droplet moves to maximum splay at the center with  $p$  pointing toward the center along negative  $n$  in accord with observations. Subsequent droplets form chains. In contrast, in the parallel geometry there is no splay localizing particles; as a result, the particles and chains undergo Brownian motion, which leads to interchain coagulation.

Finally, one of the most important features of these novel colloidal interactions is their dependence on the anchoring of the nematic at the interface. For example, the behavior of the colloidal droplets in the multiple emulsions is completely altered if the nematic is forced to align parallel to the surface of the large droplets rather than perpendicular. In the passage from homeotropic to tangential alignment, the topological charge interior to a nematic drop is changed from 1 to 0, and point defects called boojums (2) develop on its surface. Splay is a maximum in the vicinity of these boojums, and thus we would expect the colloidal droplets to congregate at these defects. We can achieve tangential boundary conditions at the surface of the nematic drops, but not at the surfaces of interior colloidal water droplets, by adding a small amount of glycerol to the continuous water phase. As expected, the colloidal droplets do indeed migrate to the boojums. Similarly, in our theory, both the chaining and the defect-mediated repulsion are a consequence of the dipolar defect configuration produced by a droplet with homeotropic boundary conditions. Droplets with tangential boundary conditions create neither a radial nor a companion hyperbolic hedgehog and should, therefore, exhibit completely different structures. To test this, we added polyvinyl alcohol to the water droplets to change boundary conditions from homeotropic to tangential. The tendency to form chains was greatly reduced; moreover, the droplets were no longer separated by large distances when they approached one another, reflecting the absence of the hedgehog defects.

The new class of colloidal interactions discussed in this paper is not restricted to thermotropic nematic LC but should be present whenever the host fluid is anisotropic. Interesting effects can be expected as the delicate balance among the magnitude of the elastic constant, the particle size, and the anchoring energies is adjusted. For example, this class of interactions should also be present for solutions of

anisotropic micelles (10), rigid-rod polymers, and even biological systems such as actin or viruses. Moreover, the ability to controllably obtain both attractive and repulsive interactions offers an opportunity to develop novel routes to colloid stabilization and structure, as well as to create new materials with potentially useful applications. The theoretical picture presented here provides the framework for understanding all of these phenomena.

#### REFERENCES AND NOTES

1. W. B. Russel, D. A. Saville, W. R. Schowalter, *Colloidal Dispersions* (Cambridge Univ. Press, Cambridge, 1989).
2. M. V. Kurik and O. D. Lavrentovich, *Usp. Fiz. Nauk*, **154**, 381 (1988) [*Sov. Phys. Usp.* **31**, 196 (1988)]; N. D. Mermin, *Rev. Mod. Phys.* **51**, 591 (1979).
3. P. G. de Gennes and J. Prost, *The Physics of Liquid Crystals* (Clarendon, Oxford, ed. 2, 1993); S. Chandrasekhar, *Liquid Crystals* (Cambridge Univ. Press, Cambridge, 1992).
4. E. M. Terentjev, *Phys. Rev. E* **51**, 1330 (1995); O. V. Kuksenpk, R. W. Ruhwandl, S. V. Shiyonovskii, E. M. Terentjev, *ibid.* **54**, 5198 (1996).
5. S. Ramaswamy, R. Nityananda, V. A. Garhunanathan, J. Prost, *Mol. Cryst. Liq. Cryst.* **288**, 175 (1996).
6. R. B. Meyer, *ibid.* **16**, 355 (1972).
7. S. Ostlund, *Phys. Rev. B* **24**, 485 (1981).
8. R. B. Meyer, *Phys. Rev. Lett.* **22**, 918 (1969).
9. A. P. Gast and C. F. Zukoski, *Adv. Colloid Interface Sci.* **30**, 153 (1989).
10. P. Poulin, V. A. Raghunathan, P. Richetti, D. Roux, *J. Phys. II France* **4**, 1557 (1994).
11. We are grateful to A. Yodh for helpful discussions and a careful reading of the manuscript and to F. Macera for help with the figures. Supported primarily by the Materials Research Science and Engineering Center Program of NSF under award number DMR96-32598.

30 September 1996; accepted 7 February 1997

## Direct Radiometric Observations of the Water Vapor Greenhouse Effect Over the Equatorial Pacific Ocean

Francisco P. J. Valero,\* William D. Collins, Peter Pilewskie, Anthony Bucholtz, Piotr J. Flatau

Airborne radiometric measurements were used to determine tropospheric profiles of the clear sky greenhouse effect. At sea surface temperatures (SSTs) larger than 300 kelvin, the clear sky water vapor greenhouse effect was found to increase with SST at a rate of 13 to 15 watts per square meter per kelvin. Satellite measurements of infrared radiances and SSTs indicate that almost 52 percent of the tropical oceans between 20°N and 20°S are affected during all seasons. Current general circulation models suggest that the increase in the clear sky water vapor greenhouse effect with SST may have climatic effects on a planetary scale.

Recent studies (1) have demonstrated that atmospheric general circulation models, when forced only with measured SSTs (in particular, tropical Pacific SSTs), can reproduce the changes in global tropospheric temperatures that have been observed during the last several decades (2, 3). Earlier results (4–6) also pointed to the existence of a relation between variations in the tropical Pacific SSTs and global tropospheric temperatures. In this context, the clear sky water vapor greenhouse effect is key to the understanding of climate change, including global warming (7). The greenhouse effect can be defined as (8–10)

$$G_a = \sigma(\text{SST})^4 - F^+ \quad (1)$$

F. P. J. Valero, W. D. Collins, A. Bucholtz, P. J. Flatau, Atmospheric Research Laboratory, Center for Atmospheric Sciences, Scripps Institution of Oceanography, University of California, San Diego, 9500 Gilman Drive, La Jolla, CA 92093-0242, USA.  
P. Pilewskie, NASA, Ames Research Center, Moffett Field, CA 94035, USA.

\*To whom correspondence should be addressed.

According to the Stefan Boltzmann law,  $\sigma(\text{SST})^4$  is the infrared black body emission by the surface at temperature SST,  $\sigma = 5.67 \times 10^{-8} \text{ W m}^{-2} \text{ K}^{-4}$  is the Stefan Boltzmann constant, and  $F^+$  is the outgoing infrared radiation flux at the top of the atmosphere.

Satellite studies (8–10) have found that for clear skies and SSTs above 298 K, the spatial variation of  $G_a$  with SST,  $dG_a/d(\text{SST})$ , exceeds the rate of increase of sea surface emission,  $d\sigma(\text{SST})^4/d(\text{SST}) = 4\sigma(\text{SST})^3$ . For a tropical SST of 300 K,  $4\sigma(\text{SST})^3 \approx 6.1 \text{ W m}^{-2} \text{ K}^{-1}$ . This effect, termed the "super greenhouse effect" (11), occurs in both hemispheres during all seasons. It is also observed for interannual variations of  $G_a$  with SST during the El Niño in the tropical Pacific (12). Observations in the tropical Atlantic ocean (11) show that the clear sky downwelling infrared flux incident on the surface ( $F_a^-$ ) also increases faster than the surface emission with increasing SST. The net result is fur-

# Tab 2

MOLECULAR CRYSTALS AND LIQUID CRYSTALS  
SCIENCE AND TECHNOLOGY

CHEM PER  
QD  
901  
M64  
v. 275

Section A

MOLECULAR CRYSTALS  
AND  
LIQUID CRYSTALS

CONTENTS

Editorial: MCLC Enters Its 30th Year	i
<b>Liquid Crystals</b>	
In Memoriam: Glenn H. Brown (1915-1995)	1
Z. MIKITYUK, O. NEVMERZHITSKA, P. ZAREMBA and M. VISTAK: Temperature Dependence of Field Hysteresis Loop in Nematic-Cholesteric Mixtures	3
M. NISHIKAWA, N. BESSHO, T. NATSUI, Y. OHTA, N. YOSHIDA, D.-S. SEO, Y. IIMURA and S. KOBAYASHI: A Model of the Unidirectional Alignment Accompanying the Pretilt Angle of a Nematic Liquid Crystal (NLC), 5CB, Oriented on Rubbed Organic-Solvent-Soluble Polyimide Film	15
J. WEN, M. TIAN, Z. GUO and Q. CHEN: Synthesis and Phase-transition of 4-alkoxycarbonylphenyl 4'-n-alkoxy-2,3,5,6-tetrafluorobiphenyl-4-carboxylates	27
D.-S. SEO, S. KOBAYASHI, M. NISHIKAWA, E.-J. HAHN and Y. YABE: Effect of the Rubbing Fabric for Surface Liquid Crystal Alignment on Various Orientation Films	37
J. CHEN, H. VITHANA, D. JOHNSON, A. ALBARICI, J. LANDO, J. A. MANN, Jr and M.-A. KAKIMOTO: Investigations on Langmuir-Blodgett Films as Alignment Layers for Liquid Crystals	49
T. NOSE, T. SATO and S. SATO: Behavior of Disclination Lines Induced by a Nonuniform Electric Field in a Nematic Liquid Crystal Cell	63
W. WEISSFLOG, E. DIETZMANN, C. STÜTZER, M. DREWELLO, F. HOFFMANN and H. HARTUNG: Novel Mesogenic Benzoic Acids with Large Branches I. Synthesis, Liquid Crystalline Properties and Crystal Structure Analyses of 3-(4-Subst.-benzyloxycarbonyl)-4-(4-n-octyloxybenzyloxy)benzoic Acids	75

(continued on back cover)

Molecular crystals and  
liquid crystals science and  
technology. Section A,  
Molecular crystals and  
liquid crystals  
Received on: 04-11-97

University of Nebraska,

Lincoln -- Libraries

GORDON AND BREACH PUBLISHERS

30th Anniversary  
1966-1996

## Investigations on Langmuir-Blodgett Films as Alignment Layers for Liquid Crystals

J. CHEN<sup>1</sup>, H. VITHANA<sup>1</sup>, D. JOHNSON<sup>1</sup>, A. ALBARICI<sup>2</sup>, J. LANDO<sup>2</sup>,  
J. A. MANN, Jr<sup>3</sup> and M.-A. KAKIMOTO<sup>4</sup>

<sup>1</sup> Department of Physics and Liquid Crystal Institute, Kent State University, Kent, OH 44242

<sup>2</sup> Department of Macromolecular Science, Case Western Reserve University, Cleveland, OH 44106

<sup>3</sup> Department of Chemical Engineering, Case Western Reserve University, Cleveland, OH 44106

<sup>4</sup> Department of Textile and Polymeric Materials, Tokyo Institute of Technology, Ookayama, Meguro-ku Tokyo 152

(Received September 28, 1994; in final form May 10, 1995)

Multilayer polyimide (PI) films were successfully fabricated using the Langmuir-Blodgett (LB) technique. These films were studied in several ways relevant to their use as liquid crystal alignment layers. (1) The influence of dipping speed and creep time on the orientational order of PI-LB films was investigated by means of birefringence measurements. (2) For comparison, we measured the pretilt angles and polar anchoring strengths of liquid crystal (LC) cells assembled with PI-LB films and rubbed PI-LB films as alignment layers. (3) The anchoring direction of the liquid crystal was found to be solely determined by the dipping direction of uppermost PI-LB layer, regardless of the dipping direction of deeper layers. (4) Combining results of the above studies with measurements of pretransitional birefringence (above the isotropic-to nematic (I → N) transition) and observations of the growth of the alignment texture just below the nematic-isotropic transition, we draw the conclusion that the range of interaction between the PI-LB film and LC molecules is quite short ( $\sim 4.5$  Å) and that the alignment mechanism is epitaxial. Therefore, anisotropic short range molecular interactions are responsible for the alignment of the first liquid crystal layer. (5) From studies of PI-LB films deposited perpendicular to the rubbing direction of underlying spin-coated PI films, we also found evidence, as expected, that the grooves induced by the rubbing process are not decisive for LC alignment on a rubbed polymer surface.

**Keywords:** Liquid crystals, alignment, LB films

### 1. INTRODUCTION

The wide application of flat displays using liquid crystals (LCDs) has stimulated extensive study of alignment.<sup>1–3</sup> Conventional processes for forming homogenous alignment layers include a rubbed polymer coating and oblique evaporation of SiO<sub>2</sub>. Although the oblique evaporation method has the advantage of giving the liquid crystal molecules a prescribed pretilt angle, the deposition process is quite complicated and it is difficult to obtain a large uniform aligning area. The rubbing process also has several serious shortcomings.<sup>4,5</sup> Static electricity generated by rubbing causes flicker during operation of LCDs. Furthermore, the delicate switching elements on the surface, for example, thin film transistors, can be destroyed by the rubbing process and rubbing can introduce dust particles which can degrade the performance of LCDs. For

these reasons, researchers have tried to develop alternative methods of alignment. Ordered polyimide Langmuir-Blodgett (PI-LB) films have recently been shown to have enormous promise as LCD alignment layers.<sup>6-11</sup> It is now clear that LB films with their well-controlled architecture, large-area capability and dust free character are contenders for the alignment layers of future LCDs. Due to this potential application in the LCD industry, we need to know the mechanism of alignment and how to control the important parameters for display, for example, anchoring strength and pretilt angle.

In this paper, we present our preliminary results on PI-LB film alignment layers. Orientational order of PI-LB films was investigated by means of the birefringence measurements on films prepared with different dipping speeds and creep times. The pretilt angle and the temperature dependence of the polar anchoring strength of liquid crystal cells assembled with PI-LB alignment films and their rubbed counterparts were also measured. We have also made the first study of the pretransitional birefringence of LC cells with PI-LB alignment films. Based on our experimental results, the LC alignment mechanism on PI-LB films is suggested. Finally, we bring into focus the advantages and problems associated with PI-LB films as alignment layers. Possible solutions for the existing problems are suggested.

## 2. EXPERIMENTAL

### 2.1 Preparation of multilayer PI-LB films

Figure 1 shows the flow chart of the PI-LB preparation. LB films were prepared in a 70 cm × 15 cm Lauda trough. Due to the non-amphiphilic nature of the PI, we first mixed poly[4,4'-oxydiphenylene] pyromellitic acid (I) with N,N'-dimethylhexa decylamine (II) in the molar ratio of 1:2 in an organic solvent of N,N'-dimethylacetamide and benzene (1:1 in a molar ratio) to form a poly[4,4'-oxydiphenylene] pyromellitic acid salt (III). 100  $\mu$ l of (III) was then spread on deionized water at 20°C. After waiting for 10 min, the monolayer was compressed at a speed of 1.8 cm/min. The value of the co-area obtained was 110  $\text{\AA}^2$ . Y-type LB films of (III) were transferred onto the indium-tin-oxide (ITO) coated patterned glass by vertical dipping at a surface pressure of 25 mN/m and dipping speed of 1 mm/min for the first round trip and 10 mm/min for subsequent dipping. Films of (III) were immersed overnight in a mixed organic solvent of acetic anhydride, pyridine and benzene (1:1:3) for imidization to obtain polyimide (IV) LB(PI-LB) films.

### 2.2 Measurements of the anchoring strength, pretilt angle and optical retardation

The liquid crystal cells were made with two identical ITO-patterned glass substrates coated with PI-LB films. We assembled the cells with the dipping direction of the last LB layer antiparallel to each other. The thickness ( $\sim 50$   $\mu$ m) of each cell was determined by the optical interference method ( $\pm 0.5$   $\mu$ m) before the cells were filled with 4-cyano-4'-n-pentybiphenyl (5CB) liquid crystal by the capillary method. These cells were heated to 80°C (above the nematic-isotropic clearing point) then slowly

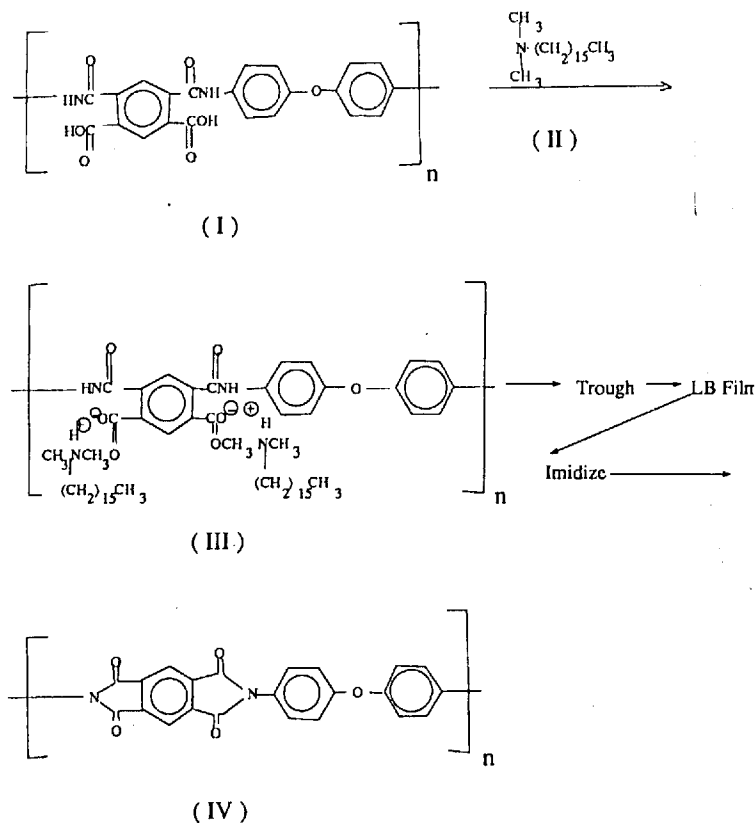


FIGURE 1 Flow chart of the multilayer PI-LB film preparation.

cooled down to room temperature to get rid of the flow alignment effect induced by filling the cell. 5CB was purchased from BDH chemicals and used without further purification.

The optical retardation of the PI-LB film was measured by ellipsometry with a resolution of  $0.01^\circ$ . The standard crystal rotation method<sup>12</sup> was used to determine the pretilt angle. To measure the polar anchoring strength, we adopted Yokoyama and VanSprang's high field method,<sup>13,14</sup> which requires simultaneous measurements of the voltage dependence of the birefringence and capacitance of a homogeneously aligned nematic LC cell. The schematic diagram for the optical phase retardation and capacitance measurement apparatus is shown in Figure 2.



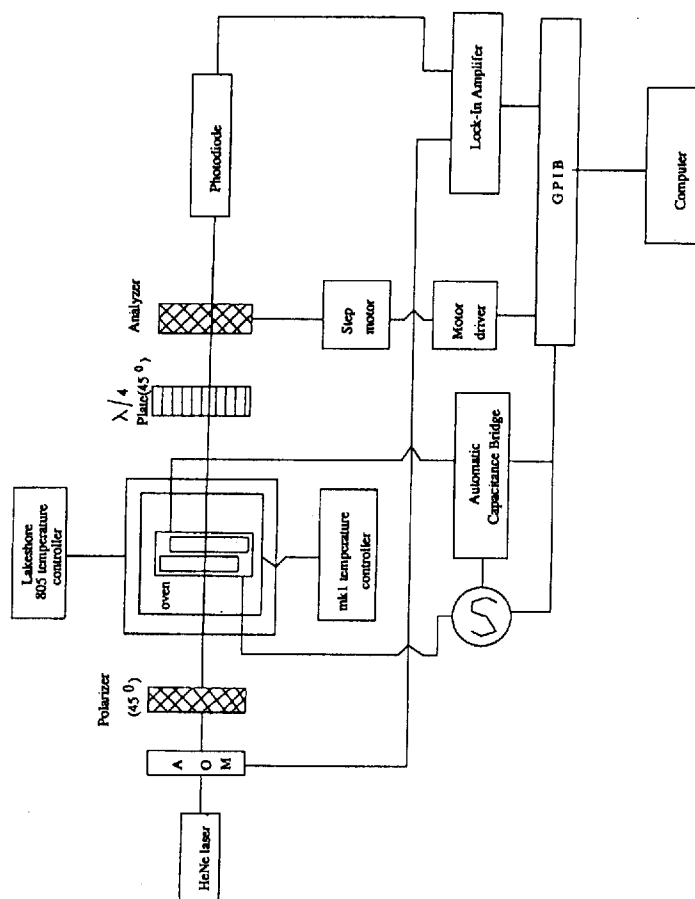


FIGURE 2. Experimental set-up for the optical phase retardation and capacitance measurements. All elements are self explanatory except the one labeled AOM which stands for Acoustic Optic Modulator.

For applied voltages,  $V$ , larger than 6 times the Freedericksz threshold voltage,  $V_{th}$ , the following relation should be accurate:<sup>13</sup>

$$R/R_0 = I_0/CV - 2d_e/d_0 \quad (1)$$

where the constant  $I_0$  is related to material parameters.  $R_0$  is equal to  $2\pi d_0(n_e - n_o)/\lambda$ .  $d_e$  is called the surface extrapolation length. The polar anchoring strength,  $W_0$ , is directly related to  $d_e$ . In particular, for the Rapini-Papoular surface potential,  $\frac{1}{2}W_0\sin^2(\theta - \theta_e)$ , we have a simple relationship  $W_0 = K_1/d_e$ , where  $K_1$  is the splay elastic constant of the LC which was measured separately.  $C$  and  $d_0$  are the capacitance and thickness of the LC cell respectively.  $n_o$  and  $n_e$  are the ordinary and extraordinary refractive indices of the LC. Temperature was controlled to  $\pm 5$  mK over 10 h. For the measurement of the pretransitional birefringence, the temperature was swept at the rate of  $0.18^\circ\text{C/h}$  and the result was independent of sweep rate at this rate.

### 3. RESULTS AND DISCUSSIONS

At least 3 PI-LB layers were needed to achieve good uniform LC alignment on PI-LB/ITO glass. The reason may be that 3 layers are enough to screen the interaction between the LC and ITO glass surfaces, and smoothly and fully cover the surface. All LC cells made with 3 to 15 PI-LB layers gave identical, good homogenous alignment. In all cases, the LC alignment direction matched with the dipping direction of LB deposition. To check the effectiveness of alignment of the last PI-LB layer, we deposited 6 layers on glass plates in such a way that the dipping direction of the sixth layer was changed by  $45^\circ$  with respect to the dipping direction of the previous five layers. Polarized microscopy showed that the LC anchoring direction was solely determined by the dipping direction of the sixth PI layer, which means that the interaction responsible for LC alignment on PI-LB films is rather short ranged, i.e., less than the thickness of one PI layer ( $\sim 4.5 \text{ \AA}$  as measured by our group.<sup>15</sup>)

As is known, LC alignment on a PI-LB film is induced by the well ordered polymer, which aligns along the dipping direction.<sup>16</sup> The dipping speed is expected to be an important parameter for controlling the quality of the LB film. The influence of dipping speed and creep time on the order of PI-LB films was investigated by measuring the optical retardation. The result is shown in Figure 3. Because of the birefringence of the ITO glass itself, microscope slides were used. Assuming that the retardation  $R = 2\pi d_0(n_e - n_o)S/\lambda$ , where  $S$  is an appropriately defined orientational order parameter of the PI-LB film, and  $n_e$  and  $n_o$  are the extraordinary and ordinary refractive indices of the polymer respectively, it seems that in our range of dipping speed, the order of the LB film doesn't change. Furthermore, we did not see any difference in retardation of the PI-LB films for creep times of 1 hour and 2 hours.

The pretilt angles of LC cells with various numbers of LB layers were measured by the standard crystal rotation method.<sup>12</sup> The results are presented in Figure 4. All samples show very small or zero pretilt angle. When we applied an electric field across these cells, all of them showed reverse tilt domains under polarized microscopy, which confirmed the tilt angle measurement results. Introducing a finite pretilt angle will be very important for the application of LB films as alignment layers.

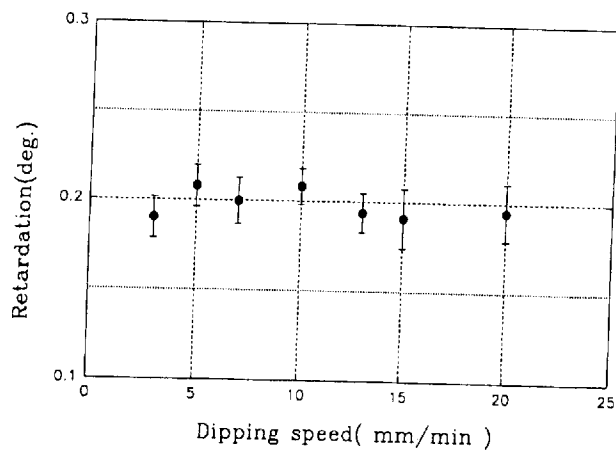


FIGURE 3 Phase retardation of PI-LB (5) film versus the dipping speed. Both sides of the microscope sheet glass have 5 layers of PI-LB films.

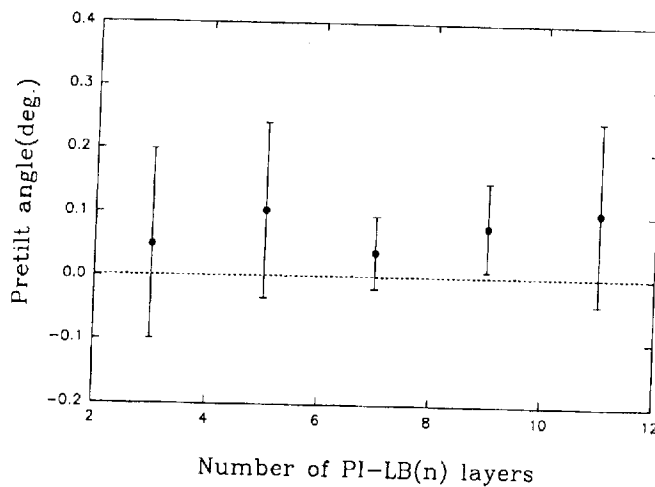


FIGURE 4 Pretilt angle versus the number  $n$  of PI-LB ( $n$ ) layers.

Figure 5 shows two typical  $R/R_0$  versus  $1/ CV$  curves of a liquid crystal cell with five PI-LB layers at two different temperatures. Fitting data of this type to Eq. (1), the polar anchoring strength and extrapolation length at different temperatures can be calculated and is shown in Figure 6. The polar anchoring strength of the PI-LB film is

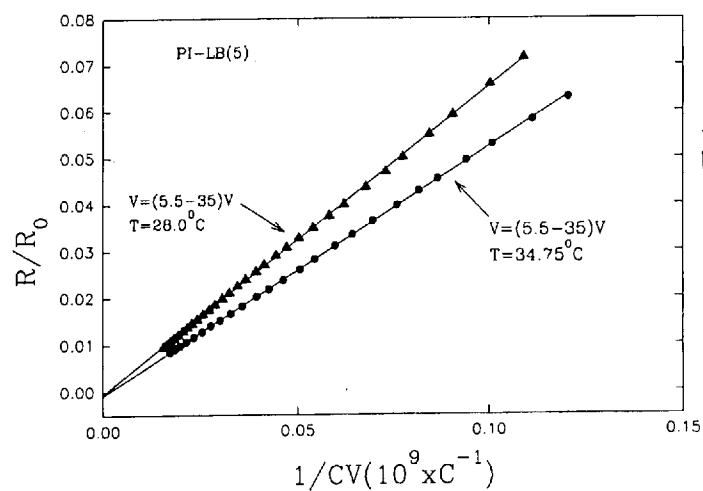
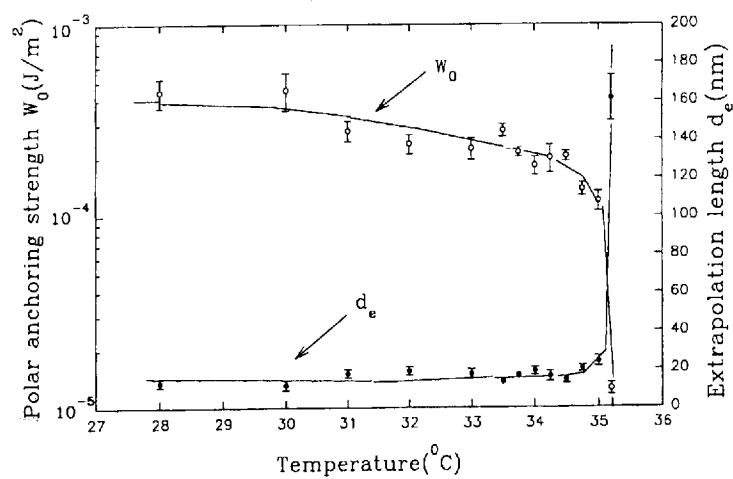

 FIGURE 5 Typical  $R/R_0$  versus  $1/CV$  curves at two different temperatures.


FIGURE 6 Polar anchoring energy and extrapolation length of PI-LB(5) versus temperature.

much stronger than that of  $\text{SiO}_x$ ,<sup>13,14</sup> but somewhat weaker than that of a spin-coated rubbed polymer film.<sup>3</sup>

As mentioned above, PI-LB films fail to align the liquid crystal with a pretilt angle, which is a prerequisite for LCDs to avoid reverse tilt domains. One technique to introduce a pretilt angle is to manipulate the side chain density of the polyimide precursor. The number of side chains can be controlled by varying the degree of imidization. It has been claimed that in this way one can control the pretilt angle of the liquid crystal on such LB films.<sup>18</sup> However, so far, we don't understand how to force the side chains to flip down unidirectionally to give pretilt angles that are uniform over the cell. Furthermore, the thermal stability of the pretilt angle has not been investigated. An alternative method to get a finite pretilt angle is to rub the PI-LB film. Due to the fact that PI-LB films are very thin (about 22 Å for 5 layers), static charge accumulation should not be a problem. Figure 7 shows two crystal rotation curves of LC cells assembled with PI-LB films with and without rubbing. Clearly, the symmetry point shifted away from zero angle after rubbing. The pretilt angle obtained in this case was about 2°. For comparison, we also measured the polar anchoring strength of the rubbed PI-LB films, which is shown in Figure 8. It seems that rubbing doesn't enhance the polar anchoring strength of PI-LB films, which is not in agreement with the results of Seo *et al.*<sup>8</sup> We also note that the polar anchoring strength of our non-rubbed PI-LB film is almost the same as that of their rubbed one. Atomic force microscopy (AFM) images indicate that our PI-LB films are already highly ordered before rubbing.<sup>15</sup> Evidently rubbing does not further improve the order of the film. Based on these results, we suggest that the polymer backbones lay statistically flat on the glass surface along the dipping direction, and, therefore, they fail to align the LC with a pretilt angle. The

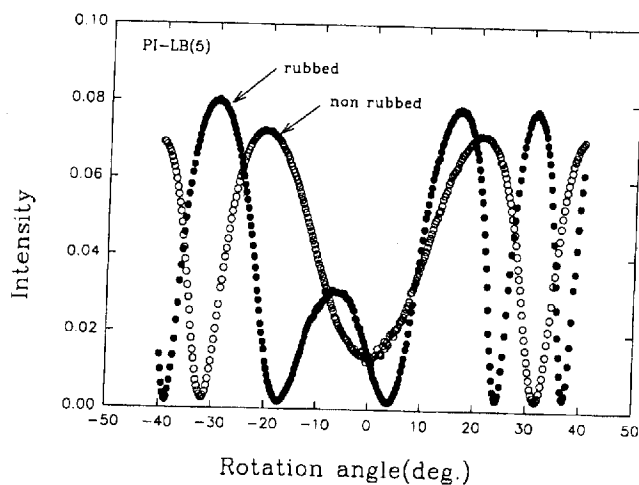


FIGURE 7 Crystal rotation curves of LC cells having PI-LB(5) films with and without rubbing.

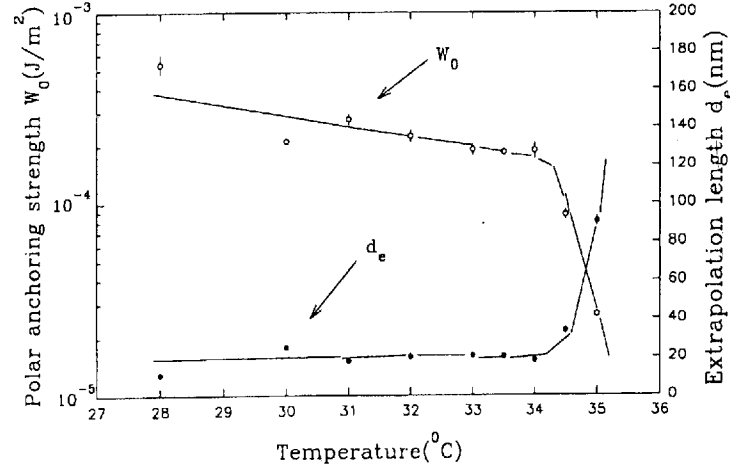


FIGURE 8 Polar anchoring strength and extrapolation length of rubbed PI-LB (5) versus temperature.

stress generated by the rubbing process apparently gives these backbones a small but finite angle with the surface plane and a finite pretilt angle is obtained.

This result is consistent with the pretilt generation model proposed by Geary *et al.*<sup>19</sup> However, it has to be mentioned here that it is hard to rub PI-LB films uniformly because of their ultrathin nature. Therefore, adjusting the rubbing strength is not a suitable way to control the pretilt angle for practical applications. We also find that hard rubbing can damage or even strip away PI-LB films. Controlling the pretilt angle of LC's aligned by PI-LB films is still a big challenge for the application of LB films in the LCD industry. Pretransitional birefringence has been used to probe the mechanism of an LC alignment for some years.<sup>20-23</sup> We report here the first surface induced pretransitional birefringence measurements of an LC cell with PI-LB films as alignment layers. Three samples were measured and results are presented in Figure 9. The alignment layers for these samples are a PI-LB (5) film, a rubbed PI-LB (5) film and a conventional spin-coated rubbed PI film. All three samples show qualitatively similar pretransitional behavior. The solid lines in Figure 9 are fitting curves using Eq. (3) derived from the Ginzburg-Landau theory of de Gennes.

Under the framework of de Gennes' theory,<sup>24</sup> the free energy density of a semi-infinite ( $z \geq 0$ ) sample near the LC isotropic to nematic phase transition is

$$F = F_0 + \frac{1}{2}a(T - T^*)Q^2(z) - \frac{1}{3}bQ^3(z) + \frac{1}{4}cQ^4(z) + \frac{1}{2}L|\nabla Q(z)|^2 \quad (2)$$

Minimizing the total free energy with respect to the functional form of  $Q(z)$  at fixed boundary condition  $Q(0) = Q_s$ , the analytic expression for total phase difference between

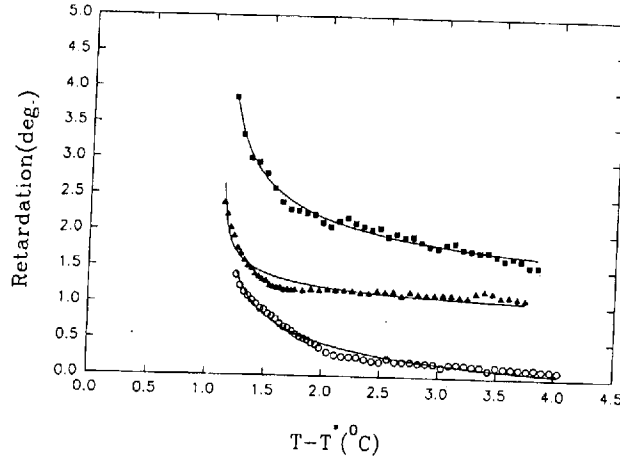


FIGURE 9 Pretransitional birefringence behavior of LC cells assembled with PI-LB (5) ( $\circ$ ), rubbed PI-LB (5) ( $\blacktriangle$ ) and spin-coated rubbed PI ( $\blacksquare$ ) films. The solid curves are fitting curves using Equation (3). Both experimental and theory values of the middle curve were shifted upward one degree on purpose in order to avoid overlapping the bottom curve.

ordinary and extraordinary rays of light passing normally through the sample is<sup>22</sup>

$$\begin{aligned}\Delta\delta &= \frac{2\pi}{\lambda}(n_e - n_o) \int_0^\infty Q(z) dz \\ &= \frac{2\pi}{\lambda}(n_e - n_o) \left(\frac{2L}{c}\right)^{1/2} \ln P(T, Q_s) \\ &= \delta_0 \ln P(T, Q_s)\end{aligned}\quad (3)$$

where

$$P(T, Q_s) = \frac{(F_1(Q_s)/Q_s^2)^{1/2} + (a(T - T^*)/2)^{1/2} + Q_s c^{1/2}/2}{(F_1(Q_s)/Q_s^2)^{1/2} + (a(T - T^*)/2)^{1/2} - Q_s c^{1/2}/2}$$

$$F_1(Q) = a(T - T^*)Q^2(z)/2 - bQ^3(z)/3 + cQ^4(z)/4$$

The parameters  $a$ ,  $b$  and  $c$  for 5CB used for all fitting were  $0.13 \times 10^6 \text{ Jm}^{-3} \text{ K}^{-1}$ ,  $1.6 \times 10^6 \text{ Jm}^{-3}$  and  $3.9 \times 10^6 \text{ Jm}^{-3}$  respectively and were obtained from the ref. 23. We selected  $Q_s$ ,  $T^*$ ,  $\delta_0$  and the background birefringence as adjustable fitting parameters to minimize the standard deviation.

Surprisingly, for all three cases, we found almost the same surface order parameters. The fitted values of  $Q_s$  were 0.38, 0.39 and 0.38 respectively for PI-LB (5),

rubbed PI-LB (5) and spin-coated rubbed PI films. The fitting results for the PI-LB film and rubbed spin-coated PI film are fairly good. However, we notice that we can't fit both the high and low temperature regions for the rubbed PI-LB film. The magnitude  $\delta_0$  for the rubbed PI-LB film is 0.33, which is quite different from values 0.70 and 0.92 we got for PI-LB (5) and rubbed PI films respectively. They are supposed to be the same in the model because the same LC materials are used (see Eq. (3)). Note that the data for this film fit de Gennes' model rather poorly by comparison with the other two films. This may indicate that the surface order parameter of the rubbed PI-LB (5) film changes with temperature instead of being fixed as we have assumed or that the uniformity of the rubbed PI-LB films is poor. More detailed work on this is under way.

The nucleation of the nematic phase of homogeneous LC cells with PI-LB (5) as alignment layers was observed under polarized light microscopy as the cell cooled slowly. As described in ref. 19, "sheet nucleation" on the cell surface was observed as the nematic phase was entered. These uniformly-aligned nematic layers grew in thickness until they met in the center of the cell, producing a flaw-free aligned texture. This behavior is strongly distinguished from the evolution of the alignment texture of an LC cell associated with obliquely evaporated  $\text{SiO}_x$  alignment layers. In the latter situation, the nematic phase nucleates at numerous isolated sites in the bulk and at the surface. These spots grow and join together with a high density of director defects. Uniform alignment of the whole cell is reached only after the defects anneal out. The PI-LB alignment behavior belongs exactly to the first category in Table II ref. 19, i.e., sheet rather than point nucleation. On the other hand, obliquely deposited  $\text{SiO}_x$  alignment surfaces belong to the second category and are strong candidates for description by the Berreman model.<sup>25</sup> This is further substantiated by their failure to give pretransitional birefringence.<sup>21</sup>

Historically, the groove model was first proposed to elucidate the LC alignment mechanism for rubbed or polished solid surfaces<sup>25</sup>. Berreman, however, was well aware that surfaces having oriented long organic molecules may align by a different mechanism. Much evidence shows that the groove structures induced by the rubbing process play a minor role in LC alignment on rubbed PI or many other polymer surfaces.<sup>19,27,28</sup> An epitaxial growth model was subsequently proposed in which the interaction between oriented polymers and LC molecules is responsible for LC alignment.<sup>19</sup> The mechanism of alignment is analogous to epitaxial formation of conventional solid crystals except it is orientational rather than translational in nature. However, to some extent there is still confusion about these two models. All of the above experimental results taken collectively provide evidence to settle this issue in favor of epitaxial alignment. This conclusion is independent of any specific macroscopic model such as that of de Gennes.<sup>24</sup>

We studied the case of LB films with a varying number of layers deposited perpendicular to the direction of rubbing on a spin-coated rubbed PI film. We also found that three PI-LB layers ( $\sim 13 \text{ \AA}$ ) were required to switch the LC orientation from the rubbing direction to the PI-LB dipping direction.<sup>7</sup> Before deposition, well-defined grooves were detected by AFM. The depth of grooves was around  $80 \text{ \AA}$ . As we mentioned above, 3 PI-LB layers were also required to achieve good LC alignment on ITO-coated glass. It seems that it also requires three PI-LB layers



to screen the interaction between the LC and the polymer on spin-coated rubbed PI films. The groove structure was still observed by AFM. After 3 layer PI-LB film deposition this result shows, not surprisingly, that while the groove structure may aid alignment, it is not an intrinsic reason for LC alignment on a rubbed polymer surface. Note also that grooves on the rubbed polymer surface increases the interaction area between polymer and LC molecules in comparison with a PI-LB film with a flat surface. This could be the reason why the polar anchoring strength of a PI-LB film is lower than that of the rubbed PI film. Whatever the true effect of the grooves may be, when the interaction between oriented polymer and LC molecules is screened by three or more perpendicularly oriented PI-LB layers, the influence of groove structure is dramatically weakened.

#### 4. CONCLUSIONS

Highly-ordered multilayer PI-LB films were successfully fabricated by the LB technique and showed a strong tendency to align liquid crystals. In order to achieve good alignment on ITO-coated glass, three or more PI-LB layers were necessary. It was also found that the anchoring direction of the LC was solely determined by the dipping direction of the uppermost PI-LB layer. This means that the alignment comes from short range molecular interactions. In our range of dipping speeds, the orientational order of our PI-LB films was almost constant. Unfortunately, they failed to align the LC with a pretilt angle. Rubbing was found to solve this problem in principle, but it was very hard to rub the whole region uniformly. The measured polar anchoring strength between the PI-LB film and 5CB is very strong ( $\sim 3 \times 10^{-4}$  J/m<sup>2</sup> at 30°C). The alignment texture and pretransitional birefringence behavior of an LC cell with PI-LB alignment films clearly showed that the aligning LC layer grows epitaxially from the surface. In the case of PI-LB films deposited perpendicular to the rubbing direction of spin-coated rubbed PI films, results indicated that while the groove structure generated by the rubbing process was not the intrinsic reason for LC alignment on rubbed polymer surface, it may enhance the anchoring strength.

#### Acknowledgements

We would like to thank Mr. Doug Bryant for helping us to use the facilities in the clean room and Dr. A. R. Baldwin, Mr. J. H. Brechtelsbauer and Mr. W. D. Burkhardt for much help during the set up of the equipment. The authors also acknowledge Prof. D. W. Allender, Dr. V. Surendranath and Mr. D. Yohannes for useful discussions. This work was supported by the Office of Naval Research under the grant # N00014-94-1-0270 and by the Advanced Liquid Crystalline Optical Materials program under NSF grant # DMR-8920147.

#### References

1. T. J. Sluckin and A. Poniewierski, In *Fluid Interfacial Phenomena* edited by C. A. Croxton (Wiley, New York, 1986) Chap. 5.
2. J. Cognard, *Mol. Cryst. Liq. Cryst. Suppl.*, **1**, 1 (1982).
3. H. Yokoyama, *Mol. Cryst. Liq. Cryst.*, **265**, 269 (1988).
4. H. Ikeno, A. Oh-sasi, N. Ozaki, M. Nitta, K. Nakaya and S. Kobayashi, *Pro. Soc. Inf. Disp. (SID)*, **52**, 45 (1988).

5. M. Kimura, H. Maeda, M. Yoshida, B. Zhang, H. Sekine, A. Mochizuki and S. Kobayashi, *Mol. Cryst. Liq. Cryst.*, **202**, 171 (1991).
6. H. Ikeno, H. Maeda, M. Yoshida, B. Zhang, M. Kimura and S. Kobayashi, *Pro. Soc. Inf. DISP. (SID)*, **30**, 329 (1989).
7. M. Murata, H. Awaji, M. Isurugi, M. Uekita and Y. Tawada, *Jpn. J. Appl. Phys.*, **31**, L189 (1992).
8. D.-S. Seo, H. Matsuda, T. OH-Ide and S. Kobayashi, *Mol. Cryst. Liq. Cryst.*, **224**, 13 (1993).
9. H. Ikeno, A. Oh-saki, M. Nitta, N. O. Zaki, Y. Yokoyama, K. Nakaya and S. Kobayashi, *Jpn. J. Appl. Phys.*, **27**, L475 (1988).
10. Y. Nishikata, A. Morikawa, Y. Takiguchi, A. Kanemoto, M. Kakimoto and Y. Imai, *Jpn. J. Appl. Phys.*, **27**, L1163 (1988).
11. Y. M. Zhu, Z. H. Lu, Q. H. Wei, X. M. Yang, Y. Wei, X. Y. Chen, J. H. Tang and W. Yan, *Phys. Lett.*, **A183**, 107 (1993).
12. T. J. Scheffer and J. Nehring, *J. Appl. Phys.*, **48**, 1783 (1977).
13. H. Yokoyama and H. A. Van Sprang, *J. Appl. Phys.*, **57**, 4520 (1985).
14. H. Yokoyama, S. Kobayashi and H. Kamei, *J. Appl. Phys.*, **61**, 4501 (1987).
15. H. Vithana and D. Johnson, to be published.
16. N. Minari, K. Ikegami, S. Kuroda, K. Saito, M. Saito and M. Sugi, *Jpn. J. of the Phys. Soc.*, **58**, 222 (1989).
17. H. Yokoyama, *Mol. Cryst. Liq. Cryst.*, **165**, 265 (1988).
18. Y. Nakajima, K. Saito, M. Murata and M. Vekita, *Mol. Cryst. Liq. Cryst.*, **237**, 111 (1993).
19. J. M. Geary, J. W. Goodby, A. R. Kmetz and J. S. Patel, *J. Appl. Phys.*, **62**(10), 4100 (1987).
20. K. Miyano, *Phys. Rev. Lett.*, **43**(1), 51 (1979).
21. H. Yokoyama, S. Kobayashi and H. Kamei, *Appl. Phys. Lett.*, **41**(5), 438 (1982).
22. J. C. Tarczon and K. Miyano, *J. Chem. Phys.*, **73**(4), 1994 (1980).
23. H. A. Van Sprang, *J. Physique*, **44**, 421 (1983).
24. P. G. de Gennes, *The Physics of Liquid Crystals* (Oxford, London, 1974).
25. D. Berreman, *Phys. Rev. Lett.*, **28**, 1683 (1972).
26. S. Isohichi, H. Wakemoto, K. Nakazima and Y. Matsuo, *Liq. Cryst.*, **4**(6), 669 (1989).
27. N. A. J. M. Van Aerle, M. Barmentlo and R. W. J. Hollering, *J. Appl. Phys.*, **74**(1), 3111 (1993).

# Tab 3

# PHYSICAL REVIEW A

STATISTICAL PHYSICS, PLASMAS, FLUIDS,  
AND RELATED INTERDISCIPLINARY TOPICS

---

Volume 43

*Third Series*

Number 10

---

15 MAY 1991



*Published by*

THE AMERICAN PHYSICAL SOCIETY

*through the*

AMERICAN INSTITUTE OF PHYSICS

MAY 29 1991

# PHYSICAL REVIEW A

STATISTICAL PHYSICS, PLASMAS, FLUIDS, AND RELATED INTERDISCIPLINARY TOPICS

## Editor

BENJAMIN BEDERSON  
(New York University)

## Assistant Editor

CAROL B. KRANER

## Assistants to the Editor

MARGARET MALLOY  
VALERIE L. MILLER

## Associate Editors

RUSSELL J. DONNELLY  
(University of Oregon)

BRANT M. JOHNSON  
(Brookhaven National Laboratory)

IRWIN OPPENHEIM  
(Massachusetts Institute of Technology)

## Editorial Board

### Term ending 31 December 1991

P. C. HOHENBERG—statistical physics  
R. M. NOYES—chemical physics  
B. H. RIPIN—plasmas

### Term ending 31 December 1992

R. S. BERRY—chemical physics  
M. E. FISHER—statistical physics  
R. E. KELLY—fluid dynamics  
T. A. WITTEN—statistical physics

### Term ending 31 December 1993

L. KRAMER—nonlinear phenomena,  
liquid crystals  
B. WIDOM—statistical mechanics

Published through the  
American Institute of Physics  
by  
**The American Physical Society**

## President

NICOLAAS BLOEMBERGEN

## President-Elect

ERNEST M. HENLEY

## Executive Secretary

N. RICHARD WERTHAMER

## Treasurer

HARRY LUSTIG

## Editor-in-Chief

DAVID LAZARUS

## Editorial Office:

1 Research Road  
Box 1000  
Ridge, NY 11961  
Telephone: (516) 924-5533  
Telex: 971599  
Cable Address: PHYSREV RIDGENY  
FAX: (516) 924-5294  
BITNET Address: pra@APSEDOFF

\*Not for transmission of manuscripts

## Production and distribution by

American Institute of Physics  
500 Sunnyside Blvd.  
Woodbury, NY 11797  
Telephone: (516) 349-7800  
FAX: (516) 349-7669

Manuscripts for publication should be submitted to the Editorial Office (please provide four copies). Information for contributors may be found in the January and July issues. Submission is a representation that the manuscript has not been published previously and is not currently under consideration for publication elsewhere. The manuscript should be accompanied by a statement transferring copyright to APS. A transfer form may be found in the back of some recent issues of *Physical Review Letters*.

To support wide dissemination of research results through publication of journal pages, the authors' institutions are requested to pay a publication charge of \$50 per page plus a \$50 abstract charge. Reprints are offered for sale to authors.

Subscription prices (table below) for American Physical Society members are for the fiscal year July 1, 1990–June 30, 1991. Member subscriptions are for personal use only. Nonmember subscription prices are for the period of January–December 1991. Back-number price: Single copies, \$65.

	No. issues	U.S.A. & Poss.	Can., Mex., Cntrl. & S. Amer., & Carib.	Europe, Asia, Africa, & Oceania		
				Surface Mail	Air Freight	Optional Air Freight
<b>Physical Review A</b>						
Members	24	\$ 140	\$ 195	\$195	—	\$275
Nonmembers	24	\$ 1150	\$ 1220	—	\$1300	—
<b>Physical Review A (1st)</b>						
Members	12	\$ 70	\$ 98	\$ 98	—	\$140
<b>Physical Review A (15th)</b>						
Members	12	\$ 70	\$ 97	\$ 97	—	\$135
<b>Phys. Rev. A,B,C,D</b>						
Nonmembers	96	\$4570	\$4830	—	\$5150	—

Inquiries regarding subscriptions, renewals, address changes, missing or damaged copies, microfilm, and single-copy orders should be addressed as follows:

**Members:** APS Membership Information Systems, 500 Sunnyside Blvd., Woodbury, NY 11797.

**Nonmembers:** MASS, American Institute of Physics, 500 Sunnyside Blvd., Woodbury, NY 11797.

Allow at least six-weeks advance notice. For address changes please send both old and new addresses, and, if possible, include an address stencil imprint from the mailing wrapper of a recent issue. A change-of-address form is included in every issue of *Physics Today*.

The Annual Index of *Physical Review* and *Physical Review Letters* may be ordered by members for \$20, and by nonmembers for \$60. Back issues are available for \$50. There are mail surcharges for non-U.S. destinations.

## Copyright 1991 by The American Physical Society

Permission is granted to quote from this journal with the customary acknowledgment of the source. To reprint a figure, table, or other excerpt requires, in addition, the consent of one of the original authors and notification of APS. No copying fee is required when copies of articles are made for educational or research purposes by individuals or libraries (including those at government and industrial institutions). Republication or reproduction for sale of articles or abstracts in this journal is permitted only under license from APS; in addition, APS may require that permission also be obtained from one of the authors. Address inquiries to the Executive Secretary, The American Physical Society, 335 East 45th Street, New York, NY 10017.

# Optical second-harmonic-generation study of the interaction of silane-covered surfaces with liquid-crystal layers

M. Barmiento, F. R. Hoekstra, N. P. Willard, and R. W. J. Hollering  
*Philips Research Laboratories, P.O. Box 80000, 5600 JA Eindhoven, The Netherlands*  
 (Received 13 November 1990; revised manuscript received 20 March 1991)

Optical second-harmonic generation has been used to determine the average molecular orientation of liquid-crystal (LC) molecules adsorbed on various silane-covered substrates. With the use of different preparation methods for the silane layers, considerable changes in molecular orientation of the polar-ordered part of the first LC monolayer were observed. Concomitantly, the number of polar-ordered LC molecules changed.

## I. INTRODUCTION

Various types of bulk liquid-crystal (LC) alignment can be induced by specific surface treatments. However, the physical mechanisms which underlie the alignment are not completely understood.<sup>1</sup> One would therefore like to probe the interaction between the treated surface and the LC molecules close to it. Optical second-harmonic generation (SHG), which is intrinsically surface specific, seems an ideal tool for studying these interfaces.

The interface-specific character of the technique stems from the fact that, in the electric-dipole approximation, SHG is symmetry forbidden in the bulk of centrosymmetric media. Efficient generation of a polarization at the second-harmonic (SH) frequency is only possible at a surface or interface where this symmetry is broken. In recent publications, the use of SHG (Refs. 2 and 3) and sum-frequency generation<sup>4</sup> (SFG) in studying liquid-crystal-surfactant interfaces has been successfully demonstrated. As a surprising result, it was found with SHG (Ref. 2) that the molecular orientation in the first LC monolayer adsorbed on glass was not affected by the presence of silane layers which yield different bulk LC alignments.

In this paper, we report that the molecular orientation strongly depends on the preparation of the silane layers.

## II. THEORY

The SH intensity  $I(2\omega)$  reflected from a monolayer of LC molecules adsorbed on a substrate is given by<sup>5</sup>

$$I(2\omega) \propto \sec^2 \phi |e_{2\omega} \cdot \chi^{(2)} : e_{\omega} e_{\omega}|^2 I^2(\omega). \quad (1)$$

Here,  $\phi$  is the angle of reflectance and  $\chi^{(2)}$  the nonlinear susceptibility tensor.  $e_{2\omega}$  and  $e_{\omega}$  denote the products of Fresnel factors and the output- and input-polarization vectors at frequencies  $2\omega$  and  $\omega$ , respectively,<sup>5</sup> and  $I(\omega)$  denotes the laser intensity at frequency  $\omega$ . In this paper, the polarization directions are denoted by  $p$ ,  $s$ , and  $q$ , where  $p$  and  $s$  are in the plane of incidence ( $x$ - $z$  plane) and normal to it, respectively, while  $q$  refers to a mixed linear polarization with the polarizer set at  $45^\circ$ .

If the nonlinear susceptibility of the substrate is relatively small, the SH signal will be dominated by the ad-

sorbed LC molecules. Assuming the interaction between molecules to be negligible,  $\chi^{(2)}$  takes the form

$$\chi_{ijk}^{(2)} = N_s \langle G_{ijk}^{\xi\eta\zeta} \rangle a_{\xi\eta\zeta}^{(2)}, \quad (2)$$

where  $a^{(2)}$  is the nonlinear polarizability tensor of a molecule and  $N_s$  is the surface density of molecules.  $\langle G_{ijk}^{\xi\eta\zeta} \rangle$  denotes an appropriate average over molecular orientation of the transformation matrix from the molecular coordinate axes ( $\hat{\xi}, \hat{\eta}, \hat{\zeta}$ ) to the laboratory system ( $\hat{i}, \hat{j}, \hat{k}$ ).

For SHG from an in-plane isotropic distribution of molecules where  $a^{(2)}$  is dominated by a single component,  $a_{\xi\xi\xi}^{(2)}$ , along the long molecular axis  $\hat{\xi}$ , the only nonvanishing elements are

$$\chi_{zzz}^{(2)} = N_s \langle \cos^3 \theta \rangle a_{\xi\xi\xi}^{(2)}, \quad (3)$$

$$\chi_{z\hat{x}\hat{x}}^{(2)} = \chi_{z\hat{y}\hat{y}}^{(2)} = (N_s/2) \langle \sin^2 \theta \cos \theta \rangle a_{\xi\xi\xi}^{(2)} \quad (i=x, y), \quad (4)$$

where  $\hat{x}$  and  $\hat{y}$  are in-plane unit vectors,  $\hat{z}$  is taken as the surface normal, and  $\theta$  denotes the tilt angle between the long molecular axis  $\hat{\xi}$  and  $\hat{z}$ . It has repeatedly been shown that from appropriate input-output polarization combinations, the average molecular tilt angle  $\theta$  can be determined, assuming some distribution of  $\theta$ .<sup>6-10</sup>

## III. EXPERIMENT

The experiments were performed using the 532-nm frequency-doubled output of a Nd:YAG laser (YAG denotes yttrium aluminum garnet) with a pulse duration of 30 ps and a pulse energy of 3 mJ. The unfocused beam was directed onto the sample at an angle of incidence of  $45^\circ$ . After appropriate spectral filtering of the specularly reflected beam, the SH output was detected using a photomultiplier and gated electronics. The SH wavelength (266 nm) is close to resonance for the 4-*n*-octyl-4'-cyanobiphenyl (8CB) molecules and therefore in all cases the SH background of the glass-silane substrates is negligible.

The silane layers were deposited onto chemically cleaned commercially available BK-7 glass prisms instead of glass plates in order to avoid interference of multiple reflections of the fundamental beam. The silanes we used were *N,N*-dimethyl-*N*-octadecylammoniumpropyltrimethoxysilane chloride (DMOAP), *N*-methyl-

aminopropyltrimethoxysilane (MAP), and octadecyltrichlorosilane (OTS). Trimethylsilyl diethylamine (TMSDEA) monolayers were used as a completely covered nonpolar reference.<sup>11</sup> DMOAP and MAP were used as received (Petrarch Systems). OTS and TMSDEA (Aldrich) were distilled before use. The liquid crystal which we used is 8CB, as obtained (British Drug Houses, Ltd.) without further purification.

The modification reactions were performed in three different ways. A first batch of substrates was modified with DMOAP and MAP, according to Kahn.<sup>12</sup> A second batch of substrates was modified in a refluxing 2% solution of the appropriate silane (MAP, DMOAP, or OTS) in toluene and in the case of DMOAP, methanol, with the exclusion of moisture under an atmosphere of argon. In this way, polymerization of the silanes in solution is minimized yielding a better-defined monolayer.<sup>13,14</sup> In order to obtain a higher density of the desired silane molecules (DMOAP and OTS), the reaction in batch 3 was catalyzed with a continuous flow of ammonia ( $\text{NH}_3$ ), which deprotonizes the glass surface.<sup>14,15</sup> It is known that afterwards no relevant fraction of  $\text{NH}_3$  is left at the surface.<sup>14,15</sup> The 8CB monolayers were deposited using an evaporation technique,<sup>2</sup> where SHG was used as an *in situ* deposition monitor.

#### IV. RESULTS AND DISCUSSION

In order to compare our results with those obtained by Mullin, Guyot-Sionnest, and Shen,<sup>2</sup> we first deposited 8CB onto clean glass and DMOAP- and MAP-coated glass substrates from the first batch (DMOAP-1, MAP-1). The variation in *p*-polarized SH intensity under *s* excitation ( $I_{ps}$ ) obtained during adsorption of 8CB on the different substrates is shown in Fig. 1. The average molecular tilt angle  $\theta = 67^\circ \pm 3^\circ$  was determined assuming a  $\delta$ -function distribution. The other input- and output-polarization combinations showed the same SH response during deposition, which indicates that the orientation is independent of 8CB packing density. In all respects, these results agree with those reported by Mullin, Guyot-Sionnest, and Shen.<sup>2</sup> For adsorption of 8CB on OTS, prepared according to Kahn<sup>12</sup> (OTS-1), we refer to the data of Mullin, Guyot-Sionnest, and Shen.<sup>2</sup> They found the same tilt angle  $\theta = 67^\circ$  and a reduction in SH intensity by more than an order of magnitude with respect to that of 8CB on clean glass.

The fact that no differences in  $\theta$  are found for 8CB adsorption on the different silanes and clean glass is surprising, since these surfactant-coated substrates yield different *bulk* LC alignments. DMOAP-1 and OTS-1 lead to homeotropic alignment (perpendicular to the surface), while MAP-1 and often clean glass induce planar alignment (parallel to the surface).<sup>1,12</sup> In addition, the SFG spectra of MAP and DMOAP behave differently upon adsorption of an 8CB monolayer.<sup>4</sup> We believe that the anomalies mentioned above can be understood from an incomplete shielding of the glass substrates for small molecules, such as 8CB, by the silanes. Indeed it is known that formation of a layer of a multifunctional silane, such as MAP, DMOAP, and OTS, according to the procedure of

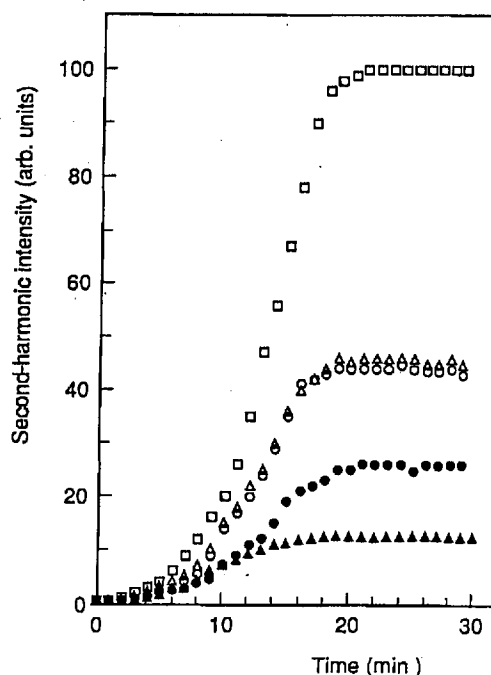


FIG. 1. Variation of the SH intensity ( $I_{ps}$ ) during adsorption of 8CB on different substrates, MAP-1 (○), DMOAP-1 (△), DMOAP-2 (●), DMOAP-3 (▲), and chemically cleaned glass (□).  $I_{ps}$  denotes the *p*-polarized SH intensity for *s*-polarized excitation.

Kahn,<sup>12</sup> leads to polymerization during deposition and gives rise to the formation of a nonuniform multilayer.<sup>13,16</sup> This means that, for instance, although no more DMOAP molecules can be attached to the surface, 8CB molecules can still penetrate the layer and a reasonably high packing density of 8CB molecules can be obtained.

To check whether the quality of the silane layers can be held responsible for the surprising results, we prepared the silane layers under various conditions. We will first discuss the results for OTS. It is known that formation of OTS-2 in batch 2 ensures polymerization of OTS only along the surface, thus yielding a better-defined monolayer.<sup>13,14</sup> Deposition of 8CB on OTS-2 reduced the tilt angle to  $\theta = 52^\circ \pm 3^\circ$ , while the SH intensity was reduced by a factor of 10 with respect to 8CB on clean glass. By catalyzing the chemisorption (OTS-3), the packing density of the OTS monolayer is improved.<sup>15,17</sup>  $\theta$  was further reduced to  $39^\circ \pm 3^\circ$ , and concomitantly the SH intensity was further decreased. In Fig. 2 the SH intensities of 8CB molecules adsorbed on differently covered OTS substrates for different input- and output-polarization combinations are shown. The decrease in overall SH intensity and the change in relative SH intensities ( $I_{ps}$ ,  $I_{sq}$ ,  $I_{pp}$ , and  $I_{pq}$ ) for 8CB adsorbed on differently prepared substrates is clear, indicating the sensitivity of SHG to changes in the preparation method of the silane layer. The significant change in  $\theta$  is not affected by introducing Gaussian distribution functions for the molecular orientation. Assuming, for instance, a standard deviation  $\sigma = 10^\circ$ , the peak positions only change from  $67^\circ$  to  $73^\circ$ , from  $52^\circ$  to  $54^\circ$ , and from  $39^\circ$  to  $37^\circ$ , respectively.

The results can be interpreted as follows. The SH signal is dominated by those molecules that are attached to

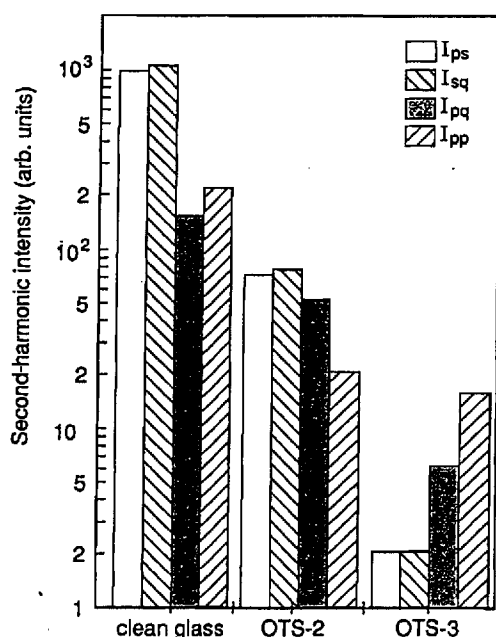


FIG. 2.  $p$ - and  $s$ -polarized SH intensities for different polarizations of the excitation beam for 8CB adsorbed on clean glass and two differently prepared OTS-covered substrates (OTS-2 and OTS-3).

polar glass sites and therefore have polar ordering. The remaining 8CB molecules presumably form electric quadrupolar pairs and contribute negligibly to the SH intensity.<sup>2</sup> The OTS-1 layer is known to be nonuniform. Therefore patches of unshielded glass are present and the polar-ordered 8CB molecules have enough freedom to align just as on clean glass. The OTS-2 layer has an improved uniformity. The polar-ordered 8CB molecules are now more closely surrounded by OTS molecules and their alignment is affected accordingly ( $\theta \approx 52^\circ$ ). On the OTS-3 surface, the distance between the OTS molecules is reduced. The influence on the alignment is therefore enhanced<sup>18</sup> ( $\theta \approx 39^\circ$ ). Concomitantly, the number of free glass sites for the 8CB molecules to attach to is reduced, which leads to a reduction of the SH intensity.

This interpretation is further supported by the results for DMOAP. The SH intensity ( $I_{ps}$ ) of 8CB on DMOAP-2 was reduced by a factor of 2 with respect to the first batch and no significant change in  $\theta$  was found. However, adsorption of 8CB on DMOAP layers, chemisorbed in the presence of  $NH_3$  (DMOAP-3), yielded a tilt angle  $\theta = 52^\circ \pm 3^\circ$  and a SH intensity ( $I_{ps}$ ) reduced

by a factor of 9 with respect to 8CB on clean glass (see Fig. 1).

The fact that the DMOAP-2 surface did not influence the alignment is not surprising, since the DMOAP head group covers more space than the OTS group and therefore the distance between the alkyl chains is greater. Since DMOAP-3 did, in fact, influence  $\theta$ , we conclude that the DMOAP packing density must have been improved. In order to test the DMOAP layers, cells have been produced from these substrates. They showed regular homeotropic alignment of the bulk LC.

Adsorption of 8CB on MAP-2 and DMOAP-2, which differ only in the presence of an alkyl chain, yielded the same results, supporting the idea that the alkyl chains of DMOAP-2 do not yet play a role in the alignment of the first polar-ordered LC monolayer. Catalyzing the chemisorption of MAP with  $NH_3$  is not possible.

Finally, adsorption experiments carried out on trimethylsilyl-covered glass substrates, which were used as a completely covered nonpolar reference,<sup>11</sup> yielded very weak SH signals. Here, the 8CB molecules are unable to find polar sites. Also for glass substrates, which were not chemically cleaned, we found that the polar character of the surface is greatly reduced. This indicates that the SH intensity can be used as a gauge of the surface density of polar sites at a surface. Adsorption of 5CB, 6CB, and 7CB (predecessors of 8CB in the homologous series) on clean glass yielded virtually the same results as for 8CB.

## V. CONCLUSIONS

We were able to prepare various surfactant layers of OTS and DMOAP, which yielded a measurable change in the molecular orientation of the first LC monolayer as measured by SHG. A change in  $\theta$  up to approximately  $30^\circ$  towards the bulk alignment could be induced, depending on the amount and structure of the silane. It is concluded that the SHG data yield information only on LC molecules attached to polar glass sites. Such molecules may constitute only a (minor) fraction of the first LC monolayer.

## ACKNOWLEDGMENTS

We would like to thank I. G. J. Camps for carefully preparing the silane layers and Dr. A. H. Bergman, Dr. A. H. M. Sondag, and Dr. Q. H. F. Vrehen for valuable discussions.

<sup>1</sup>See, for example, J. Cognard, *Alignment of Nematic Liquid Crystals and Their Mixtures* (Gordon and Breach, London, 1982).

<sup>2</sup>C. S. Mullin, P. Guyot-Sionnest, and Y. R. Shen, *Phys. Rev. A* **39**, 3745 (1989).

<sup>3</sup>W. Chen, M. B. Feller, and Y. R. Shen, *Phys. Rev. Lett.* **63**, 2665 (1989).

<sup>4</sup>J. Y. Huang, R. Superfine, and Y. R. Shen, *Phys. Rev. A* **42**,

3660 (1990).

<sup>5</sup>V. Mizrahi and J. E. Sipe, *J. Opt. Soc. Am. B* **5**, 660 (1988).

<sup>6</sup>Y. R. Shen, *Chemistry at Surfaces and Interfaces*, edited by R. B. Hall and A. B. Ellis (VCH, Deerfield Beach, FL, 1986).

<sup>7</sup>T. F. Heinz, C. K. Chen, D. Richard, and Y. R. Shen, *Phys. Rev. Lett.* **48**, 478 (1982).

<sup>8</sup>Y. R. Shen, *J. Vac. Sci. Technol. B* **3**, 1664 (1985).

<sup>9</sup>G. Berkovic, Th. Rasing, and Y. R. Shen, *J. Opt. Soc. Am. B* **4**,



- 945 (1987).
- <sup>10</sup>R. W. J. Hollering and W. J. O. V. Teesselink, *Opt. Commun.* **79**, 224 (1990).
- <sup>11</sup>J. J. Ponjée, V. B. Marriott, M. C. B. A. Michielsen, F. J. Touwslager, P. N. T. van Velzen, and H. van der Wel, *J. Vac. Sci. Technol. B* **8**, 463 (1990).
- <sup>12</sup>F. J. Kahn, *Appl. Phys. Lett.* **22**, 386 (1973).
- <sup>13</sup>E. P. Plueddemann, *Silane Coupling Agents* (Plenum, New York, 1982).
- <sup>14</sup>F. Deyhimi and J. A. Coles, *Helv. Chim. Acta* **65**, 1752 (1982).
- <sup>15</sup>F. P. Blitz, R. S. Shreedhara Murthy, and D. E. Leyden, *J. Colloid Interface Sci.* **126**, 387 (1988).
- <sup>16</sup>V. M. J. Vankan, J. J. Ponjée, J. W. de Haan, and L. J. M. van de Ven, *J. Colloid Interface Sci.* **126**, 604 (1988).
- <sup>17</sup>J. N. Kinkel and K. K. Unger, *J. Chromatogr.* **316**, 193 (1984).
- <sup>18</sup>K. Hiltrop and H. Stegemeyer, *Ber. Bunsenges. Phys. Chem.* **85**, 582 (1981).

# Tab 4

# Applied Physics B Lasers and Optics

Editor-in-Chief: F. Träger  
 Board of Editors: S.N. Baggey, H. Coural, W. Dämmeler, T. W. Hansen, G. Huber, J. Keller, E. Kratzig, G. Marowsky, G. A. Mourou, Y.R. Shan, T. Shimizu, E. K. Ueda, K. J. Wilbur, J. Wolfrum  
 Founding Editor: H.K.W. Loetsch

Volume B 62 Number 6 June 1996

**M. Falconieri, A. Lanzi, G. Salvetti**

Spectroscopic investigation of the visible and mid-infrared emission in Tm- and Ho-doped YAG and YLF crystals 537

**C. Mavroyannis**

Stimulated emission of a laser photon by the excited states of a three-level atom 547

**G. Stareev, A. Balter, S. Gawrilow, D. Sowada**

Laser-excited fluorescence of perylene by using self-induced second-harmonic and sum-frequency radiation emanating from high-power AlGaAs double hetero-type diodes 557

**A. Seas, C. Christofides**

Photopyroelectric spectroscopy in the presence of an air gap transparent phase-shifter 563

**H.S. Dhadwal, K. Suh, D.A. Ross**

A direct method of particle sizing based on the statistical processing of scattered photons from particles executing Brownian motion 575

**R. Kienle, M.P. Lee, K. Kohse-Höinghaus**

A detailed rate equation model for the simulation of energy transfer in OH laser-induced fluorescence 583

**F. Bormann, T. Nielsen, M. Burrows, P. Andresen**

Single-pulse collision-insensitive picosecond planar laser-induced fluorescence of OH  $A^2 \Sigma^+$  ( $v'=2$ ) in atmospheric-pressure flames 601

**J. Förster, M. von Hoesslin, J. Uhlenbusch**

Temperature measurements in CO<sub>2</sub>-laser-induced pyrolysis flames for SiC and ternary SiC/C/B powder synthesis by means of CARS 609

**H.-M. Wu, J.-H. Tang, Q. Luo, Z.-M. Sun, Y.-M. Zhu, Z.-H. Lu, Y. Wei**

Liquid-crystal alignment of rubbed polyimide films: A microscopic investigation 613

**L. Kong, S. Chunyu, S. He, Y. You, Q. Zhang, Y. Cai, S. Yang, W. Huang, Y. Gu, A. He, X. Yang, X. Li, Y. Wang, X. Cheng, W. Xie**

Cu-like Pd and Ag inner-shell photoionization phenomena 619

*Contents of Volume 62 B and A*

Forthcoming papers A5

*Contents of Applied Physics A*

Volume 62, Number 6, June 1996 A5

*Indexed in Current Contents*

Evaluated and abstracted for *PHYS on STN*

APBOEM 62 B (6) 537-622 (1996)

Printed on acid-free paper

Published monthly - June 1996



0928-2171(199606)62:6:1-B

# Applied Physics B Lasers and Optics

Founded by H.K.V. Lotsch

In Cooperation with the German Physical Society (DPG)

## Editorial Policy

**Applied Physics** is a monthly journal for the rapid publication of experimental and theoretical investigations in applied research and is issued in two parts. **Appl. Phys. A**, with the subtitle "Materials Science & Processing" mainly covers the condensed state, including surface science and engineering. **Appl. Phys. B**, subtitled "Lasers and Optics", mainly covers the gaseous state, including the applications of laser radiation in chemistry and biochemistry. Further details can be inferred from the appropriate listings of PACS numbers [American Institute of Physics, AIP PUB. R-261.12 (1994)].

For speedy publication this journal appears monthly in single issues of varying size, according to the material received. Six issues usually constitute one volume, and two volumes are normally published per year.

Once a manuscript is accepted, it will be published quickly and *free of page charges* up to a prescribed maximum length: 4 printed pages for rapid communications, 8 printed pages for contributed papers, and 15 printed pages for invited papers; authors of papers that exceed these limits will be charged DM 150 per excess printed page.

A signed Copyright Transfer Agreement must accompany each manuscript submitted (see **Appl. Phys. B** 58, No. 1 for further details; see also section "Copyright" on this page).

## Copyright

Submission of a manuscript implies: that the work described has not been published before (except in the form of an abstract or as part of a published lecture, review, or thesis); that it is not under consideration for publication elsewhere; that its publication has been approved by all coauthors, if any, as well as by the responsible authorities at the institute where the work has been carried out; that, if and when the manuscript is accepted for publication, the authors agree to automatic transfer of the copyright to the publisher; and that the manuscript will not be published elsewhere in any language without the consent of the copyright holders.

All articles published in this journal are protected by copyright, which covers the exclusive rights to reproduce and distribute the article (e.g., as offprints), as well as all translation rights. No material published in this journal may be reproduced photographically or stored on microfilm, in electronic data bases, video disks, etc., without first obtaining written permission from the publisher.

The use of general descriptive names, trade names, trademarks, etc., in this publication, even if not specifically identified, does not imply that these names are not protected by the relevant laws and regulations.

*While the advice and information in this journal is believed to be true and accurate at the date of its going to press, neither the authors, the editors, nor the publisher can accept any legal responsibility for any errors or omissions that may be made. The publisher makes no warranty, express or implied, with respect to the material contained herein.*

**Special regulations for photocopies in the USA:** Photocopies may be made for personal or inhouse use beyond the limitations stipulated under Section 107 or 108 of U.S. Copyright Law, provided a fee is paid. All fees should be paid to the Copyright Clearance Center, Inc., 21 Congress Street, Salem, MA 01970, USA, stating the ISSN 0946-2171, the volume, and the first and last page numbers of each article copied. The Copyright owner's consent does not include copying for general distribution, promotion, new works, or resale. In these cases, specific written permission must first be obtained from the publisher.

The Canada Institute for Scientific and Technical Information (CISTI) provides a comprehensive, world-wide document delivery service for all Springer-Verlag journals. For more information, or to place an order for a copyright-cleared Springer-Verlag document, please contact Client Assistant Document Delivery, Canada Institute for Scientific and Technical Information, Ottawa, Canada K1A 0S2 (Tel: +1-613/993-9251; Fax: +1-513/952-8243; e-mail: cisti.docdel@nrc.ca).

## Subscription information

ISSN 0946-2171

Volumes 62 and 63 (6 issues each) will appear in 1996.

**North America:** Recommended annual subscription rate: approx. US \$ 1,729.00 (single issue price approx. US \$ 170.00) including carriage charges. Subscriptions are entered with prepayment only. Orders should be addressed to:

Springer-Verlag New York Inc.  
Journal Fulfillment Services Department  
333 Meadowlands Parkway  
Secaucus, NJ 07094, USA  
Tel.: +1-201/348-4033, Fax: +1-201/348-4505

**All other countries:** Recommended annual subscription rate: DM 2,300.00, plus carriage charges; [Federal Republic of Germany: DM 32.40 incl. value added tax; all other countries: DM 52.20, except for the following countries to which SAL delivery (Surface Airmail Lifted) is mandatory: Japan, India, Australia/New Zealand. SAL charges and airmail delivery to all other countries are available upon request]. Volume price: DM 1,150.00, single issue price: DM 230.00, plus carriage charges. Subscriptions can either be placed via a bookdealer or sent directly to: Karin Tiks, Springer-Verlag, Postfach 311340, D-10643 Berlin, Germany  
Tel.: +49-30/8207-358, Fax: +49-30/8207-448

A reduced rate of DM 3,998.00 plus carriage charges (or for USA approx. US \$ 3,021.00 including carriage charges) applies if both Journals A and B are ordered simultaneously. For carriage charges see above.

**Cancellations** must be received by September 30 to take effect at the end of the same year.

**Changes of address:** Allow six weeks for all changes to become effective. All communications should include both old and new addresses (with Postal Codes) and should be accompanied by a mailing label from a recent issue.

According to §4 Sect. 3 of the German Postal Services Data Protection Regulations, the German Federal Post Office can inform the publisher of a subscriber's new address even if the subscriber has not submitted a formal application for mail to be forwarded. Subscribers not in agreement with this procedure may send a written complaint to Springer-Verlag's Berlin office within 14 days of publication of this issue.

**Back volumes:** Prices are available on request.

**Microform editions** are available from: University Microfilms International  
300 N. Zeeb Road, Ann Arbor, MI 48106, USA

## Production

Springer-Verlag, Margret Grasshoff  
Journal Production Department II  
Postfach 105280  
D-69042 Heidelberg, Germany  
*Address for courier, express and registered mail:*  
Tiergartenstrasse 17  
D-69121 Heidelberg, Germany  
Tel.: +49-6221/487-327, Fax: +49-6221/487-188

## Responsible for advertisements

Springer-Verlag, E. Lückermann  
Heidelberger Platz 3  
D-14197 Berlin, Germany  
Tel. (0) 30/8207-0, Fax (0) 30/8207300

## Printers

Universitätsdruckerei H. Stürtz AG, Würzburg  
© Springer-Verlag Berlin Heidelberg 1996  
Springer-Verlag GmbH & Co. KG  
D-14197 Berlin, Germany  
Printed in Germany



Springer

# Liquid-crystal alignment of rubbed polyimide films: A microscopic investigation

H.-M. Wu<sup>1,3,\*</sup>, J.-H. Tang<sup>4</sup>, Q. Luo<sup>2,3</sup>, Z.-M. Sun<sup>2,3</sup>, Y.-M. Zhu<sup>1,3</sup>, Z.-H. Lu<sup>1,3</sup>, Y. Wei<sup>1,3</sup>

<sup>1</sup> National Laboratory of Molecular and Biomolecular Electronics, Southeast University, Nanjing 210096, People's Republic of China (Fax: + 86-25/771-2719)

<sup>2</sup> State Key Laboratory of Solid State Microstructures, Nanjing University, Nanjing 210093, People's Republic of China

<sup>3</sup> Center for Advanced Studies in Science and Technology of Microstructures, Nanjing 210093, People's Republic of China

<sup>4</sup> Nanjing Electronic Devices Institute, Nanjing 210016, People's Republic of China

Received: 15 May 1995/Accepted: 8 November 1995

**Abstract.** Rubbed polyimide films were investigated by Atomic Force Microscopy (AFM). On a large scale, microgrooves due to rubbing treatment were observed, whilst on a small scale, polyimide chain molecules were found to be non-uniformly oriented. Liquid-crystal monolayers were adopted in this study as visualizing media for AFM observation.

PACS: 61.30; 61.16; 68.35

To shed light on the mechanism by which such a polymer alignment method works, it is desirable to directly observe the rubbed polymer film on a small scale. In this paper, rubbed polyimide films, which were coated and uncoated with LC monolayers, were investigated by the newly invented Atomic Force Microscopy (AFM). AFM should represent an ideal tool for surface characterization due to its high resolution and the simplicity for sample preparation [12].

It has been established empirically that homogeneous alignment of liquid-crystal (LC) mesophases (average molecular orientation parallel to the surface along some easy axis) can be induced by the rubbing of polymer-coated substrates between which the LC layer is sandwiched [1]. However, the rubbing process and the related physical mechanism responsible for the LC alignment is not yet fully understood. One possible alignment mechanism is that alignment acts through the elastic interactions between the rubbing-induced microgrooves and the LC molecules [2], which is applicable in some cases [3]. According to Berreman's calculation [2], it is preferable in energy for all the molecules to lie along the grooves, creating a uniformly aligned cell along the rubbing direction. But Geary et al. [4] have found that such a mechanism is unsuitable for some reasons. On the other hand, Castellano [5] adopted an alternative concept that LC alignment is induced by the orientation of the polymer chains with the hypothesis that rubbing of the films orients the polymer chains along a preferred direction through localized melting. Recently, a variety of techniques have been employed to investigate the rubbed polymer films [4, 6–8] and the orientational distribution of LC molecules on polymer films [9–11]. However, the mechanisms proposed above are still lacking direct experimental verification of the microscopic pictures they purport.

## 1 Materials and experimental details

Polyimide PI-1 was purchased from Shanghai Jiaotong University and used without further purification. Freshly cleaned glass plates were first treated with a silane coupling agent, after which a thin polymer layer was applied by spin coating (3000 rev/min) followed by a thermal baking step to evaporate the solvent remainder (30 min at 80° and 60 min at 180°). All drying were carried out in a fan circulated box oven with nitrogen purging. The resulting layer thickness was about 200 Å. Polymer-coated substrates were unidirectionally rubbed using a cylinder 620 mm in diameter. The height of the revolving cylinder is adjusted until it just moves the substrate; this is defined as the zero position. The height of the drum is then lowered down a distance  $L_d = 0.75$  mm. During the rubbing process, the cylinder was spinning at 560 rev/min and the glass substrate was passed beneath it by means of a moving table at a velocity of 15 mm/min. It is the standard rubbing process used by the LC display industry [3].

A liquid-crystal cell was assembled using two substrates prepared above with their rubbing directions antiparallel. The distance of the cell was controlled by glass fibers with a nominated diameter of 20 µm. The liquid-crystal, 8CB, was introduced into the cell by the capillary action. To minimize the effects of flow alignment, the cell and the 8CB were heated up to the clearing point of 8CB when filling. Then the cell was slowly cooled down to the nematic and smectic phase of 8CB for observation.

For monolayer deposition, 8CB was dissolved in chloroform to a concentration of  $1.0 \times 10^{-3}$  M. The solu-

\* To whom all correspondence should be addressed

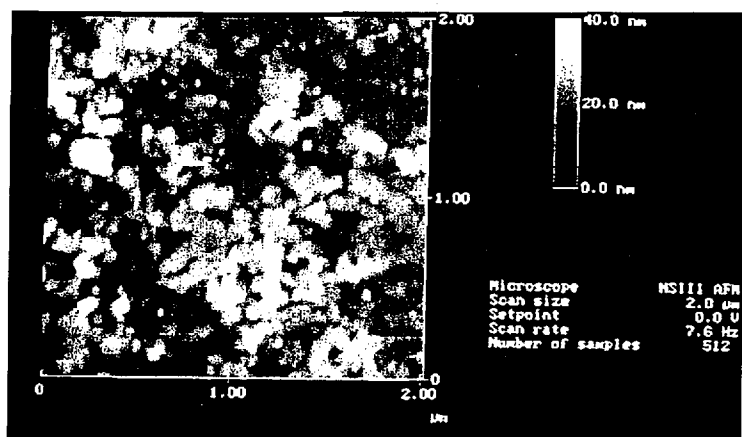


Fig. 1. AFM image of the unrubbed polyimide film

tion was then spread onto a double-distilled water surface on a Langmuir trough to form a monolayer. The temperature of the subphase was held at 18°C with a precision of 0.5°C. Each monolayer was compressed at a constant velocity of 15 Å<sup>2</sup>/min/molecule to the expected pressure and held automatically during monolayer film preparation. The surface pressure was measured by a Wilhelmy balance with an accuracy better than 0.1 mN/m. To deposit 8CB monolayer films, the surface pressure was kept at 3.5 mN/m and the dipping speed was 1 mm/min.

The 8CB covered- and uncovered-samples were examined with a commercially available AFM (Nanoscope III, Digital Instruments, Santa Barbara, CA) under ambient conditions. AFM operated in the contact mode with a loading of about 10 nN. We used microfabricated pyramidal shaped Si<sub>3</sub>N<sub>4</sub>-tips integrated into a rectangular cantilever with a typical force constant of 0.12 N/m.

## 2 Results and discussion

### 2.1 Polarizing microscope observation of LC cells

To determine the alignment capability of rubbed polyimide films, the LC cell was observed under a polarizing microscope (with crossed polarizers). The incident light was normal to the polymer-coated glass plates, and the cell could be rotated around the direction of the incident light. Under this microscope, the 8CB texture in the cell is uniform. The intensity of the transmission light in the cell changes periodically with a period of 90° when the cell is rotated. When the rubbing direction is oriented at 0° with respect to the analyzer, the transmission reaches the minimum value. While when the rubbing direction is oriented at 45°, the transmission increases to its maximum value. This indicated that 8CB molecules are homogeneously aligned along the rubbing direction on the surface of rubbed polyimide films.

### 2.2 AFM characterization of rubbed polyimide films

For comparison, we first image a pristine surface. The result is given in Fig. 1. The scan size is 2.0 μm × 2.0 μm.

Aggregations of polyimide domains are visible in this figure. The mean roughness of this unrubbed polyimide film is about 7.5 nm.

Fig. 2a shows the typical morphology of rubbed polyimide film. The rubbing direction is shown by the arrow in this figure. Several microgrooves due to rubbing treatment could be observed, which are similar to those observed by scanning electronic microscopy [3]. These microgrooves should play some role in LC alignment, though it has been realized that rubbing-induced microgrooves are not dominant in either LC bulk or LC monolayer alignment.

A closer look at the rubbed polyimide surface (Fig. 2b) reveals clearly the effect of rubbing on polymer layers. In contrast to Fig. 1, the surface of rubbed polyimide film is much more smooth, with a mean roughness of only about 2.5 nm. Furthermore, the boundary of polyimide domains on the rubbed surface is more blurring than that of their precursors, leaving the vestiges of rubbing. According to aforementioned rubbing process, the total length of rubbing cloth that passes a unit length of the polyimide-coated substrate, denoted by  $L_u$ , is

$$L_u = [2\pi(r + l - L_d)\omega + v]L_d/v \quad (1)$$

where  $L_d$  is the distance of the drum lowered from the zero position,  $\omega$  and  $r$  are the rotation speed and the radius of the cylinder,  $v$  is the rate of moving table and  $l$  is the pile length of rubbing cloth. In this experiment, because

$$r \gg l - L_d \quad (2)$$

(1) can be rewritten as

$$L_u = (2\pi r\omega + v)L_d/v. \quad (3)$$

Thus  $L_d$  can be used as a direct measure of rubbing strength as long as other parameters in (3) are kept constant. Figure 2c and d show the AFM image of rubbed polyimide films with  $L_d = 0.25$  mm and  $L_d = 1.00$  mm accordingly. In comparison with Fig. 2b, one can see clearly the difference in surface structures when changing the rubbing strength. The calculated mean roughness of Fig. 2c and d are on the order of 5.0 and 1.5 nm, respectively. Summarizing the results presented above, the rubbing cannot only produce microgrooves on polyimide film surface, but also force a top layer of polyimide molecules

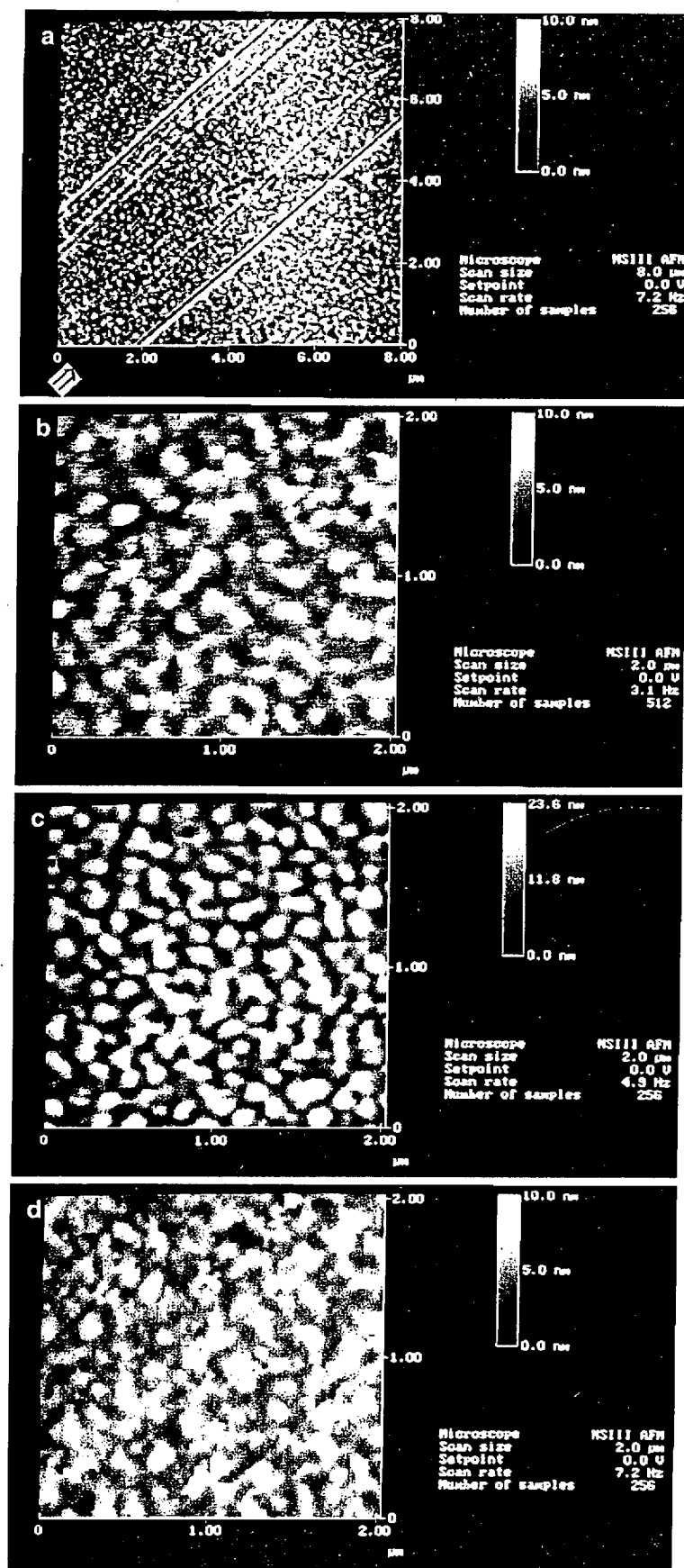


Fig. 2a-d. AFM images of rubbed polyimide films (a)  $L_d = 0.75$  mm (b)  $L_d = 0.75$  mm (c)  $L_d = 0.25$  mm (d)  $L_d = 1.00$  mm. The rubbing direction is indicated by the arrow ( $\Rightarrow$ ) in this figure

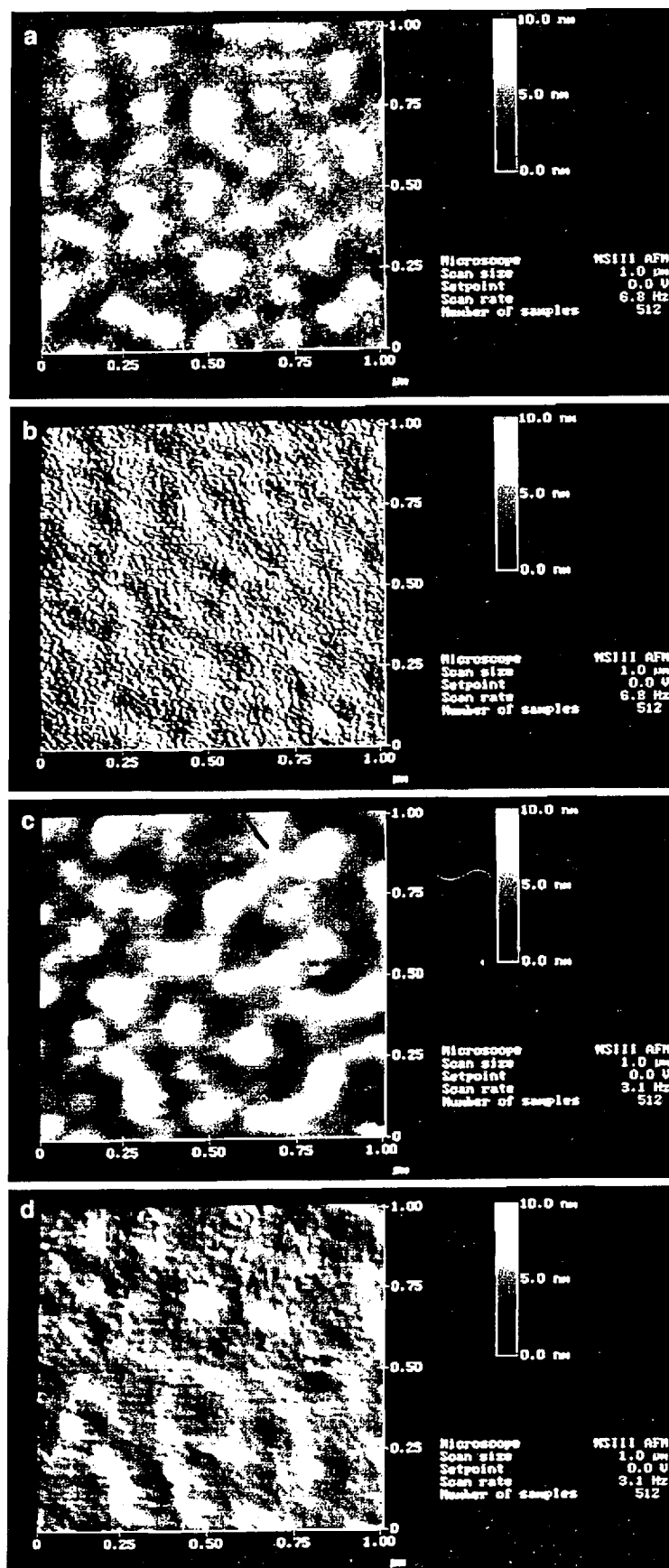


Fig. 3a-d. AFM image of 8CB monolayer-coated rubbed polyimide film (a) and its high-pass transform (b); rubbed polyimide films ( $L_d = 0.75$  mm) (c) and its high-pass transform (d)



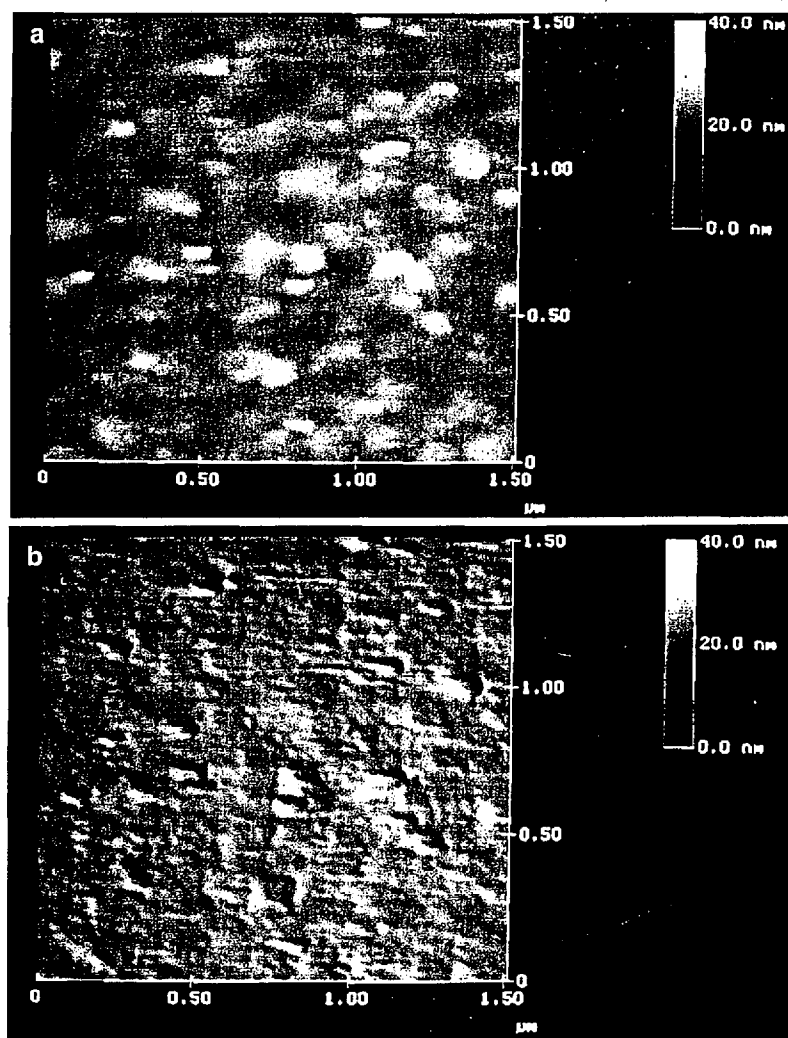


Fig. 4a, b. AFM image of 8CB monolayer-coated polyimide LB film deposited on rubbed polyimide film (a) and its high-pass transform (b)

to move on the surface resulting in a more smooth surface. These processes will cause the permanent shear deformation of polymer chains [4]. The rubbing strength can be simply changed by the alteration of  $L_d$ .

For the sake of imaging the detail structure of polyimide chain molecules, we still imaged the rubbed films to a nanometer scale so as to check the detailed structure of polyimide chains. However, no meaningful images of chain molecules could be obtained, though our AFM machine has the ability to achieve a molecular resolution when imaging polyimide molecules in polyimide LB films [13]. It has been well established that chain molecules under rubbing could be oriented in the rubbing direction when subjected to the shear force of rubbing [4]. This phenomenon has already been demonstrated by several techniques such as optical-phase retardation [4, 6, 7] and X-ray-scattering measurements [8]. We were unable to observe a single polyimide chain in the rubbed cast film in the mentioned condition, probably because the polyimide chains were not uniformly oriented in the rubbing direction on a small scale. According to Weihs' models [14], it seems unable for our AFM to determine a single polyimide chain in a non-periodic arrangement. However, Weihs'

model [14] does not eliminate the possibility of images with apparent atomic or molecular scale periodicity (This is the case for polyimide LB films [13]) due to moire or multiple imaging [15]. For a better understanding of the surface structure of rubbed samples on a microscopic scale, we carried out the following experiments.

### 2.3 AFM characterization of 8CB-monolayer-coated rubbed polyimide films

It has been known for many years that if a liquid crystal is spread on top of an anisotropic polymer substrate, the energy of the LC molecules at the LC-polymer substrate will depend on orientation, thus inducing preferential alignment of the LC director. So the structure of aligned LC layers may provide some information of the underlying polymer alignment layers. In order to obtain more detailed information about the surface structures within polyimide orienting layers, we deposited LC molecules of 8CB onto rubbed films as a visualizing media for AFM studies. Only one monolayer was deposited so as to rule out the bulk effect. Figure 3a shows the result. For

comparison, the AFM image of the uncoated sample is also shown in Fig. 3c. It is clear that the surface of 8CB-monolayer-covered rubbed polyimide film looks much rougher. This feature is much more distinctive after a high-pass transform of the originally obtained AFM image (see Fig. 3b and d, respectively). It is certain that these rough structures were formed by LC molecules and LC molecules were not uniformly aligned on the rubbed surface on a microscopic scale. We conjecture that this phenomenon was correlated with the local non-uniform orientation of chain molecules within polymer alignment layers and thus the previously measured in-plane anisotropy [4, 6–8] in rubbed polyimide films is only an average effect on a relatively macroscopic scale. This conclusion was further supported by the following experiments. Rubbed polyimide film was first covered with two monolayers of polyimide LB films and then a monolayer of 8CB molecules. Figure 4a shows the AFM observation results. Its high-pass transform is shown in Fig. 4b. No visible difference in surface structure could be observed before and after the coverage of 8CB monolayer. The surface in Fig. 4a is much more smooth than that in Fig. 3a and no similar rough microstructures are visible. This observation result is in agreement with our previous STM studies on 8CB-coated polyimide LB films, in which perfect local and global ordering of chain molecules was observed [13, 16] and all 8CB molecules were uniformly aligned along the dipping direction [16].

In conclusion, through atomic force microscopy investigations, we found that rubbing cannot only produce microgrooves on polymer surfaces, but also induce a macroscopic orientation of polyimide chains in

the rubbing direction. However, on a small scale, the chain molecules were not uniformly oriented, resulting a local non-uniform alignment of LC monolayers.

*Acknowledgement.* This work was supported by the National Natural Science Foundation of China.

## References

1. J. Cognard: *Mol. Cryst. Liq. Cryst. Suppl.* **1**, 1 (1982)
2. D.W. Berreman: *Phys. Rev. Lett.* **28**, 1683 (1972)
3. A. Mosley, B.M. Nicholas, P.A. Gass: *Displays* **8**, 17 (1987)
4. J.M. Geary, J.W. Googby, A.R. Kmertz, J.S. Patel: *J. Appl. Phys.* **62**, 4100 (1987)
5. J.A. Castellano: *Mol. Cryst. Liq. Cryst.* **94**, 33 (1983)
6. S. Kuniyasu, H. Fukuro, S. Maeda, K. Nakaya, M. Nitta, N. Ozaki, S. Kobayashi: *Jpn. J. Appl. Phys.* **27**, 827 (1988)
7. N.A.J.M. van Aerle, M. Barmentlo, R.W.J. Hollering: *J. Appl. Phys.* **74**, 3111 (1993)
8. M.F. Toney, T.P. Russell, J.A. Logan, H. Kikuchi, J.M. Sands, S.K. Kumar: *Nature* **374**, 709 (1995)
9. M. Barmentlo, R.W.J. Hollering, N.A.J.M. van Aerle: *Phys. Rev. A* **46**, R4490 (1992)
10. W. Chen, M.B. Feller, Y.R. Shen: *Phys. Rev. Lett.* **63**, 2665 (1989)
11. M.B. Feller, W. Chen, Y.R. Shen: *Phys. Rev. A* **43**, 6778 (1991)
12. H.M. Wu, S.J. Xiao, Z.H. Tai, Y. Wei: *Phys. Lett. A* **199**, 119 (1995)
13. X.M. Yang, N. Gu, Z.H. Lu, Y. Wei: *Phys. Lett. A* **183**, 111 (1993)
14. T.P. Weihs, Z. Nawaz, S.P. Jarvis, J.B. Pethica: *Appl. Phys. Lett.* **59**, 3536 (1991)
15. J.D. Todd, J.B. Pethica: *J. Phys. Condens. Matter* **1** 9823 (1989)
16. J.Y. Fang, Z.H. Lu, G.M. Min, Y. Wei: *Liq. Cryst.* **14**, 1621 (1993)

# Tab 5

QD

923

.C58

1982

MLCA5 1 1-78(1982)

ISSN 0026-8941

# MOLECULAR CRYSTALS AND LIQUID CRYSTALS

## SUPPLEMENT SERIES

SUPPLEMENT 1

### ALIGNMENT OF NEMATIC LIQUID CRYSTALS AND THEIR MIXTURES

Jacques Cognard

ISBN 0 677 05905-1

G+B

GORDON AND BREACH SCIENCE PUBLISHERS · LONDON · NEW YORK · PARIS

MOLECULAR CRYSTALS AND LIQUID CRYSTALS  
SUPPLEMENT SERIES

A series of monographs and other special publications.

**SUPPLEMENT 1**

Alignment of Nematic Liquid Crystals  
and Their Mixtures by **Jacques Cognard**

Additional volumes in preparation.

MOLECULAR CRYSTALS AND LIQUID CRYSTALS  
SUPPLEMENT SERIES



3 1858 025 411 277  
phys Alignment of nematic liquid crystals  
s and their mixtures /Cognard, Jacques.  
QD 923 .C58 1982 /\*c.1

## SUPPLEMENT 1

# Alignment of Nematic Liquid Crystals and Their Mixtures

by

JACQUES COGNARD

*Chemistry Group, ASULAB S.A., Neuchâtel, Switzerland*

GORDON AND BREACH SCIENCE PUBLISHERS

London • New York • Paris

*Copyright © 1982 by Gordon and Breach, Science Publishers, Inc.*

Gordon and Breach, Science Publishers, Inc.  
One Park Avenue  
New York, NY 10016

Gordon and Breach Science Publishers Ltd.  
42 William IV Street  
London WC2N 4DE

Gordon & Breach  
58, rue Lhomond  
Paris 75005

ISSN: 0026-8941. ISBN 0 677 059 05-1. All rights reserved. No part of this book may be reproduced or utilized in any form or by any means, electronic or mechanical, including photocopying, recording, or by any information storage or retrieval system, without permission in writing from the publishers. Printed in the United States of America.

00  
2  
257  
101

## Preface

Research in the field of Molecular and Liquid Crystals has reached a certain degree of maturity. It was considered timely, therefore, to inaugurate a supplement series to the journal of *Molecular Crystals and Liquid Crystals*. The aim of this series is to provide in-depth reviews, in the form of monographs, of specific topics within this wide and rapidly growing field. As a result of expansion and diversification, regular research articles must be highly specialized. It is important, therefore, to provide the mechanism whereby researchers, students and practitioners can readily obtain a balanced view of the important results in various areas of the overall field. This is the aim of this new supplement series.

G. J. Dienes  
Managing Editor

The University of Iowa  
LIBRARIES



# Alignment of Nematic Liquid Crystals and Their Mixtures

JACQUES COGNARD

*Chemistry Group, ASULAB S.A., Neuchâtel, Switzerland*

## INTRODUCTION

### I A CRITICAL REVIEW OF THE LITERATURE

- I.1 The alignment of liquid crystals on smooth surfaces
  - I.1.1 Inorganic substrates
  - I.1.2 Organic polymers
- I.2 Alignment on grooved surfaces
- I.3 Alignment by surface active agents
- I.4 Alignment by silane treated surfaces
- I.5 Tilted alignment

### II ALIGNMENT MECHANISMS OF NEMATIC LIQUID CRYSTALS AND THEIR MIXTURES

- II.1 Physicochemical interactions
  - II.1.1 The Friedel-Creagh-Kmetz rule
  - II.1.2 Surface tension
    - II.1.2.1 Liquid crystal surface tension
    - II.1.2.2 Anisotropy of the surface tension of a LC
    - II.1.2.3 The surface tension of solids
  - II.1.3 Solid liquid crystal contact angle
    - II.1.3.1 The contact angle
    - II.1.3.2 The contact of a LC with a solid
  - II.1.4 The critical surface tension of a solid
  - II.1.5 The polar and dispersive components of surface tension
    - II.1.5.1 Polar interactions of LCs and surfaces
    - II.1.5.2 Dispersive interactions of LCs and polymers
  - II.1.6 The smecticlike interfacial layer
  - II.1.7 Nonuniform coverage
  - II.1.8 Alignment by surfactants

- II.1.9 Surface hydrolysis
- II.1.10 Measurement of LC surface tension
- II.1.11 Summary
- II.2 Elastic orientation on grooved surfaces
  - II.2.1 Geometrical factors
  - II.2.2 Mixed alignment
- II.3 Anchoring energies
  - II.3.1 Anchoring and the interfacial layer
  - II.3.2 In-plane anchorage energy
  - II.3.3 Azimuthal anchorage
- II.4 Conclusions

### III RECOMMENDED PROCEDURES

- III.1 Cleaning
- III.2 Parallel alignment
  - III.2.1 Rubbed PVA
  - III.2.2 Rubbed polyimide
  - III.2.3 Evaporated  $\text{SiO}_x$
- III.3 Homeotropic alignment
  - III.3.1 Lecithin (DMOAP)
  - III.3.2 DMCS
- III.4 Tilted alignment
  - III.4.1 Tangentially evaporated  $\text{SiO}_x$
  - III.4.2 Crossed evaporation
  - III.4.3 "Tilted homeotropic" alignment

### ACKNOWLEDGMENT

### REFERENCES

### INDEX

## INTRODUCTION

The most recent reviews concerning the alignment of liquid crystals (LC) appeared five years ago.<sup>1-3</sup> Since then studies of LC alignment have proceeded actively: the tangential evaporation of oxides and fluorides has found wide industrial acceptance; aligning properties of layers deposited in various ways have been well documented and studies of LC surface interactions are numer-

ous. Many methods of aligning LCs have been described but attempts to utilize or even reproduce published results are often discouraging.

It is the purpose of this paper to review the various methods described, to extend them to other commercial LC mixtures and point out the most reliable ones, as found through our own experience in developing displays for electronic watches.

We have sought to be comprehensive up to December 1979 and cite any English, French or German references available to us through computer search, abstracts bibliography and cross referencing. It was thus impossible to cover all studies and we considered only the most practical methods of LC alignment compatible with practical requirements. We insist on those processes that give reproducible results.

An evaluation of an alignment process has to consider its reproducibility, applicability to various LCs, lifetime and compatibility with the associated

#### LC Code

##### (1) LC commercial mixtures

( from our chromatographic analysis )

Code	Composition	T <sub>NI</sub> °C	Source
Zli 1132	0.15 BCH-5 ; 0.24 PCH-3 ; 0.36 PCH-5 0.25 PCH-7	70	Merck
E 3	0.55 K15 ; 0.14 M 15 ; 0.13 M 21 ; 0.18 M 24	54.3	BDH
E 7	0.51 K15 ; 0.25 K 21 ; 0.16 M 24 ; 0.08 T 15	59.8	BDH
E 8	0.45 K15 ; 0.16 M9 ; 0.12 M15 ; 0.16 M 24 0.11 T 15	70.5	BDH
ROTN 103	0.05 PEPN 4 ; 0.24 PEPN5 ; 0.13 PEPN 6 0.18 PEPN 7 ; 0.12 P <sub>3</sub> 5 ; 0.08 P <sub>3</sub> 7 ; 0.20 T P <sub>3</sub> 4	81.4	Roche
ROTN 200	0.33 S3 ; 0.67 S6	65.2	Roche
ROTN 404	0.31 M15 ; 0.14 M 24 ; 0.14 T 15 ; 0.09 P <sub>3</sub> 5 0.18 P <sub>3</sub> 7 ; 0.14 T P <sub>3</sub> 4	105	Roche

Merck—Frankfurter Str. 250 D 6100 Darmstadt 1

BDH —Poole Dorset BH 124 NN England

Roche—Liquide Crystals group RA/LC CH-4002 Basel

sealing process. Sealing of LC displays involves either a high temperature (500°C) glass frit technique or adhesives cured around 200°C.

Most alignment methods have been tested on MBBA,† a very sensitive Schiff's base LC, while biphenyls, esters or phenylcyclohexane eutectic mixtures are of current industrial interest. Our evaluations considered the commercial mixtures ROTN 200, ROTN 103, ROTN 404, E7, E8 and Zli 1132. † On filling a cell, the nematic director generally aligns in the direction of flow (4a), but the resulting orientation is temperature sensitive (4b). Heating the LC to its isotropic phase will often promote a uniform alignment, and slow

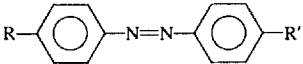
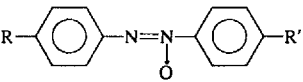
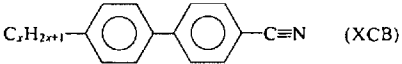
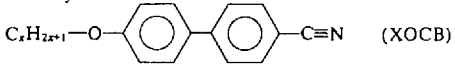
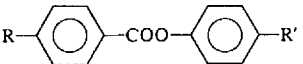
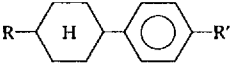
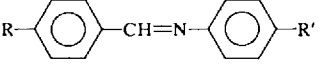
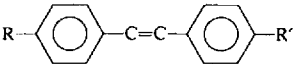
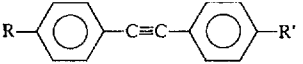
### LC Code

#### (2) LCs of current industrial use

C B 13		PCH-5	
S 3		PCH-7	
S 6		HPE-33	
K-15		HPEH-23	
K-21		HPEH-43	
M-9		PEPN 4	
M-15		PEPN 5	
M-21		PEPN 6	
M-24		PEPN 7	
T-15		P3 5	
BCH-5		P3 7	
PCH-3		TP3 4	

† See LC code.

## (3) Abbreviations used in the text

Azo	LCs with an azo linkage	
Azoxys (A)	LCs with azoxy linkage	
Azoxys eut. mixt.	Azoxys eutectic mixture	
BAB	4,4'-Bis( <i>n</i> -butoxy)azoxybenzene	
BBCA	4-Butoxybenzylidene-4'-cyanoaniline (pSB)	
BECS	4- <i>n</i> -Butyl-4'-ethoxy- $\alpha$ -chlorostilbene	
CB	Cyanobiphenyls	
CBOA	4-Cyanobenzylidene-4'- <i>n</i> -octylaniline	
CE	Cyano esters	
CN	Cholesteryl nonanoate	
DIBAB	4,4'-Di- <i>n</i> -butylazoxybenzene	
$\Delta\epsilon$	Dielectric anisotropy	
Esters	LCs with an ester linkage	
MBAB	4-Methoxy-4'-butylazoxybenzene	
MBBA	4-Methoxybenzylidene-4'- <i>n</i> -butylaniline (nSB)	
MPT	4-Methoxy-4'-pentyltolan	
<i>n</i>	Negative dielectric anisotropy ( $\Delta\epsilon < 0$ )	
OCB	Alkoxycyanobiphenyls	
<i>p</i>	Positive dielectric anisotropy ( $\Delta\epsilon > 0$ )	
PAA	<i>Para</i> -azoxyanisole	
PAP	<i>Para</i> -azoxyphenetol (4,4'-ethoxyazoxybenzene)	
PCH	Phenylcyclohexane	
<i>p</i> Esters mixt.	Mixture of positive LC esters	
PHT	4-Propyloxy-4'-heptyltolans	
SB	LCs with a Schiff base linkage	
Stilbenes (S)	LCs with a double bond linkage	
Tolans (T)	LCs with a triple bond linkage	

cooling also favors the LC alignment but such tricks characterize a weak aligning mechanism with reproducibility not guaranteed.

For practical purpose a good aligning process has to produce a uniform alignment immediately on filling the cell. In the case of weak effects the real cause of alignment may not be the supposed mechanism.

## I A CRITICAL REVIEW OF THE LITERATURE

### I.1 The alignment of liquid crystals on smooth surfaces

#### I.1.1 *Inorganic Substrates*

The surfaces of glasses, oxides and metals exhibit an aligning influence on liquid crystals (Table I). The reproducibility and uniformity of this type of alignment is poor as the substrate surface is ill defined. The cleaning procedures employed in the substrate preparation also play a role, e.g., MBBA molecules will align perpendicular to the surface (homeotropically) of acid treated glasses<sup>5</sup> or oxides,<sup>6,7</sup> but nonuniform alignment parallel† to the substrate surface is obtained with fired<sup>5</sup> or detergent cleaned glasses.<sup>6,8</sup> Homeotropic alignment on acid treated surfaces is limited to a few Schiff bases, and attempts to rationalize the alignment effect observed on 12 different LCs led to the hypotheses that it was due to a homeotropic aligning impurity,<sup>7</sup> as most polar molecules tend to induce perpendicular alignment (see paragraph 3). Recent investigations gave elegant evidence of the dramatic influence of impurities on LCs alignment in many compounds.<sup>9</sup> Boiling a glass plate in sulfuric acid is supposed to unpolish it, as does dipping in HF solution,<sup>10</sup> which may help homeotropic orientation, as observed with MBBA, however, acid washed glasses align azoxys parallel to the substrate.<sup>10</sup> Oxidation of SnO<sub>2</sub> or In<sub>2</sub>O<sub>3</sub> coating in an oxygen plasma lead to layers causing parallel alignment of biphenyls.<sup>25,26</sup>

In Table I reported alignment effects of cleaved crystals and evaporated layers have been collected. One sees that, although some layers have been observed to induce homeotropic alignment of certain LCs, generally parallel alignment is observed. We have been unable to obtain reproducible homeotropic alignment using evaporated inorganic layers although it does occur sometimes. It has to be considered that reliable homeotropic alignment may not be obtained from such surfaces.

#### I.1.2 *Organic polymers*

Polymer coatings on glass substrates can be employed to align liquid crystals, but film uniformity and the substrate used influence the observed results.

---

† The terms "homogeneous and parallel" imply parallel uniform, and nonuniform alignment, respectively.

TABLE I  
Alignment of nematic LCs on inorganic substrates<sup>a</sup>

I a	II a	III b	IV b	V b	VI b	VII b	VIII	I b	II b	III a	IV a	V a
LiF $\perp$ 12	CaF <sub>2</sub> $\times$ 20 $\perp$ 12									BN $\times$ 19	C $\times$ 6,20,24	
NaF $\times$ 11	MgF <sub>2</sub> $\times$ 15,20,22									Al $\times$ 17,20 Al <sub>2</sub> O <sub>3</sub> $\times$ 17,20,21 $\perp$ 13,14,20	Si <sub>3</sub> N <sub>4</sub> $\times$ 18 SiO <sub>2</sub> $\times$ 17,19,20	
NaCl $\times$ 20,90b	Mg(OH) <sub>2</sub> $\perp$ 10 (Brucite)									Aluminosilicates: $\times$ 10,23		
KBr $\times$ 20,90b KI $\times$ 3			TiO <sub>2</sub> $\times$ 19 20 22		Cr <sub>2</sub> O <sub>3</sub> $\times$ 21 Cr $\times$ 17	Fe <sub>2</sub> O <sub>3</sub> $\perp$ 16	NiO $\times$ 21 Ni $\times$ 47		ZnS $\times$ 21 $\perp$ 13 ZnO $\times$ 11		GeO <sub>2</sub> $\perp$ 16	As <sub>2</sub> S <sub>3</sub> $\times$ 10,23 (Orpiment)
		Y <sub>2</sub> O <sub>3</sub> $\times$ 19	ZrO <sub>2</sub> $\times$ 20 $\perp$ 20							In <sub>2</sub> O <sub>3</sub> $\times$ 17,20 $\perp$ 17,20	SnO <sub>2</sub> $\times$ 6,7,20,21 $\perp$ 6,7,20	
Cs <sub>2</sub> O $\times$ 19	BaTiO <sub>3</sub> $\times$ 22	CeO <sub>2</sub> $\times$ 19 ThF <sub>4</sub> $\perp$ 13		TaN $\times$ $\perp$ 16			Pt $\times$ 17,20 Au $\times$ 17,20	HgF <sub>2</sub> $\times$ 19			PbO <sub>2</sub> $\times$ 21	

<sup>a</sup> Often the same layer has been reported to induce either parallel or perpendicular alignment. Our investigations have generally shown the nematic orientation to be parallel to the surface. Impurities or surface hydrolysis may cause a homeotropic orientation of some LCs which is not characteristic of the surface.  $\perp$  = homeotropic alignment;  $\times$  = parallel, nonuniform. Reference 20 to our work means that we have observed these alignments on our test LC mixtures.

Polyimide layers have been claimed to align MBBA homogeneously<sup>27</sup> but our investigation proved that the alignment is generally parallel but not uniform. The alignment properties of most polymers have been evaluated, and Table II summarizes our results for cast films, together with the available published data. A wide variety of methods<sup>34</sup> has been used to form the polymer layer which is preferably thin in order to avoid an excessive potential drop in the dielectric layer. The film may be transferred to the surface from a liquid, while polymer casting and thermal or plasma polymerization of the monomer have also been used. The most common method is to form the polymer from partially polymerized solution by dipping or spin coating followed by curing. That the condition of film formation determines the final result may be indicated by the case of polytetrafluoroethylene (PTFE) films. As a result of an experiment with a series of photopolymerized 1000 Å PTFE films we observed that some films gave a homeotropic alignment while others did not. An attempt to determine the critical surface tension of these films proved that a continuous variation of the contact angle of liquids of different surface energy could not be obtained on those films which did not align LCs. It was also observed that films obtained from fluorinated polymer suspensions did not give homeotropic alignment of ester or biphenyl mixtures. It has been reported that MBBA does not align on PTFE films transferred by sliding contact on to glass substrates,<sup>38</sup> while sputtered PTFE films align most LCs, including MBBA.<sup>34</sup> Such a discrepancy is evidently related to the state of the surface of the deposited film.

Smooth, uniform polymer layers of PTFE and silicones induce homeotropic alignment of most commercial LCs with the exception of phenylcyclohexane (Merck Zli 1132) and tolan<sup>34</sup> mixtures. Alignment of these mixtures may be obtained by plasma polymerization of fluorinated alkene monomers<sup>25</sup> or perfluorocycloalkanes<sup>31</sup> and by films deposited from silicone solutions (see also paragraph 4). These homeotropically aligning plastic films excepted, other polymers, including plasma deposited films, do not give an uniform parallel alignment and a further rubbing is needed to provide uniformity.

Polymer coatings do not sustain high temperatures and displays employing such coatings must be sealed with an adhesive which is compatible with the polymer layers. This calls for a careful choice of adhesive in the case of silicones. Fluorinated polymers deposited by plasma polymerization of perfluorocycloalkanes,<sup>31</sup> as well as polyimide layers<sup>30</sup> are reported to be compatible with a glass frit sealing.

In general, smooth layers of glasses, oxides or polymers orient the nematic director parallel to the substrate but do not induce uniform, reproducible LC alignment.



TABLE II  
Alignment of nematic LCs on organic polymers<sup>a</sup>

Polymer	Commercial name	Source	$10^{-3} \text{ J m}^{-2}$	Mode of coating	Surface state	Liquid crystals	Alignment	Ref.
Polyalkenes								
p. ethylene	Suprathen Skyn	Kalle	28-36	Thick film	Natural	MBBA/TN200/ E7/TN103	×	20
p. ethylene	Suprathen Skyn	Kalle	28-36	Thick film	Rubbed	MBBA/TN200/ E7/TN103		20
p. isobutene	...	...	27	Plasma polym.	Rubbed	MBBA/esters/ tolanes		34
p. butadiene	Polyoil 1300	Hüls	33 (34) 31	Polym. sol.	Rubbed	n. Schiff base mixt.		36
Polyacrylates								
p. acrylate	RE 377	Mitsubishi Rayon	35-42 33-44	Polym. sol.	Rubbed	n. Schiff base mixt.		36
p. methyl methacrylate	...	...	...	Plasma polym.	Rubbed	MBBA/esters/ tolanes		34
p. cyanoacrylate	Ep 1	Taoka Chem.	37 (34) 33-34	Polym. sol.	Rubbed	n. Schiff base mixt.		36
p. acrylonitrile	Barex	Wipf	44	Film	Natural	MBBA/TN103/E7	×	20
					Rubbed	MBBA/TN103/E7		20
Polyvinyls								
p. vinyl alcohol	Polyviol 13/140	Wackez	37	Polym. sol.	Rubbed	MBBA, azoxys, TN103, E7		20
p. vinyl acetate	Vinyon	Nichia Paint	37	Polym. sol.	Rubbed	n. Schiff base mixt.		36
p. vinyl butyral	Rhovinal B 20-30	Rhodia	24-32	Polym. sol.	Rubbed	MBBA, azoxys, TN103, E7		20
p. vinyl chloride	Genotherm	Kalle	39	Film	Natural	MBBA, azoxys, TN103, E7	×	20
p. vinyl chloride	Genotherm	Kalle	39	Film	Rubbed	MBBA, azoxys, TN103, E7		20
p. vinyl pyridinium	...	...	...	Polym. sol.	Natural	5CB, 80CB	⊥	120
Polystyrenes								
p. styrene	Styrite	Daido Kogyo	27-33	Polym. sol.	Rubbed	MBBA/esters/ tolanes/CB		36
	...	...	...	Sol. p. styrene + divinyl benzene	Rubbed	Schiff base mixt., 5CB		34

TABLE II (continued)

Polymer	Commercial name	Source	$10^{-3} \text{ J m}^{-2}$	Mode of coating	Surface state	Liquid crystals	Alignment	Ref.
Polyparaxylylene p. xylylene)	Parylene	(Union Carbide) (Bakelite) (BXC)	...	Vapor polym.	Rubbed	DIBAB		29
Polyesters, polyurethanes p. esters p. esters	Lumirror Mylar A, B, C	Toray Dupont	40-43 40-43	Polym. sol. Thick film	Rubbed Natural	Schiff base mixt. MBBA/TN200/ TN103. E7	 X	34 20
p. esters	Mylar A, B, C	Dupont	40-43	Thick film	Rubbed	azoxy ent. MBBA/TN200/ TN103. E7		20
p. esters	Melinex	ICI	40-43	Thick film	Natural	azoxy ent. MBBA/TN200/ TN103. E7	X	20
p. esters	Hostaphan	Kalle	40-43	Thick film	Rubbed	azoxy ent. MBBA/TN200/ TN103. E7		20
p. esters	Hostaphan	Kalle	40-43	Thick film	Natural	azoxy ent. MBBA/TN200/ TN103. E7	X	20
p. urethane	V. Chroma	Dai Nippon Toray	40-43	Polym. sol.	Rubbed	azoxy ent. MBBA/TN200/ TN103. E7		36
Polyamides p. amide p. amide p. methylamide (Nylon 6)	Capran Versamid Sumitherm	All Chem. Gen. Mills Sumi Denks	33-42 33-42 ...	Thick film Sol. in LC Polym. sol.	Natural Rubbed Natural	TN200, TN103. E7 TN200, TN103. E7 MBBA	X    ⊥	20 20 56
Polyimides p. imide	Nolimid	Rhône Poulenc	...	From monomer sol.	Rubbed	Schiff bases TN200, TN103. TN104. E7	X 	36 20

## ALIGNMENT OF LIQUID CRYSTALS

11

p. imide	Nolimid	Rhône Poulenc	...	From monomer sol.	Rubbed	E8, ZLI1132		20
p. imide	Nolimid	Rhône Poulenc	...	From monomer sol.	?	MBBA		27
p. imide	Nolimid	Rhône Poulenc	...	From monomer sol.	Rubbed	Schiff bases, CB		30,31
p. imide	Kapton	Dupont	...	Thick film	Natural	Esters azoxys. azo	×	20
p. imide	Kapton	Dupont	...	Thick film	Rubbed	TN200, TN103, TN404, E7, E8	×	20
						TN200, TN103, TN404, E7, E8		20
Polysulfone								
p. sulfone	S 179	Appl. Sc. Lab	41	Polym. sol.	Natural	TN103, E7, azoxy	×	20
					Rubbed	n. esters mixture		20
Polyheterocycles								
p. quinoxaline	...	Monomer	...	Polym. sol.	Rubbed	p. nematic mixt.		28
p. benzthiazole	...	Monomer	...	Polym. sol.	Rubbed	p. nematic mixt.		28
p. benzoxazole	...	Monomer	...	Polym. sol.	Rubbed	p. nematic mixt.		28
Cellulose derivatives								
Methyl cellulose	...	Shinetsu Kagaku	35-42	Polym. sol.	Rubbed	Schiff base mixt.		36
65SH4000	...	Ceta SA	39	Thick film	Natural	MBBA/TN103/ E7/azoxys	×	20
Cellulose acetate					Rubbed	MBBA/TN103/ E7/azoxys		20
Cellulose acetate								
Cellulose acetate	LT105	Daicel	39	Polym. sol.	Rubbed	Schiff base mixt.		36
Cellulose triacetate	LT105	Daicel	39 -	Polym. sol.	Rubbed	Schiff base mixt.		36
and various esters								
Nitrocellulose	HIG40	Asai Kasei	34-42	Polym. sol.	Rubbed	Schiff base mixt.		36
Nitrocellulose	Celluloid	...	34-42	Thick film	Natural	TN200/TN103/ E7/azoxys	×	20
Nitrocellulose	Celluloid	...	34-42	Thick film	Rubbed	TN200/TN103/ E7/azoxys		20
Polysilanes								
p.(glycidopropyl- trimethoxysilane)	...	...	41 (34)	Dipping in monomes sol.	Nat ?	MBBA, esters, tolans, CB		34
p. hexamethylsiloxane	...	...	24 (34)	Plasma polym.	Natural	MBBA, esters, tolans, CB	⊥	34
Silicone rubber	KE45	Shinetsu Kagaku	22-24	Polym. sol.	Natural	Schiff base mixt.	⊥	36
Silicone rubber	CAF RTV	Rhône Poulenc	22-24	Polym. sol.	Natural	TN200/103-E7, azoxys	⊥	20

TABLE II (continued)

Polymer	Commercial name	Source	$10^3 \text{ J m}^{-2}$	Mode of coating	Surface state	Liquid crystals	Alignment	Ref.
Silicone rubber	Elcon 111	Chemie Moudon	22-24	Polym. sol.	Natural	TN200/103-E7, azoxys	$\perp$	20
p. ester silicone	...	Frabera	22-24	Thick film	Natural	TN200/103-E7, azoxys	$\perp$	20
p. methylphenylsiloxane	...	...	22-24	Dipping	Natural	MBBA/EBBA	$\perp$	91
p. methyl p. dimethylsiloxane mixt.	...	...	22-24	Dipping	Natural	MBBA/EBBA	$\perp$	91
p. methylsiloxane	...	...	22-24	Polym. sol.	Natural	p. S. Bmüt	$\perp$	86
p. methyl, phenyl (45%) siloxane	Si 996	Rhône Poulenc	...	Sol.	Natural	E7	$\perp$	20
p. methyl, phenyl (45%) siloxane	Si 996	Rhône Poulenc	...	Sol.	Natural	103	$\times$	20
p. methyl, phenyl (45%) siloxane	Si 996	Rhône Poulenc	...	Sol.	Natural	1132	$\times$	20
Fluorinated polymers								
p. tetrafluoroethylene	Teflon	Dupont	16-22	Sputtering	Natural	MBBA, esters, tolans	$\perp$	34
p. tetrafluoroethylene	...	...	22 (34)	Plasma polym.	Natural	CB	$\parallel$	25a
p. tetrafluoroethylene	...	...	16 (38)	Sliding contact	Natural	MBBA, Chlorostilbene, azoxys	$\times$	38
p. tetrafluoroethylene	...	...	not measurable	Photo polym.	Natural	CB, TN103	$\times$	20
p. fluoropropyl Co tetrafluoroethylene FEP	...	Dupont	16-16.5	Thick film			$\times$	20
p. vinylidene fluoride	Tedlar	Dupont	32.3	Thick film	Rubbed		$\parallel$	20
p. 1,3-dimethylcyclohexane	...	...	18 (32)	Plasma polym.	Natural	Schiff base mixt.	$\perp$	32
p. perfluorocyclohexene	...	...	22-24 (32)	Plasma polym.	Natural	Schiff base mixt.	$\perp$	32
p. perfluoro dimethylcyclobutane	...	...	20-22 (32)	Plasma polym.	Natural	Schiff base mixt.	$\perp$	32
p. acetylene Co perfluoro-1,3-dimethylcyclohexane	...	...	...	18-31	Natural	Schiff base mixt.	$\perp$ - $\parallel$	37
Others								
Urea-formaldehyde resins/viole	...	Mitsubishi Toaku	61	Polym. sol.	Rubbed	Schiff base mixt.	$\parallel$	36

Epoxies	ER 664	Asahi Kasei	35	Polym. sol.	Natural	Schiff base mixt.		36
Phenolic resins	Beckosol	Dai Nippon	52	Polym. sol.	Natural	Schiff base mixt.		36
Casein	...	...	43	...	Natural	Schiff base mixt.		35
Ionomere	Surlyn Na	Dupont	...	Thick film	Natural	103.E7.	X	20
Coumarone-Indene	Surlyn Na	Dupont	...	Thick film	Rubbed	103.E7.		20
	...	...	...	...	...	—		35

\* Critical surface tension from *Polymer Handbook*, 2nd ed., edited by J. Brandrup and E. H. Immergut, (Wiley, New York, 1975), except as otherwise indicated.

⊥ = homeotropic alignment (perpendicular to glass surface); || = alignment, uniform, parallel to glass surface; ● = molecular alignment too difficult to distinguish between perpendicular and parallel alignments and to obtain consistent experimental results; ||/⊥ = molecular alignment changed near the phase transition temperature from the parallel alignment at lower temperatures to the perpendicular alignment at higher temperatures; X = parallel nonuniform.

## 1.2 Alignment on grooved surfaces

Rubbing, tangential evaporation or shallow angle ion beam etching (SAIBE) produce a wavy surface. It has long been acknowledged that the rubbing of glass plate induces uniform alignment of LCs,<sup>39,40</sup> with the nematic director nearly parallel to the substrate surface.<sup>41</sup> For some time it was considered that the material used for rubbing determined the efficiency of the process.† It is now clear, however, that, as proposed many years ago,<sup>39</sup> any rubbing material, e.g., paper, tissues, brushes and polishing powders, gives good results. Some LCs align more easily than others and reproducibility is not very good on substrates that are simply rubbed. The use of polishing powder, such as diamond paste, improves the alignment and is a requisite for hard layers of silica or fluoride.

Glass has a surface layer extending one micron in depth which has higher entropy than the bulk<sup>42</sup> and may be easily deformed by rubbing, producing a wavy surface. Because of its higher energy this surface layer melts 125°C below the softening point of the glass<sup>42</sup> (i.e., around 475°C for soda lime glass) and, therefore, the effects of rubbing disappear above this temperature. Glass frit sealed cells, therefore, require the use of layers of high melting point compounds. SiO<sub>2</sub> deposited by sputtering, CVD or an electron gun, as well as MgF<sub>2</sub>,<sup>15,20</sup> BaTiO<sub>4</sub>, TiO<sub>2</sub>,<sup>22</sup> Cs<sub>2</sub>O, Y<sub>2</sub>O<sub>3</sub>, BN,<sup>19</sup> CeO<sub>2</sub><sup>19</sup> or Si<sub>3</sub>N<sub>4</sub><sup>18</sup> layers give, after rubbing with diamond paste or cerium oxide powder,<sup>43,20</sup> good, homogeneous aligning layers but the results are very sensitive to further processing. It is likely that these hard materials are difficult to groove sufficiently.

Oxides,<sup>17</sup> fluorides and metal layers evaporated obliquely to a substrate generally align the LC molecules parallel to, or at a slight angle from, the surface<sup>44</sup> but tangentially evaporated calcium fluoride is reported to align the molecules nearly perpendicular<sup>12</sup> although we could not reproduce this result. Slant evaporation of a metal and subsequent thermal oxidation<sup>21</sup> or shallow angle ion beam etching (SAIBE)<sup>45a</sup> produce the same results. Obliquely evaporated SiO<sub>x</sub> and MgF<sub>2</sub> layers give reproducible results and this method is widely used for the fabrication of small displays; it is further compatible with any type of sealing.

When high temperature resistance is not required, as in experimental cells or plastic sealed displays, it is advantageous to coat the electrodes with a soft polymeric layer which is rubbed afterwards. Any polymer is suitable, pro-

---

† Alignment of LCs by rubbed surfaces is sometimes wrongly attributed to J. F. Dreyer who omitted, in his paper "Orientation of the surface of glass" [Glass. Ind. **29**, 197 (1948)], to quote the work of Zocher and Coper (Ref. 39). This point has been cleared up in a letter to the editor by C. D. West [Glass. Ind. **30**, 272 (1949)], which provides an English translation of the main paragraph of Ref. 39. P. Chatelain,<sup>40</sup> who studied in detail LC alignment by rubbed surfaces, also ignored this work which clearly established the influence of rubbed glass surfaces on the orientation of PAA (which was used to prove the glass surface anisotropy) and that it was a property of the clean surface.

vided that it is possible to deposit it as a thin film (Table II) and most LCs will align homogeneously. Rubbed polyvinyl alcohol or polyvinyl butyraldehyde have been proposed as a method of forming an internal polarizer and an aligning layer simultaneously,<sup>33</sup> but the polarizing effect is weak. The quality of the alignment depends on the polymer layer thickness and the substrate uniformity. It is often advantageous to provide the electrodes with an intermediate layer that promotes adhesion and uniformity. As previously described, a wide variety of methods has been used to form films on a glass substrate. The rubbing of substrates on which a polymer powder was spread, or rubbing with a piece of polymer, have also been described as producing good aligning layers.<sup>46</sup> Although the surface deformation of glasses and polymers has not been clearly shown, the grooves produced by rubbing with a polishing paste<sup>43,47</sup> and the striated nature of tangentially evaporated layers<sup>48-53</sup> has been shown by photomicrographs. A grating made of a photoresist layer<sup>47,54</sup> or of  $\text{SiO}_2$ <sup>51</sup> induces homogeneous alignment of a LC.<sup>47,50</sup> Many surfaces tend to align LC's parallel and striations on these surfaces provide uniformity, which has led to the claim that any striated surface, whatever the substrate and the method used to produce them,<sup>55</sup> induces homogeneous alignment. In fact homeotropic aligning layers, e.g., evaporated  $\text{CaF}_2$ , show at most a leaning of the molecular axis when striations are induced by oblique evaporation, and polymethylsiloxane still promotes an homeotropic alignment after it has been rubbed (see Figure 9).

One point which is not clear is the surface nature of evaporated inorganic layers which are sometimes found to induce homeotropic alignment (not in a reproducible manner) but, once rubbed, promote a homogeneous alignment.

### 1.3 Alignment by surface active agents

It has long been observed<sup>56</sup> that surface active agents promote LC alignment. They may be either dissolved in a LC, or deposited on the cell walls. Small amount of surfactants may be dissolved in LCs conveniently through a common solvent which is evaporated afterwards. Spontaneous homeotropic alignment of the mixtures is observed on glass or oxide surfaces. Most surfactants have been described as effective (Table III) and examples are given for negative LC mixtures. These observations have been hastily extended to "liquid crystals" in general. As surfactant induced alignment is complex depending on the substrate, mode of application, LC composition (see § II.1.8), the use of these data needs critical evaluation.<sup>57,65</sup> For displays operating in the field effect mode, the increase in conductivity due to an ionic dopant is a disadvantage and, therefore, nonionic compounds are preferred. Cationic surfactants, which are long chain substituted ammonium salts, are very effective in promoting homeotropic alignment of negative<sup>58-60</sup> and positive<sup>20,117</sup> LCs although they increase the LC conductivity. Figures obtained for various con-

TABLE III

Surfactants agents reported to induce homeotropic alignment of nematic LCs

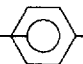
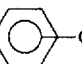
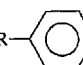
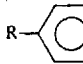
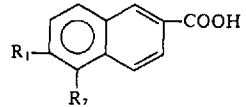
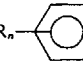
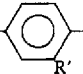
Surfactants	Liquid crystal	Ref.
<b>1. ANIONIC</b>		
<b>1.1. ACYCLIC CARBOXYLIC ACIDS: R-COOH</b>		
R = C <sub>n</sub> H <sub>2n+1</sub> n > 10	MBBA	5
n = 8, 11, 19	n-Schiff base mixt.	61
	n-Ester mixt.	
R = C <sub>8</sub> H <sub>17</sub> CH=CH-(CH <sub>2</sub> ) <sub>n</sub> n = 18 (stearic acid)	MBBA	60
R = C <sub>n</sub> F <sub>2n+1</sub> (oleic acid)	MBBA	60
n = 18	Esters	3
R-(COOH) <sub>2</sub>		
R = C <sub>n</sub> H <sub>2n+1</sub> n = 18 (octadecylmalonic acid)		64
<b>1.2. AROMATIC ACIDS: R--COOH</b>		
R = 4NH <sub>2</sub> ; 4 OH; 3 OH	n-Schiff base mixt.	
R = C <sub>n</sub> H <sub>2n+1</sub> O      n = 9, 10, 12, 14, 16, 18	n-Ester mixt.	61
	n-Azoxy mixt.	62
R = C <sub>n</sub> H <sub>2n+1</sub> n = 8		66
R = C <sub>n</sub> H <sub>2n+1</sub> -COO      n = 6, 12		62
R = C <sub>n</sub> H <sub>2n+1</sub> -COO      n = 3, 17		
R-  -CH <sub>2</sub> COOH	n-Schiff base mixt.	
R = 4NH <sub>2</sub> , 4 OH, 2-5 OH	n-Ester mixt.	
	n-Azoxy mixt.	61
R-  -(CH <sub>2</sub> ) <sub>2</sub> -COOH		
R = 4NH <sub>2</sub> , 4 OH, 3-4 OH	n-Schiff base mixt.	61
	n-Ester mixt.	
	n-Azoxy mixt.	
R-  -CH=CH-COOH	n-Azoxy mixt.	62
R = C <sub>n</sub> H <sub>2n+1</sub> O      n = 10, 12, 18		
R = C <sub>n</sub> H <sub>2n+1</sub> -COO      n = 1, 12, 18	n-Azoxy mixt.	
 -COOH		
R <sub>1</sub> = C <sub>6</sub> H <sub>13</sub> O      R <sub>2</sub> = Cl	n-Ester mixt.	56
R <sub>1</sub> = C <sub>16</sub> H <sub>33</sub> O      R <sub>2</sub> = Cl		
<b>1.3. CARBOXYLIC ACID WITH LC STRUCTURE</b>		
<b>1.3.1. Derivatives of Schiff's base</b>		
R <sub>n</sub> -  -CH=N-  -COOH		



TABLE III (continued)

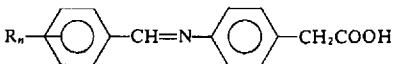
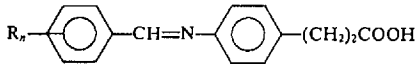
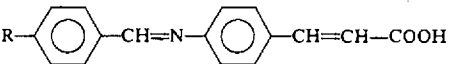
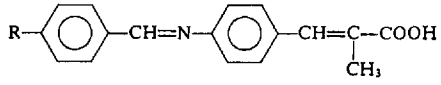
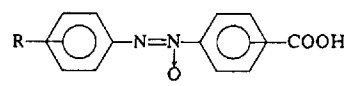
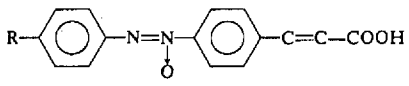
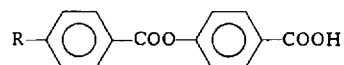
Surfactants	Liquid crystal	Ref.
$R' = H, R_n = 4 \text{ OH}, 3 \text{ OH}, 2 \text{ NO}_2\text{-}3 \text{ OH}, 3\text{-}4 \text{ OH}, 2\text{-}4 \text{ OH}, 2\text{-}4\text{-}6 \text{ OH}$ $R_n = C_nH_{2n+1}O \quad n = 1, 7, 13,$ $R_n = C_nH_{2n+1} \quad n = 1, 4, 7, 13$ $R' = OH, R_n = C_nH_{2n+1}O \quad n = 0, 1, 3, 7, 13$	n-Schiff base eut. mixt. n-Esters eut. mixt. n-Azoxy eut. mixt. n-Azo eut. mixt.	61, 62
$R_n$  $R_n = 4 \text{ OH}, 3 \text{ OH}, 3\text{-}4 \text{ OH}$ $R_n = C_nH_{2n+1}O \quad n = 1, 3, 4, 15$ $R_n = C_nH_{2n} \quad n = 1, 4, 7, 13$	As above	61
$R_n$  $R = 4 \text{ OH}$ $R = C_nH_{2n+1}O \quad n = 1, 4, 7, 13$ $R = C_nH_{2n+1} \quad n = 1, 4, 7, 11$		
$R$  $R = C_6H_{17}O$	n-Ester mixt.	56
$R$  $R = CH_3O \quad R = C_2H_5O \text{ (slow)}$	n-Ester mixt.	56
1.3.2. Derivatives of LC azoxy structure		
$R$  $R = C_nH_{2n+1}O \quad n = 1, 2, 4, 6, 12, 18$ $R = C_nH_{2n+1}COO \quad n = 3, n = 15$ $R_n = C_nH_{2n+1} \quad n = 14$	n-Azoxy eut. mixt.	62
$R$  $R = C_nH_{2n+1}O \quad n = 2, 4$	n-Azoxy eut. mixt.	62
1.3.3. Derivatives of LCs with ester structure		
$R$ 	n-Azoxy mixt. n-Ester eut. mixt.	62

TABLE III (continued)

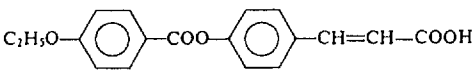
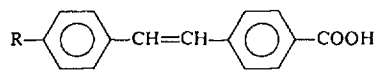
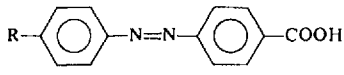
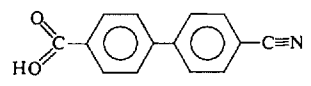
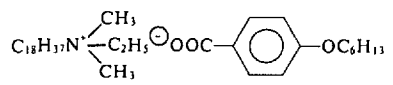
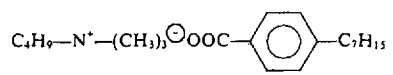
Surfactants	Liquid crystal	Ref.
$R = C_nH_{2n+1}O \quad n = 10, 14$ $R = C_nH_{2n+1} \quad n = 4, 8, 18$ $R = C_nH_{2n+1}COO \quad n = 3, 15, 17$		
	n-Azoxy eut. mixt.	62
1.3.4. Derivatives of LCs stilben structure		
	n-Azoxy mixt. Chloro stilben mixt.	62
$R = C_nH_{2n+1}O \quad n = 8, 18$ $R = C_nH_{2n+1}COO \quad n = 6, 9$		
1.3.5. Derivatives of LCs azo structure		
	n-Azo eut. mixt.	62
$R = C_nH_{2n+1}O \quad n = 1, 6, 12, 18$ $R = C_nH_{2n+1} \quad n = 6, 10, 14$ $R = C_nH_{2n+1}COO \quad n = 3, 7, 15$		
1.3.6. Derivatives of cyanobiphenyls		
	E7	45c
1.4. ANIONIC SURFACE ACTIVE AGENTS		
Cobalt, zinc naphthenate	MBBA	58
Sulfated alcohols	MBBA	58
Sulfated ethers	MBBA	58
2. CATIONIC		
2.1. ALKYL AMMONIUM SALTS $C_nH_{2n+1}-N^+(R_3) X^-$		
2.1.1. $X^- = \text{halogen}$		
$n > 10$	MBBA	75
$n = 16$ (Cetyl trimethyl ammonium bromide)	MBBA	58, 57
$n = 16$ (Cetyl trimethyl ammonium bromide)	n-Ester mixt.	58, 59
$n = 16$ (Cetyl trimethyl ammonium bromide)	PAA	58
$C_8F_{17}SO_2NH(CH_2)_3N^+(CH_3)_3$	MBBA-E7, TN103, ZLI1132	75-20
2.1.2. $X^- = \text{benzoate}$		
	n-Schiff base mixt.	70 59
	n-Schiff base mixt.	70

TABLE III (continued)

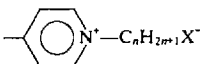
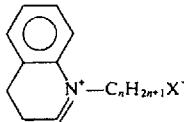
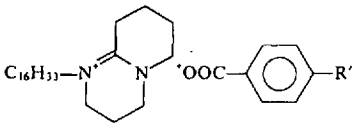
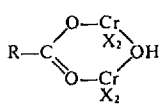
Surfactants	Liquid crystal	Ref.
2.1.3. $X^-$ = tetraphenyl borate		
$(C_{18}H_{37})_2N^+(CH_3)_2-(C_6H_5)_4B^-$	n-Schiff base mixt.	69
2.2. ALKYL PYRIDINIUM SALT		
	n-Schiff base mixt. n-Ester mixt.	59 59
$n = 16, 12$ ( $X^- = Br^-$ ) $n = 16$ ( $X^- = (C_6H_5)_4B^-$ )	n-Ester mixt.	68
2.3. ALKYL ISOQUINOLINIUM SALTS		
	PAA n-Schiff base mixt.	54 54
$n = 12$		
2.4. 7-ALKYL-1,8-DIAZABICYCLO[5.4.0]UNDECENAMMONIUM		
	n-Schiff base mixt.	
$R' = NH_2, NO_2, Cl, H, CH_3, C_2H_5, C_4H_9, C_6H_{13}$	n-Azoxy mixt. n-Ester mixt.	
2.5. CARBOXYLATOCHROMIUM COMPLEXES		
	n-Schiff base mixt. CB p-Schiff base	73
3. NONIONIC		
3.1. ALIPHATICS ESTERS, NITRILES, UREA, AMINES OR ALCOHOL		
$R-COO-C_nH_{2n+1}$ $n = 8, 18$ $R = CH_3$	n-Schiff base mixt.	74
$C_nH_{2n+1}COO R$ $n = 11$ $R = 6$	n-Schiff base mixt.	61
$C_nH_{2n+1}-CN$ $n = 7$	MBBA	60
$C_nH_{2n+1}-HN-CO-NH_2$ $n = 16$	MBBA	66
$C_nH_{2n+1}-NH_2$ $n > 12$	MBBA	5
$n = 16$	MBBA	75
$n = 18$	MBBA	60

TABLE III (continued)

Surfactants	Liquid crystal	Ref.	
$C_nF_{2n+1}CF=CF(CH_2)_2NH(CH_2)_3N(CH_3)_2$ $n = 6$	MBBA/EBBA	92	
$C_nH_{2n+1}-OH$ (amine catal.) $n = 12, 14, 16, 18$	n-Ester eut. mixt.	76	
$C_nF_{2n+1}(CH_2)_mOH$ $n = 7, m = 3$	MBBA	66	
	MBBA/EBBA	92	
3.2. AROMATIC ACID ESTERS			
$H_2N-\text{C}_6\text{H}_4-(CH_2)_m-COOC_nH_{2n+1}$ $n = 6 \text{ to } 16 \quad m = 0, 1, 2$	n-Schiff base mixt.	63	
$X_n-\text{C}_6\text{H}_4-COO-C_nH_{2n+1}$ $n = 4 \text{ to } 12 \quad X_n = 4 \text{ OH}$ $n = 2 \text{ to } 18 \quad X_n = 1, 2, 6 \text{ OH}$	n-Schiff base mixt.	63 61	
3.3. PHENOLS, AROMATIC AMINES			
2,6 Di- <i>t</i> -butyl-4-methylphenol	MBBA	71	
Hydroquinone	MBBA	71	
4- <i>t</i> -butylpyrocatechin	MBBA	71	
2- <i>t</i> -butylhydroxyanisole	MBBA	71	
Nisopropyl- <i>N</i> -phenyl p. phenylenediamine	MBBA	71	
Phenyl- $\beta$ -naphthylamine	MBBA	71	
<i>p</i> -hydroxyphenyl- $\beta$ -naphthylamine	MBBA	71	
3.4. NONIONIC SURFACTANTS			
Epoxy resins (low molecular weight)	MBBA	67	
Polyamid resins (low molecular weight)	MBBA	56	
Alkyl phenyl ethers	MBBA	67	
Polyoxyethylated glycols	MBBA	67	
Fluoro polymers	MBBA	67	
4. AMPHOLYTICS			
Lecithin	egg Lecithin	MBBA	79-6
	egg Lecithin	E7, E8, TN103, TN404, 1132	20
$\alpha$ Lecithin $\begin{array}{c} CH_2-CH-CH_2O^+PO_3^-(CH_2)_2N^+(CH_3)_3 \\   \quad   \\ R_1 \quad R_2 \end{array}$	PCH, Schiff bases, azoxy, esters	65	

centrations of cetyl ammonium bromide in a positive ester mixture ROTN 103 are given in Table IV.

The use of these agents has, therefore, been proposed for dynamic scattering mode displays.<sup>46,59</sup> Alignment of positive LCs is also observed with these compounds. Alkylvinyl pyridinium halides provide stronger orientation than ammonium derivatives, being able to align even smectic phases. In fact most

TABLE IV

Alignment and conductivity ( $\sigma$ ) of p. ester mixture TN103, with added CTAB

% CTAB	0	0.01	0.1	0.25	0.5	1
$\sigma$	$1.8 \times 10^{-10}$	$2 \times 10^{-10}$	$10^{-9}$	$1.7 \times 10^{-9}$	$2.9 \times 10^{-9}$	$7.4 \times 10^{-8}$
LC alignment				●	⊥	⊥⊥

compounds of this type, dissolved in LCs, favor homeotropic alignment of the LC. Fatty nitriles, amines,<sup>60</sup> acids<sup>6,61</sup> and esters<sup>61</sup> align MBBA. The effect of nitriles and esters is weak, depends on the substrate, and fails to align biphenyl and ester mixtures. Substituted benzoic acid<sup>61,62</sup>, its ester, phenols<sup>15,52,54</sup> and octadecyl malonic acid<sup>64</sup> are also effective, but branched isopalmitic acid does not align a LC.<sup>65</sup> Derivatives of benzoic acids which possess a liquid crystal structure have been thoroughly investigated<sup>61,62</sup> and a critical study<sup>57</sup> has assessed the more effective dopants. Such compounds, being frequently present as impurities or decomposition products in a LC, cause wrong assignment of the influence of aligning agents or prevent accurate correlations between LC structures and surface treatments. Their effect appears stronger when they are formed in the cell by LC degradation than when added to the LC. Effective concentrations of additives to the LC are in the range 0.5% to 2%. At smaller concentrations, the alignment presents defects, and higher concentrations lower the nematic to isotropic transition temperature significantly. The main drawback of this method of alignment is that on filling a cell provided with only one fill port, as preferred in industry, the additives absorb strongly in the neighborhood of the aperture and the liquid crystal at the end of the cell contains a lower concentration of additive, producing defects and a conductivity gradient across the cell. Attempts have been made to treat the cell walls before filling. Most of the surfactants described above for doping LC mixtures are effective, as the dissolved surfactant aligns the LC through absorption on the cell walls.

The orientation of the LC depends on its molecular structure: while most LCs are homeotropically aligned by adsorbed lecithin, azoxy derivatives and 4-methoxypropylcarboxybenzylidene aniline are not aligned.<sup>65</sup> The packing density of the adsorbed amphiphilic layer also plays a role. While homeotropic alignment of MBBA on glasses covered with hexadecyl(=cetyl)trimethyl ammonium bromide(CTAB) occurs at high coverage,<sup>8</sup> lecithin's orienting power decreases with increasing packing density.<sup>65</sup> Fatty amines<sup>5</sup> and alkyl substituted ammonium derivative<sup>66</sup> chains with a carbon content over 10 promote homeotropic alignment, while shorter chains orient the nematic director at an angle from the surface, smaller angles being observed for shorter chains. Heating destroys the aligning layer and cells provided with one fill port must be treated with a solution of the surfactant in a volatile solvent, rinsed,

dried and filled. Although often used in experimental work with lecithin in ether, or CTAB in alcohol, this method has not found industrial acceptance.

These methods give good results on many substrates except plastic coatings but long term stability is not obtained as the absorbed layer slowly dissolves in the LC.

Attempts have been made to bind the surface active molecule covalently to the surface. Baking octadecyltrimethyl ammonium tetraphenyl boride absorbed on cell walls from a solution has been claimed<sup>69</sup> to improve the alignment of the negative Schiff's bases. Reaction of fatty alcohols with silica covered electrodes catalyzed by amines<sup>45b</sup> seems to depend on the quality of the silica layers as we did not obtain reproducible results on silica layers deposited by CVD or solutions of organosilicon compounds. Tributyltin oxide<sup>71</sup> or chloride<sup>72</sup> dissolved in the LC produces homeotropic alignment, probably due to reactions with the electrode surface. The best results are obtained with carboxylatochromium complexes<sup>73</sup> or silanes which are substituted with one long chain polar group,<sup>77</sup> e.g., *N*-octadecyl-*N,N*-dimethyl-3-aminopropyltrimethoxysilyl chloride. We have checked that the aligning power is strong for most positive nematic mixtures and effective on rubbed layers, providing a way of realizing both homogeneous and homeotropic domains in the same cell by selective treatment of the walls. Nevertheless, these compounds, being ionic, increase slightly the LC conductivity even with thoroughly cleaned surfaces. Surfactants may also be included in a polymer layer, where they act as plasticizers: long term stability has not yet been evaluated. Long chain polar compounds generally induce homeotropic alignment of most practical LC mixtures. Few additives, however, promote planar alignment. Dicarboxylic acids added to LC mixtures are claimed to impart horizontal orientation.<sup>76</sup> Also, surfaces treated with *N*-methyl-3-aminopropyltrimethoxysilane align MBBA and *N*-*p*-(cyanobenzylidene)-*p*-*N*-octylaniline homogeneously after rubbing,<sup>77</sup> but we found that the very similar *N*-ethyl-3-aminopropyltrimethoxysilane aligns E7 and ROTN 103 homeotropically. Chromium complexes of dicarboxylic acids align negative LCs homogeneously, whereas homeotropic alignment is observed for positive mixtures.<sup>78</sup> Diazapolyoxycycloalkanes (crown ethers) improve homogeneous alignment on most oxides.<sup>80</sup> A large increase in LC conductivity, however, is observed when these compounds are used.

It is interesting to note that reacting tin oxide layers with long chain alcohols ( $C_nH_{2n+1}OH$ ,  $n = 1$  to 20), triethanolamine, phenols, cyclohexanol, phenyl acetic acid or valeric acid under pressure promotes homogeneous alignment of LCs as opposed to previous observations. An example is given for tin oxide treated either with *n*-decanol or cinnamic alcohol on an alkyloxyphenylpyrimidine mixture.<sup>81</sup>

#### 1.4 Alignment by silane treated surfaces

Alkoxys and chlorosilanes interact strongly with glass surfaces. The proposed mechanisms are either reaction with surface silanol groups, or hydrolysis of the silane to a silanol which will further condense into a linear polysiloxane layer (Figure 1). Thus silanes are sometimes considered as surface active agents and sometimes as polymer forming compounds. As they are of interest for LC alignment they justify a special paragraph.

Surface treatments with silanes have been effected by dipping during 5 s to 1 hr., (generally 5 min) in 1%–5% solution of the silane in water, toluene, dilute acetic in water, DMF or acetone. Water solutions are stable for only a few hours (except aminosilanes). After rinsing with the solvent used to dissolve the silanes.<sup>72a</sup> In the case of quaternary ammonium silyl compounds these methods gave poor results with most LCs and dipping in hot (75°C) solutions<sup>83</sup> improved the efficiency of the treatment. Silanation also occurs if the substrate is exposed to silane vapor, for low boiling point compounds, or treated in a refluxed solution of silane in toluene, for others. We have often observed that depositing a drop of pure silane on a spinning substrate often gave better results than dipping in silane solutions. Hydrolysis of the surface before coating is sometimes recommended. An evaluation of silane alignment efficiency for the alignment of the positive ester mixture ROTN 103, and the biphenyl mixture E7, is presented in Table V together with some published results. It can be seen that the effect of the silane layer depends on the mode of deposition and the nature of the LC. Among the different silanes which have been tried, monodimethyldichlorosilane shows a strong effect, unlike the similar ethyl substituted derivatives, and methyltrichlorosilane or trimethylchlorosilane. Stearyltrichlorosilane has been reported to align Schiff's bases and biphenyls homeotropically.<sup>87</sup> Those silanes which do not align homeotropically can only be persuaded to align a wide range of LCs uniformly and parallel to the substrate, after rubbing, as has already been noted. It seems that most silanes influence the LC alignment by the *in situ* formation of a polysiloxane surface layer. Deposition of silicones which are formed by bulk polymerization of silanes shows that only methylpolysiloxane (and for some LCs, methylphenylsiloxane) aligns LCs homeotropically, while the remainder promote a planar alignment, contrary to certain reported observations.<sup>86</sup> In fact, silanes may be used in two ways: either to form a polysiloxane layer or to bind a long chain to the substrate, as with stearylsilane or dodecylammonium compounds. A substrate may alter the film properties and it is advantageous to form an initial surface layer by decomposition of an organometallic compounds. A substrate may alter the film properties and it is advantageous to form an initial surface layer by decomposition of an organometallic compound before silane treatment. Silylated surfaces degrade upon heating and

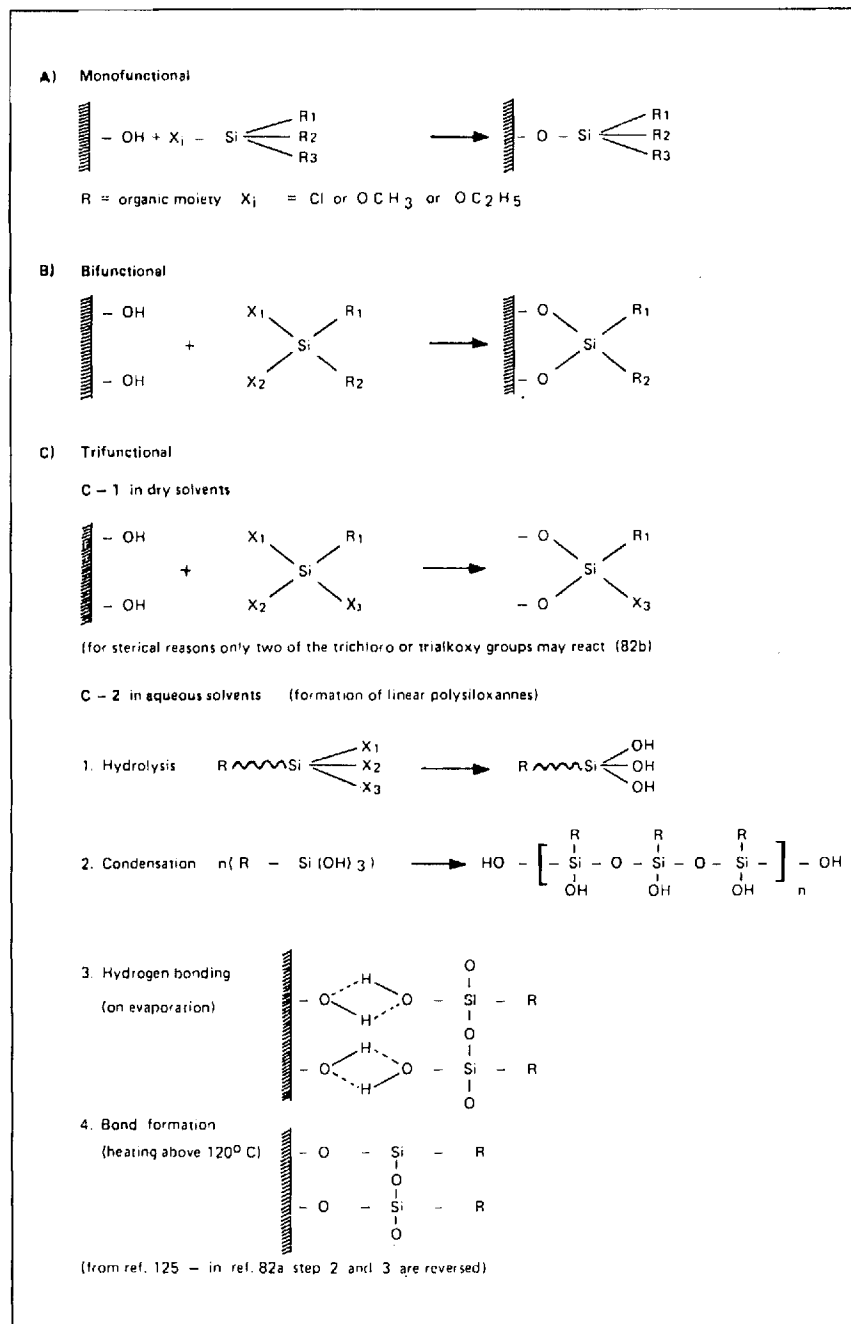


FIGURE 1 The reaction of silanes with oxides. Silane reaction with superficial hydroxyl groups produces either covalently bound alkyl chain or linear polysiloxanes.



TABLE V  
Alignment of nematic LCs by silylated substrates, under various treatment conditions<sup>a</sup>

Silane	Supplier	$10^{-3} \text{ J m}^{-2}$	Liquid crystal	Treatment	Time	Temp. °C	Ref.	Align.
<b>1. CHLOROSILANES</b>								
<i>Monochlorosilanes</i>								
Trimethyl	Fluka 92360	36-38	TN103	1% in toluene	1 h	room temp.	20	X
	Fluka 92360	36-38	TN103	vapor phase	10 sec	boil. 55°C	20	X
	Fluka 92360	36-38	TN103	vapor phase	1 h	boil. 55°C	20	X
	Fluka 92360	36-38	MBBA	solution	...	...	5	X
	Fluka 92360	36.5-38.5	TN403	10% in toluene	15 min	room temp.	20	X
				rinsed air dried, cured 120°C 1 h				
	Fluka 92360	36.5-38.5	TN404	10% in toluene	15 min	room temp.	20	X
				rinsed air dried, cured 120°C 1 h				
	Fluka 92360	36.5-38.5	ZLI1132	10% in toluene	15 min	room temp.	20	X
				rinsed air dried, cured 120°C 1 h				
Dimethyl	Fluka 92360	36.5-38.5	E7	10% in toluene	15 min	room temp.	20	X
				rinsed air dried, cured 120°C 1 h				
	Fluka 92360	36.5-38.5	E8	10% in toluene	15 min	room temp.	20	X
				rinsed air dried, cured 120°C 1 h				
				vapor phase	1 h	boil. 40°C	20	X
	Wacker HM	20.1	TN103	1% in toluene	1 h	room temp.	20	⊥ slow
	Fluka 40140	20.1	TN103	5% in toluene	1 h	room temp.	20	⊥ slow
	Fluka 40140	20.1	TN103	10% in toluene	1 h	room temp.	20	⊥ slow
	Fluka 40140	20.1	TN103	vapor phase	...	boil. 65°C	20	⊥ fast
	Fluka 40140	20.1	TN E7	spin coated	...	room temp.	20	⊥ fast
Dichlorosilanes	Fluka 40140	20.1	TN E7	spin coated	...	room temp.	20	● fast
	Fluka 40140	20.1	TN1132	spin coated	...	room temp.	20	● fast
	?	20.1	LC	50% in benzene 80°C curing for 5 min.	5-10 min	room temp.	72	⊥
Dimethyl	?	20.1	CH <sub>3</sub> O-φ-CH=N-φ-C-N	5% in toluene	10 min	room temp.	87	
			C <sub>6</sub> H <sub>5</sub> O-φ-CH=N-φ-C-N				87	
			C <sub>6</sub> H <sub>5</sub> O-φ-CH=N-φ-C-N				87	
			C <sub>6</sub> H <sub>5</sub> O-φ-CH=N-φ-C-N				87	⊥
			C <sub>6</sub> H <sub>5</sub> O-φ-CH=N-φ-C-N				87	⊥







		29	(84)	MBBA PBA SCB	0.5% in water	15 min	room temp.	X
3-Aminopropyl TES	Dow Corning XZ-2024	35	(82)	TN103	1% in toluene	1 h	room temp.	X
	Wacker A 1100 or	35 (glass)	(82)	TN103	spin coated 0.1% in toluene + sol. rinse	5 min	room temp.	X
	Dyn. Nobel AMEO	35 (glass)	(82)	TN103		...	room temp.	X
	Dyn. Nobel AMEO	35 (glass)	(82)	TN103		5 min	room temp.	X
	Dyn. Nobel AMEO	35 (glass)	(82)	404		...	room temp.	X
	Dyn. Nobel AMEO	35 (glass)	(82)	E7		...	room temp.	X
	Dyn. Nobel AMEO	35 (glass)	(82)	1132		...	room temp.	X
	Tokyo Kasei	38	(84)	SCB		15 min	room temp.	X
	Kogyo Co.							
	Kogyo Co.							
3-Aminopropyl TMS	Dyn. Nobel AMMO	35	(82)	TN103	spin coated	...	room temp.	
	Dyn. Nobel AMMO	35	(82)	E7	spin coated	...	room temp.	
	Dyn. Nobel AMMO	35	(82)	TN103	spin coated 0.1% in toluene + sol. rinse	5 min	room temp.	●
	Dyn. Nobel AMMO	35	(82)	TN103	spin coated 0.1% in toluene + sol. rinse	5 min	room temp.	X
N-2-Aminoethyl-3-Aminopropyl TMS	Dyn. Nobel AMMO			404				X
	Dyn. Nobel AMMO			E7				X
	Dyn. Nobel AMMO			1132				X
	Wacker GF 91	36-38	(84)	TN103	vapor phase	30 min	Boil. 260°C	X
	Wacker GF 91	36-38	(82)	TN103	spin coated	...	room temp.	X
	Wacker GF 91	36-38	(82)	E7	spin coated	...	room temp.	X
N-2-Aminoethyl-3-Aminopropyl TMS	Dyn. Nobel DAMO	36-38	(82)	TN103	0.1% in toluene + sol. rinse	5 min	room temp.	X
				404				X
				E7				X
				1132				X
	Shin Etsu chem	36	(84)	SCB	0.5% in water drying at room temp. 130°C	15 min	room temp.	X
	Shin Etsu chem	36		MBBA	curing for 20 min	15 min	room temp.	X
N-2-Aminoethyl-3-Aminopropyl TMS	Shin Etsu chem	36		PAB				X
	Dyn. Nobel DAMO	36	(82)	TN103	spin coated	...	room temp.	X
	Dyn. Nobel DAMO	36	(82)	E7	spin coated	...	room temp.	X
	Dyn. Nobel			TN103	spin coated	...	room temp.	X
	TRIAMO				0.1% in toluene + sol. rinse	5 min	room temp.	
	TRIAMO				0.1% in toluene + sol. rinse	...	room temp.	
N-2-Aminoethyl-3-Aminopropyl TMS	TRIAMO			404	0.1% in toluene + sol. rinse	...	room temp.	subst.
	TRIAMO			E7	0.1% in toluene + sol. rinse	...	room temp.	subst.
N-2-Aminoethyl-3-Aminopropyl TMS					0.1% in toluene + sol. rinse	...	room temp.	subst.
					0.1% in toluene + sol. rinse	...	room temp.	subst.

TABLE V (continued)

Silane	Supplier	$10^{-3} \text{ J m}^{-2}$	Liquid crystal	Treatment	Time	Temp. °C	Ref.	Align.
	TRIAMO		1132		...	room temp.	20	rubbed subst.
3-Chloropropyl TMS	Dyn. Nobel CPTMO	40.5	E7 TN103	0.1% in toluene + sol. rinse spin coated	...	room temp.	20	●
3-Chloropropyl TES	Dyn. Nobel CPTMO	40.5	(82) TN103	spin coated	...	room temp.	20	rubbed subst.
3-Glycyloxypropyl TMS	Dyn. Nobel GLYMO	38-42	(82) TN103	spin coated	...	room temp.	20	rubbed subst.
3-Glycyloxypropyl TMS	Shin Etsu chem	38.5	(84) 5CB MBBA	1.5% in water	15 min	room temp.	84	rubbed subst.
3-Morpholinopropyl TMS	Shin Etsu chem	42	(84) 5CB MBBA	0.5% in water	15 min	room temp.	84	rubbed subst.
3-Methacryloxypropyl TMS	Shin Etsu chem	28/31 28	(84) 5CB MBBA	1% in water/ 1 methanol			84	rubbed subst.
Hexamethyldisilazane	Fluka 52619 Fluka 52619		1 h TN103	vapor phase spin coated	1 h	boil. 124°C	20	rubbed subst.
Imidazoln	Dyn. Nobel IMEO		5 min TN103	0.1% in toluene + sol. rinse	5 min	room temp.	20	rubbed subst.
		404					20	rubbed subst.
		E7					20	rubbed subst.
Imidazol TES	Dyn. Nobel IMEO		1132 TN103	spin coated	...	room temp.	20	rubbed subst.
M-Phenyl-3-aminopropyl TMS	Shin Etsu chem	42	E7 5CB	spin coated	...	room temp.	20	rubbed subst.
	Shin Etsu chem	MBBA		3% in 5 water/ 1 methanol	15 min	room temp.	84	●
3-Mercaptopropyl TMS	Shin Etsu chem	41-42	(84) 5CB	3% in 7 water/ 1 methanol	15 min	room temp.	84	●
		41	(82) MBBA				84	●
		41	(82) PBA				84	●
Polyamino TMS	Toray	26	(84) 5CB	0.5% in water	15 min	room temp.	84	●

	Silicone	26	(84)	MBBA							X
N,N-Dimethyl-N-Octadecyl-3-amino-propyl TMS-chloride (DMOAP)	Dow Corning XZ-2-2300	26	(84)	PBA							⊥
	Dow Corning XZ-2-2300	26	(84)	MBBA		0.1% in water	5 min	room temp.	(77)		⊥
	Dow Corning XZ-2-2300	26	(84)	CBOA							⊥
	Dow Corning XZ-2-2300	26	(84)	MBBA + esters		0.5% in water	10 min	75°C			⊥
	Dow Corning XZ-2-2300	26	(84)	MBBA/EBBA							⊥
	Dow Corning XZ-2-2300	26	(84)	n-azoxy LC mixt.							⊥
DMOAP	Toray Silicone	23	(84)	5CB		water	15 min	room temp.	(84)		⊥
				MBBA							⊥

\* Concerning the difference between vapor and solution coated substrates, see also Ref. 88. T.E.S. = triethoxysilane; T.M.S. = trimethoxysilane. <sup>1</sup> % from Ref. 82 except as otherwise indicated. <sup>2</sup> These silanes hydrolyze strongly. <sup>3</sup> || and X are often not distinguished in the literature. In our observations only rubbed surfaces either before or after silane treatment lead to || alignment for these silanes which do not induce homeotropy.

⊥ = homeotropic alignment (perpendicular to glass surface); || = alignment, uniform, parallel to glass surface; ● = molecular alignment too difficult to distinguish between perpendicular and parallel alignments and to obtain consistent experimental results; ||/⊥ = molecular alignment changed near the phase transition temperature from the parallel alignment at lower temperatures to the perpendicular alignment at higher temperatures; X = parallel nonuniform.

preclude glass frit sealing. Treatment of the assembled cell by the organic vapor could be used, but the toxicity of chlorosilanes renders the process hazardous. From Ref. 88 it seems that the surface configuration of silane films deposited from vapor and solution phases is different. Dissolution of dimethyldichlorosilane and phenyltrichlorosilane, in EBBA-MBBA has been used to promote homeotropic and homogeneous alignment, respectively, but the process is impractical as the conductivity is increased and  $T_c$  decreased.

### 1.5 Tilted alignment

In evaluation studies of alignment effects, classification of LC alignment into homeotropic or parallel is an oversimplification, as often, in the literature, nonhomeotropic alignment is referred to as parallel (or homogeneous). In fact, the nematic director of LC molecules generally makes an angle  $\phi$  with the substrate surface. This "tilt angle" is required in practical twisted nematic displays in order to obtain a rotation of all the LC molecules in the same direction on the application of an electric field. The tilt suppresses the formation of diffracting walls between domains with reverse twist. A careful choice of tilt on each electrode leads to a better optical appearance.

In the neighborhood of a particular surface, tilt angles are distributed around a mean value.<sup>93</sup> Experimental figures refer to the mean orientation of the LC director in the bulk. Literature data show some variations in tilt angle values which arise either from the precision of the measurements or from different experimental conditions. Accuracy of measurement has been discussed<sup>94</sup> and some indicative data are collected in Table VI. The tilt angle on  $\text{SiO}_x$  evaporated layers shows slight variations with the substrate. Layer thicknesses in the range 50–100 Å cause variations of  $\phi$  from 16° to 22°.<sup>95</sup> The rate of evaporation,<sup>96</sup> the pressure,<sup>95</sup> boat temperature, and any subsequent thermal treatment<sup>96</sup> also changes  $\phi$  by several degrees. The variation of  $\phi$  with evaporation rate has been used to monitor the tilt angle of different LC composition.<sup>97</sup> The nature of the LC material,<sup>93,95</sup> its purity,<sup>93</sup> and—as shown in the case of cyanobiphenyls—the chain length,<sup>85</sup> also modify tilt values. We have observed wide variations of the tilt angle values in various cells where measurements have been made just after filling and subsequently after a period of stabilization: measurements on 11 cells have shown that, for ROTN 200, on obliquely evaporated  $\text{SiO}_x$  ( $\theta$ : 85°), the tilt angle values vary from 13° to 23°; however, after 500 hr, the different cells gave  $\phi = 17.5^\circ \pm 0.5^\circ$ . Despite experimental discrepancies, in general, rubbed layers give low tilt angles and rubbed polymers produce larger tilt angles (1°–5°) than rubbed inorganic surfaces (0°–2°), although 0° tilt angle has been measured on rubbed polyvinyl alcohol for a wide range of LC mixtures<sup>95</sup> and  $\phi = 1^\circ$  has been measured for an ester mixture aligned by polyamide-imide layers deposited on



TABLE VI

Indicative values of nematic director tilt angles on some typical aligning layers

Substrate	LC	Angle (°)	Method	Reference
Evaporated:				
SiO <sub>x</sub> 63°	?	3°	magneto capacit.	(102)
SiO <sub>x</sub> 85°	5CB	27	moving isogyre	(96)
	6CB	29	moving isogyre	(96)
	6CB	29.4 ± 0.7	$\Delta n$	(110)
	7CB	31	moving isogyre	(96)
	7CB	24.1	magneto capacit.	(94)
	8CB	34	moving isogyre	(96)
	50CB	34		
	70CB	37		
	90CB	39		
	60CB	38		
	80CB	41	moving isogyre	(96)
SiO <sub>x</sub> 85°	E8	25–27 (25 after 300 h)	magneto capacit.	(20)
SiO <sub>x</sub> 82°	E7	25.3	magneto capacit.	(94)
	MBBA	23.3–26	magneto capacit.	(94)
	TN103	21.8	magneto capacit.	(95)
	TN200	15–22 (17 after 910 h)		(20)
	TN200	22.2		(95)
	TN403	22.7		
	E7	25.4		
SiO <sub>x</sub> 82°	E7	25.3	magneto capacit.	(95)
SiO <sub>x</sub> 85°/60°	E7, TN200	25 → 0	capacitance	(104)
100 Å/0 → 30 Å				
SiO <sub>x</sub> 60°/85°	E7	0 → 25		(103)
100 Å/0 → 10 Å				
	(5CB/60CB)	0 → 33		(111)
SiO <sub>x</sub> 85 → 80°	nSB	30 → 45	capacitance	(41)
84 → 74°	nSB	15 → 25	magneto capacit.	(94)
76 → 72°	?	3 → 9	magneto capacit.	(102)
Rubbed:				
In <sub>2</sub> O <sub>3</sub>	E3	0.05	magneto null.	(93)
Glass	SB	0.5–5	capacitance	(41)
PVA	103.200.	0	magneto capacit.	(95)
	403. E7			
In <sub>2</sub> O <sub>3</sub>	E7	2.15 ± 0.1	magneto capacit.	(112)
NMAP silane	E3	0	magneto null.	(93)
Rhodiakermid	E3	0.95	magneto null.	(93)

SiO<sub>2</sub> rubbed with diamond paste.<sup>89</sup> A tilt angle of 2° has been measured for pentylcyanobiphenyl on rubbed glass as well as for a biphenyl mixture on rubbed SiO<sub>x</sub> layers evaporated at 60°C incidence.<sup>95</sup> SiO<sub>2</sub> layers rubbed with diamond paste align ester mixtures parallel to the substrate ( $\phi = 0^\circ$ ).<sup>89</sup>

Evaporation of metals or oxides obliquely to the substrate leads to layers which align LCs differently depending on the angle  $\theta$  of the evaporation beam

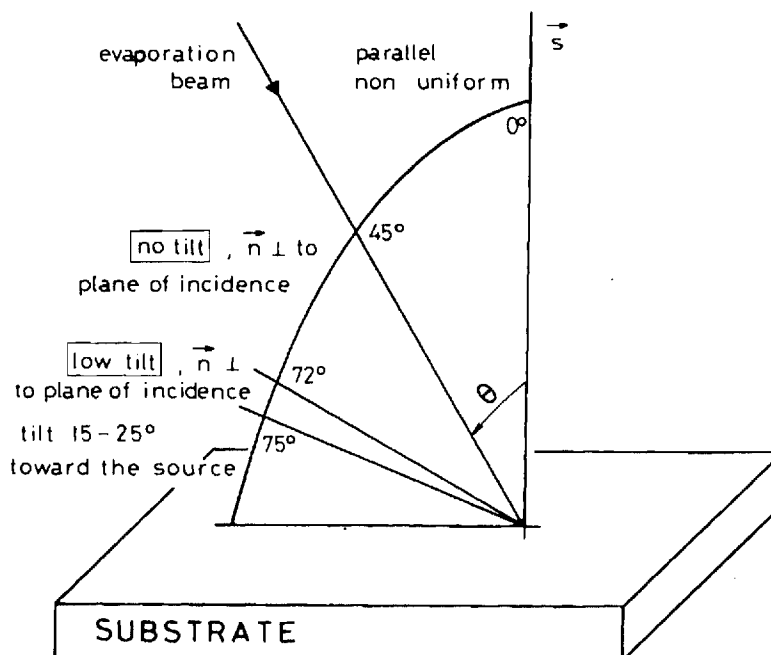


FIGURE 2 LC nematic director orientation induced by evaporated silicon oxide (or magnesium fluoride). Depending upon the angle of incidence of the evaporation beam different orientations are observed.

with respect to the normal to the surface<sup>44</sup> (Figure 2). If  $\theta < 45^\circ$ , parallel but nonuniform alignment is observed, but when  $45^\circ < \theta < 75^\circ$  LC molecules align in a direction perpendicular to the incident beam with a tilt angle very close to zero. Tangential evaporation at  $\theta > 75^\circ$  results in the nematic director being oriented towards the source at an angle of approximately  $15^\circ$ , increasing to  $25^\circ$  as  $\theta$  increases from  $75^\circ$  to  $88^\circ$ .<sup>48,102</sup> When  $\theta$  is  $72^\circ$ – $75^\circ$  the LC molecules lie parallel to the substrate plane, with the director axis perpendicular to the plane of incidence of the evaporation beam, at a low tilt angle ( $3^\circ$ – $9^\circ$ ).<sup>102</sup> These values have been widely confirmed by numerous authors and repeatedly obtained in industrial practice for all of the practical LC mixtures.

Tangentially evaporated  $\text{MgF}_2$  gives similar results but with smaller tilt angles than  $\text{SiO}_x$  for the same angle of evaporation.<sup>15b</sup> Oblique evaporation of  $\text{CaF}_2$  is reported<sup>12</sup> to produce homeotropic alignment ( $\phi = 90^\circ$ ) when  $\theta < 45^\circ$ ,  $\phi = 75^\circ$  for  $45 < \theta < 70^\circ$  and  $\phi = 60^\circ$  for tangentially evaporated layers ( $\theta > 75^\circ$ ). Surfactants, some silanes and polymers produce homeotropic alignment. Rubbing and tangential evaporation of oxides give low tilt angles while oblique evaporation induces a  $25^\circ$  tilt angle. When other tilt angles are desired, any combination of high and low-tilt-angle-producing

methods can be employed. The tilt angle of a tangentially evaporated layer may be lowered by rubbing<sup>98</sup> or by crossed evaporation of two layers of different thickness at the same angle of incidence  $\theta$ .<sup>99</sup> Deposition of a very thin (less than 5 Å) layer of  $\text{SiO}_x$ , evaporated at an angle of  $6^\circ$  from the substrate ( $\theta = 84^\circ$ ), on to a layer deposited at  $60^\circ$  incidence, after  $90^\circ$  rotation of the plate, gives a tilt angle of  $0^\circ$  to  $6^\circ$ .<sup>102</sup> By employing the reverse order<sup>104</sup> i.e., an initial evaporation of a 50 Å  $\text{SiO}_x$  layer at an incidence angle of  $5^\circ$ , followed by a rotation of  $90^\circ$ , and 100 Å evaporation of  $\text{SiO}_x$  at  $80^\circ$ , low tilt angles ( $5^\circ$ ) are obtained with the LCs E7 or ROTN 200. Variation of the layer's thickness allows tilt angles to be controlled from  $0^\circ$  to  $30^\circ$ . Variation of  $\phi$  from 0 to  $45^\circ$  for E<sub>3</sub> has been obtained by simultaneous evaporation of SiO from two sources.<sup>105</sup> Electron gun deposition of an initial layer, 350 Å thick, at  $6^\circ$  incidence, followed by a 20–50 Å thick layer deposited at  $30^\circ$  without rotation of the substrate, gives a  $6^\circ$  tilt angle.<sup>102</sup> Variations of  $\phi$  from  $11^\circ$  to  $3^\circ$  can be produced by monitoring the thickness of the second layer. SAIBE  $\text{SiO}_2$  covered with long chain alcohol allows tilt angles to be varied from  $75^\circ$  to  $90^\circ$  depending on the surfactant chain length,<sup>45b</sup> while plasma deposition of an 8 Å Teflon layer on to  $70^\circ$  evaporated  $\text{SiO}_x$  gives a tilt angle of  $15^\circ$ .<sup>106</sup>

A  $\text{SiO}_x$  layer evaporated at a low angle, which would normally result in a tilt angle of  $25^\circ$ , when treated with a homeotropic aligning layer of lecithin, orient the LC at the complementary angle of  $\phi = 65^\circ$  (Figure 3), as has been observed when this layer is treated with octadecylammonium bromide,<sup>44</sup> or deposited on glass cleaned with sulfochromic acid.<sup>108</sup> Evaporation of two dissimilar materials, such as gold and indium oxide, on adjacent sides of the grooves of a wavy surface gives a LC alignment slightly tilted from the normal for LC mixtures containing a homeotropically aligning surfactant.<sup>107</sup>

Orientation of thin LC layers may be obtained with the nematic director oriented in any direction from  $\phi = 0$  to  $25^\circ$ – $35^\circ$  and  $60^\circ$  to  $90^\circ$  by a suitable aligning layer (Diagram 1).

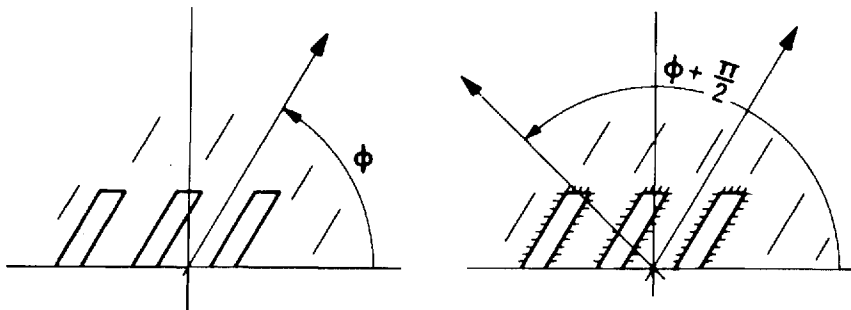


FIGURE 3 Where an inorganic surface produces an average orientation of the LC molecules at an angle  $\phi$ , treatment by a homeotropic aligning surfactant leads to an orientation at the complementary angle.

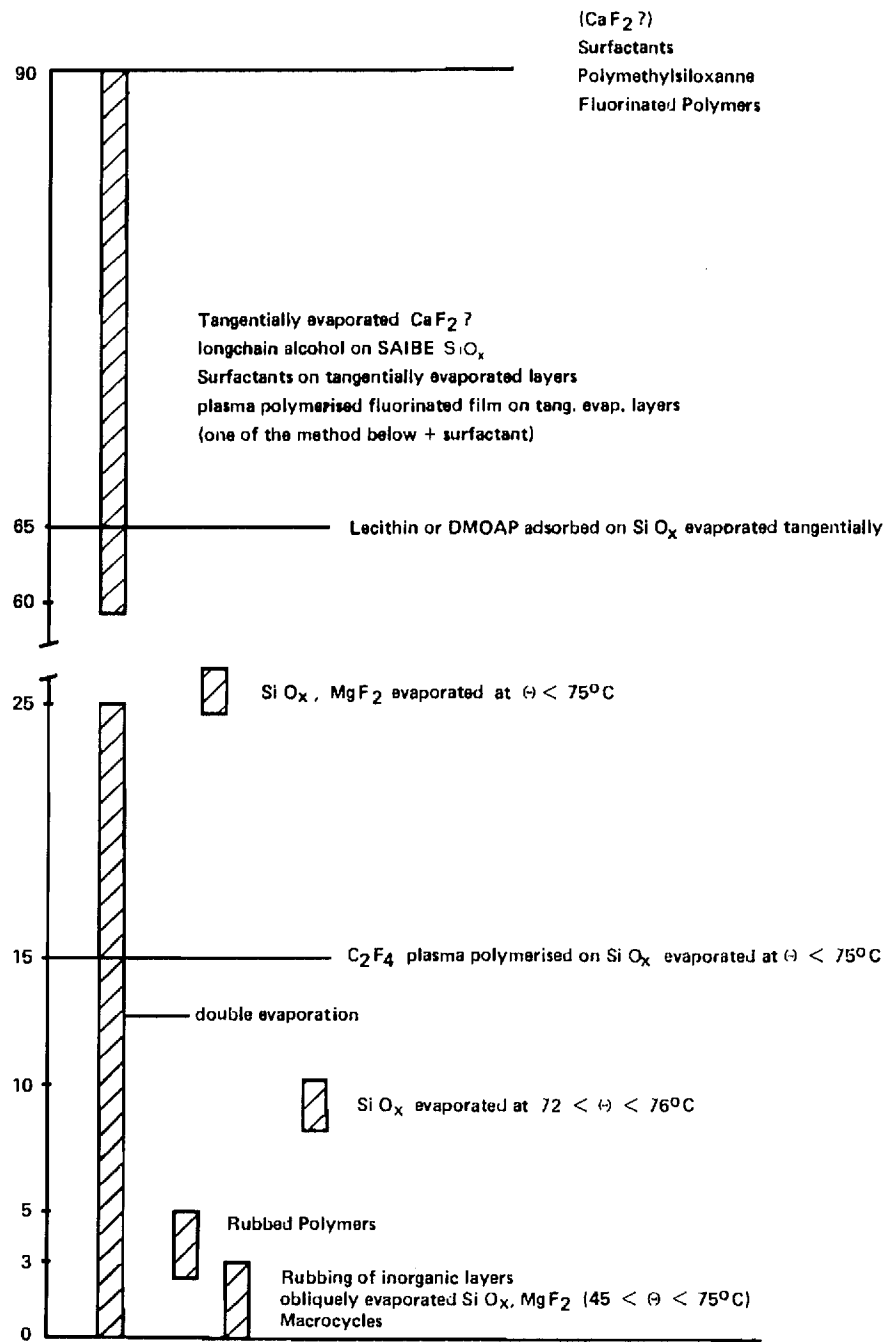


DIAGRAM 1 Tilt angle of the LC nematic director produced by different surface treatment.

## II ALIGNMENT MECHANISMS OF NEMATIC LIQUID CRYSTALS AND THEIR MIXTURES

Evaluating the various alignment methods reviewed in § I aided greatly in clarifying some general guidelines for LC-surface interactions.

The difficulties encountered, while attempting to obtain meaningful experimental data, due to ill-defined substrates, LC decomposition, and surface chemistry misconception have hindered progress in the understanding of the subject. LC molecules are composed of an aromatic core, an alkyl chain and a polar group, thus giving rise to complex dispersive polar and hydrophobic interactions.

### II.1 Physicochemical Interactions

#### II.1.1 *The Friedel-Creagh-Kmetz rule*

An old, but neglected study of the alignment of LCs (mainly azoxy compounds) on freshly cleaved crystals<sup>23</sup> suggested that the orientation of the LC molecules was determined by their physicochemical interactions: of 80 studies of LC alignment on crystal surfaces, 77 showed parallel orientation. If, however, a hole was drilled in the solid substrate, homeotropic alignment ensued in the suspended film. This led to the conclusion that LC films aligned parallel to a solid substrate if any interaction occurred and homeotropically in the absence of interactions.<sup>10</sup>

Solid-liquid surface interactions are phenomenologically described by the surface tensions of the solid substrate,  $\gamma_s$  and of the liquid  $\gamma_L$ .  $\gamma_L$  is a macroscopic description of the strength of the LC-LC interaction while  $\gamma_s$  describes the solid surface excess energy.

Thus, the above observations may be stated as<sup>6</sup>

$\begin{aligned}\gamma_s < \gamma_{LC} &\longrightarrow \text{homeotropic alignment} \\ \gamma_s > \gamma_{LC} &\longrightarrow \text{parallel alignment}\end{aligned}$
---

This empirical rule has been widely supported by experimental data, although not all results are in agreement. We will call it the "Friedel-Creagh-Kmetz" (FCK) rule.

#### II.1.2 *Surface tension*

##### II.1.2.1 *Liquid crystal surface tension*

In order to have thermodynamic significance, the LC surface tension,  $\gamma_{LV}$ , should be measured with the LC in equilibrium with its vapor. Most of the available data are relevant to an air-LC interface,  $\gamma_{LA}$ . Although the precision

of the different methods used to measure the LC surface tension should be  $10^{-4} \text{ J m}^{-2}$ , comparison of the published values, (Table VII), shows a dispersion, that may amount to 30% with the same method. This is probably due to non-equilibrium conditions and/or atmospheric contamination of the LC (for the influence of different methods see § II.1.10).

The surface tension of MBBA has been found impossible to measure precisely,<sup>113</sup> as the LC interface drifts continuously. LC surface tensions are of the order of  $25\text{--}40 \text{ erg/cm}^2$ .

### II.1.2.2 *Anisotropy of the surface tension of a LC*

The existence of a liquid crystalline state implies an anisotropic intermolecular potential. As surface tension results from the excess energy of the molecules at the surface, it would be expected to vary according to whether the LC molecules were oriented parallel or perpendicular to the surface.

Calculations of the surface tension anisotropy, taking into account only van der Waals interactions<sup>118,119</sup> leads to  $\gamma_{\parallel} < \gamma_{\perp}$ . This calculation is applicable to LCs of negative  $\Delta\epsilon$  as their long axis dipole moment ( $\mu_{\parallel}$ ) is weak and the off axis dipole moment ( $\mu_{\perp}$ ) averages out. As a result the LC molecules lie flat at the LC-air interface (e.g., PAA, Ref. 115).

MBBA has  $\mu_{\parallel} = 0.4 \text{ D}$  and is slightly tilted<sup>114</sup> at the free surface, which could be due to the angle between the molecular axis and the dipole moment. For LCs of strong positive  $\Delta\epsilon$ , experimental observations show that the LCs align normal to the free surface<sup>120</sup>, thus  $\gamma_{\parallel} < \gamma_{\perp}$ , which contradicts the theoretical evaluation of dipole interactions in LCs.<sup>119</sup> The calculated value of  $\gamma_{\parallel} - \gamma_{\perp}$  is  $7 \times 10^{-3} \text{ J m}^{-2}$  for PAA (Ref. 116) while  $\gamma_{\parallel} - \gamma_{\perp}$  of the order of  $5 \times 10^{-6} \text{ J m}^{-2}$  (Ref. 75, 120) is obtained from experimental observations (see Table VII). The Kirkwood-Buff approximation leads to  $\gamma_{\parallel} - \gamma_{\perp} = \gamma_0 (S/9) [10 - 7S/6]$  (Ref. 119)† with the previously mentioned limitations.

It has been suggested<sup>5</sup> that a situation could exist where the solid substrate surface tension,  $\gamma_s$ , has an intermediate value  $\gamma_{\parallel} < \gamma_s < \gamma_{\perp}$ , leading to a tilted orientation of the nematic director. Experimental values are much too small to explain the observed tilted alignment of MBBA on glasses onto which fatty derivatives of medium chain length ( $\text{C}_6\text{--C}_{10}$ ) have been adsorbed ( $\gamma_s \sim 26 \times 10^{-3} \text{ J m}^{-2}$ ). Such an effect would require  $\Delta\gamma \geq 8 \times 10^{-3} \text{ J m}^{-2}$  as calculated from theory. Further work seems to be required to ascertain the real order of magnitude and its relation to various LC classes.

### II.1.2.3 *The surface tension of solids*

The surface tension of a solid cannot be measured directly. Calculation of the excess surface energy from the energy of the broken bonds necessary to create

† Reference 113 suggests that after correction of errors in the evaluation of the integral,  $\gamma_{\parallel} - \gamma_{\perp} = \gamma_0 (S/3)(5 - 19/32S)$ .

a surface, give values of  $0.5$  to  $5 \text{ J m}^{-2}$ <sup>121</sup>; these values refer to the solid-vacuum interface,  $\gamma_s^0$ .

As soon as the solid surface is brought into contact with air, atmospheric constituents strongly adsorb onto the surface, lowering the surface tension from the uncontaminated value of the "surface pressure"  $\pi_0$ .

The solid-air interface has thus a surface energy,

$$\gamma_{SA} \approx \gamma_s^0 - \pi_0,$$

where  $\pi_0$  is approximately  $0.1 \text{ J m}^{-2}$ .<sup>128</sup>

Due to the fact that the solid surface chemical state is poorly defined, it has been suggested that oxide surfaces should be considered as covered by a thin layer of water, with  $\gamma_{SA} = 7 \times 10^{-2} \text{ J m}^{-2}$ .<sup>117</sup>

Cleaning procedures, as well as further thermal treatment, will modify the properties of a solid surface. In the case of silica layers, heating will desorb the physically absorbed water at around  $150^\circ\text{C}$  and following this will be condensation of surface hydroxy groups between  $170^\circ\text{C}$  and  $400^\circ\text{C}$ , to form oxygen bridges. Above  $400^\circ\text{C}$ , the oxygen bonding becomes irreversible, and above  $750^\circ\text{C}$ , the silica surface become irreversibly hydrophobic.<sup>122</sup> Irreversibly absorbed water causes  $\text{TiO}_2$  surfaces to become hydrophobic.<sup>123</sup>

In general, hydrophobic oxide surfaces consist of areas incapable of specific molecular interactions.<sup>123</sup> Complete removal of the specific interactions on inorganic substrates supposes thermal treatment at very high temperatures, which are not suitable for glass cells.

Tin oxide thin films, formed by CVD are hydrophobic; acid cleaning renders them hydrophilic.<sup>20</sup>

Even in the case of a uniform solid surface, its surface energy is difficult to predict. The same oxide may show different surface energies, depending on preparation conditions, subsequent thermal treatment, (which is unavoidable during display sealing) and cleaning procedures. For inorganic solid surfaces, however,  $\gamma_{SA}$  is greater than  $4 \times 10^{-2} \text{ J m}^{-2}$ .

To reliably establish the validity of the FCK rule it would be necessary to measure the surface tension of the solid in equilibrium with the LC vapor ( $\gamma_{sv^0}$ ), at the saturated vapor pressure. In this case  $\pi_0$  would be the pressure of the absorbed LC film. It is often claimed that LC alignment is not understood; the situation is not worse than that of surface chemistry.

### II.1.3 Solid-liquid crystal contact angle

#### II.1.3.1 The contact angle

When a liquid is deposited on a surface it often happens that it remains as a drop. The angle  $\theta_{SL}$  between the edge of the drop and the surface is related to  $\gamma_{LV}$ ,  $\gamma_{sv^0}$  and the interfacial energy,  $\gamma_{SL}$ , by the expression

$$\gamma_{sv} \cos \theta_{SL} = \gamma_{sv^0} - \gamma_{SL}. \quad (3.1)$$

TABLE VII  
Surface tension  $\gamma_L$  of some nematic LCs\*

X	L. C.	$\gamma_L$ 10 <sup>-3</sup> Jm <sup>-2</sup>	Ref.	Method	Remarks
SCHIFF'S BASE	MBBA	38	117	--	<ul style="list-style-type: none"> <li>One group of value <math>38 \pm 2</math> an other group <math>28 \pm 2</math></li> <li><math>\gamma_L</math> of MBBA impossible to measure accurately (113)</li> <li>Effect of impurities is slight (38)</li> <li>MBBA aligns nearly <math>\perp</math> at the free surface (114 b) <math>\Rightarrow</math>  <math>\gamma_{\parallel} &gt; \gamma_{\perp}</math></li> <li><math>\gamma_{\parallel} = 34</math> <math>\gamma_{\perp} = 26</math> (5)</li> </ul>
		$38 \pm 3$ (23°C)	114	VI	
		35.8	38	III	
		$35.3$ (25°C)	116	III	
		35.3	115	V	
		34	37	II	$\gamma_D = 29$ $\gamma_P = 9$ (117)
		34	34	I	$\gamma_D = 33$ $\gamma_P = 1$ (37)
		$32 - 34$	6	II	corr - uncorrected
		32.6*	1	II	$\gamma_L = 28.8$ corr. Harkins and Jordan (1)
		30	5	I	
		36.5	37	II	$\gamma_D = 34$ $\gamma_P = 1.5$ (37)
	80 MBBA/ 20 BBBA				
	PAA (120°C)	$39.6 \pm 0.4$	117 a	II	PAA aligns $\parallel$ to the free surface $\Rightarrow$ $\gamma_{\perp} > \gamma_{\parallel}$
AZOXY'S		39 (120°C)	117 b	VIII	
		38.9	115	V	
		$38.8 \pm 0.4$	138	VII	
		$38 \pm 4$	114 b	VI	$\gamma_{\parallel}^d$ (calc) = 37.8 $\gamma_{\perp}^d = 44.6$ (118)
		37.9	117 c	VIII	
		37 (120°C)	116	III	



	PAP (158°C)	29.1 29.2 29.8	117 b 115 117 a	VIII V II	
STILBENE	MBAB	37.3	38	III	
ESTER $\Delta \epsilon < 0$	BES	35.7	38	III	
$\Delta \epsilon > 0$	MPPB	24.5	34	I	
	HCPB	27	34	I	
TOLANES	ROTN 103	27.5 $\pm$ 0.3 (22°C)	20	III	
	MPT+PHT	25	34	I	not aligned on plasma PTFE I {34}
BIPHENYLS	5 CB	40	133	I	• C.B. aligns $\perp$ to the free surface $\Rightarrow$ $\gamma_{II} > \gamma_I$
		34.4	84	II	
		32 $\pm$ 0.5	20	III	
		30	32	I	
		28.1 (31.5°C)	113	I	• (Plates treated for homeotropic alignment)
	8 CB	27.9 (20°C)	113	I	• $\gamma_I = 30$
	E 7	26.2 (41°C)	113	I	
	E 8	29.3 (22°C)	20	III	
		30.6 $\pm$ 0.2 (22°C)	20	III	
PHENYLCYCLOHEXANE	ZLI 1132	31 $\pm$ 0.5 (22°C)	20	III	• Difficult to align homeotropically (20)

\* Methods: I, with hemy plate; II, de Nouy ring; III, hanging drop; IV, contact angle; V, capillary; VI, light scattering spectrum; VII, radii of curvature; VIII, maximum bubble pressure.

At equilibrium it should not matter whether the drop is deposited on the surface (advancing angle) or whether it is formed by pulling out a film of the liquid (receding angle).<sup>124</sup> On a LC drop, in practice, variations in  $\theta_{SL}$  as great as  $50^\circ$  may be observed, and experimentalists generally choose the advancing angle. When studying hydrophobicity, the receding angle is a better characterization of the surface.

The existence of hysteresis has been attributed to contamination of either the liquid or the solid, rough surfaces or absorbed surface film immobility.<sup>121</sup>

### II.1.3.2 *The contact of a liquid crystal with a solid*

Whatever the method used to measure the contact angle of a LC drop on a solid, observations are hampered by the continuous drift of  $\theta_{SL}$ . On the one hand the absorbed atmospheric constituents have to exchange with the LC molecules; on the other hand the elastic energy of the misaligned layer is weak and the evolution of surface attached disclinations is slow. Four days have been selected as the time necessary for a LC to attain equilibrium with an adjacent surface when making accurate measurements.<sup>113</sup> Liquid crystal hydrolysis and/or oxidation under the influence of both UV light and oxygen<sup>45c</sup> complicate experimental studies. Frequently the edges of LC drops are observed to be homeotropically aligned after 10 days, due to the formation of polar decomposition products.

On substrates which induce parallel LC alignment, the viscous flow of the LC tends to determine the direction of alignment, but many defects are formed and they evolve constantly, resulting in constant movement of the LC drop. It seems that reliable values can only be obtained with carefully controlled experimental conditions which has rarely been the case in the published studies.

### II.1.4 *The critical surface tension of a solid*

A useful empirical parameter has been proposed to characterize a solid surface. It has been observed that the contact angle  $\theta_{SL}$  of homologous alkanes varies linearly with the liquid surface energy. Extrapolation to  $\cos \theta_{SL} = 1$  led to a critical value  $\gamma_C$  which was characteristic of the solid employed.<sup>128</sup>

From Eq. (3.1)

$$\gamma_{LV} \cos \theta = \gamma_{SV} - \gamma_{SL}$$

and, therefore,

$$\gamma_C = \gamma_{SV} - \gamma_{SL}.$$

The introduction of a critical surface tension is only valid inasmuch as the values  $\gamma_{SL}$  and  $\pi_0$  ( $\gamma_{SV} = \gamma_S - \pi_0$ ) of different liquids are constant. If this is the case for polymers and nonpolar liquids, the use of polar liquids to measure

$\gamma_c$  may cause large variations of the extrapolated value. Therefore,  $\gamma_c$  values for polar oxide surfaces relate to the nature of the surface and the choice of the solvents. The following observations indicate that in these cases  $\gamma_c$  is not a useful parameter for the characterization of LC-oxide interactions.

- The critical surface tension of fused silica is  $\gamma_c = 78 \times 10^{-3} \text{ J m}^{-2}$ .<sup>125</sup>
- On  $\text{SiO}_x$  tangentially evaporated films,  $\gamma_c$  has been measured to be approx.  $38 \times 10^{-3} \text{ J m}^{-2}$  after correcting for surface roughness<sup>126</sup> with an anisotropy which depends on whether the edge of the drop is parallel or perpendicular to the evaporation direction.
- Normal evaporation is reported to produce films of  $\gamma_c = 48.7 \times 10^{-3} \text{ J m}^{-2}$  while obliquely evaporated layers show  $48.7 \times 10^{-3} \text{ J m}^{-2} < \gamma_c < 55.9 \times 10^{-3} \text{ J m}^{-2}$  for evaporation angles between  $0^\circ$  and  $60^\circ$ .<sup>127</sup>
- On SAIBE etched  $\text{SiO}_2$  surfaces, values of  $\gamma_c$  as low as  $24 \times 10^{-3} \text{ J m}^{-2}$  have been measured<sup>45a</sup> which is nearly the critical surface tension of water [ $\gamma_c(\text{H}_2\text{O}) = 22 \times 10^{-3} \text{ J m}^{-2}$ ].<sup>45c</sup>
- Atmospheric humidity causes the critical surface tension of glass to vary from between  $\gamma_c = 75 \times 10^{-3} \text{ J m}^{-2}$  for dry glass, to  $\gamma_c = 30 \times 10^{-3} \text{ J m}^{-2}$  at 100% humidity.
- Although water has a  $\gamma_c$  value of  $22 \times 10^{-3} \text{ J m}^{-2}$ , LCs ( $\gamma_c = 3 \times 10^{-2} \text{ J m}^{-2}$ ) do in fact align parallel on water.<sup>120</sup>

As developed in the following paragraph  $\gamma_c$  is equal to the solid surface tension  $\gamma_{sv}$  when the ratios of polar and dispersive interactions of both phases are equal. For this reason the critical surface tension of polymers may be employed to give a qualitative description of polymer-LC interactions. Measurements made on plasma polymerized films<sup>34,37</sup> showed acceptable agreement with theory, although some unexpected results were observed, i.e., tolans ( $\gamma_{LC} \sim 22 \times 10^{-3} \text{ J m}^{-2}$ ) were not aligned homeotropically by a sputtered Teflon layer ( $\gamma_c \sim 18 \times 10^{-3} \text{ J m}^{-2}$ ).<sup>34</sup>

Adsorbed surfactants reduce the solid surface tension. Fatty acids or their derivatives (alcohols and amines) exhibit a continuous range of  $\gamma_c$  values with alkyl chain length<sup>5,75</sup> but reported relations to LC alignment are somewhat conflicting (Figure 4). The same discrepancies are observed with alkyl trimethyl ammonium bromide derivatives.<sup>73</sup> The influence of the surface coverage (or packing density) is of the utmost importance<sup>8</sup> and consideration of  $\gamma_c$  is generally misleading (see paragraph 18).

The FCK rule has generally been quoted<sup>1,6</sup> using  $\gamma_c$  in place of  $\gamma_s$ , i.e.,

$\begin{aligned} \gamma_c < \gamma_{LC} &\longrightarrow \text{homeotropic} \\ \gamma_c > \gamma_{LC} &\longrightarrow \text{parallel alignment} \end{aligned}$
---

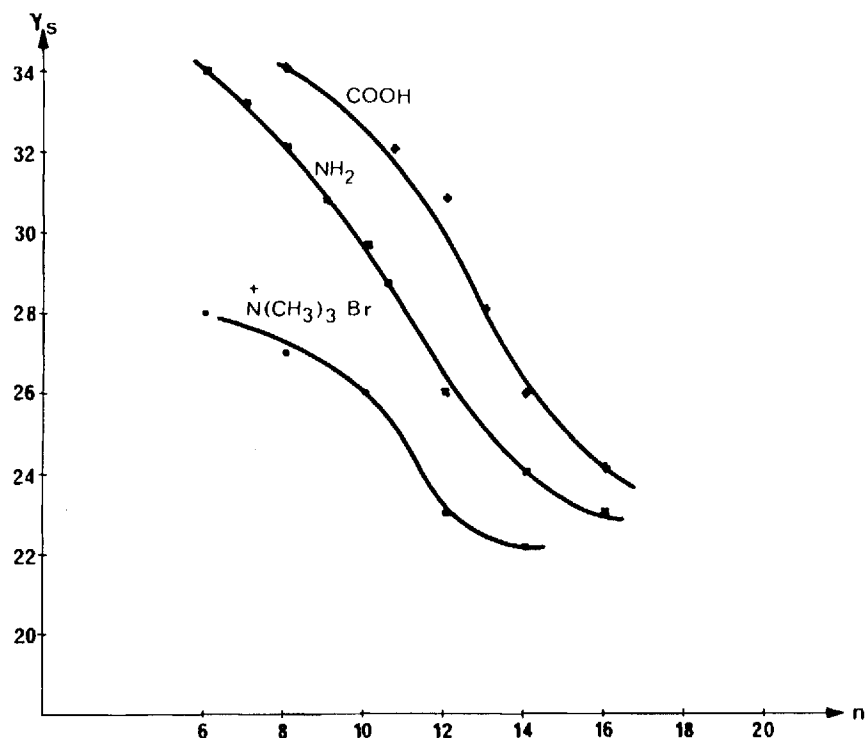


FIGURE 4 Variation of the surface tension of surfactant treated glass surfaces with increasing carbon content of the surfactant alkyl chain. [● from Ref. 75a, × Ref. 5a + Ref. 56].

and it is, therefore, not surprising that it encountered strong criticism. Compared to the expression of § II.1.1, where  $\gamma_s = \gamma_s^0 - \pi_0$ , it is evident that the above inequality employs values that are relevant to nonpolar solvents, to describe the behavior of LCs which have to be highly polar for practical application.

#### II.1.5 The polar and dispersive components of surface tension

Surface interactions are long range forces; either dispersive (van der Waals) forces, dipole-dipole interactions or double layer interactions.<sup>121</sup> These contributions are considered additive and the surface tension  $\gamma_i$  ( $i = s$  or  $l$ ) may be written as the sum of the dispersive  $\gamma_i^d$  and polar  $\gamma_i^p$  contributions,

$$\gamma_i = \gamma_i^d + \gamma_i^p.$$

Let  $d_i$  and  $p_i$  be the ratios of dispersive and polar contributions to the surface tension:  $d_i = \gamma_i^d / \gamma_i$ ,  $p_i = \gamma_i^p / \gamma_i$ . It is shown that the critical surface tension  $\gamma_c$

is  $\gamma_c = \phi \gamma_{sv}$  where  $\phi = \sqrt{d_L d_s} + \sqrt{p_L p_s}$ . When  $d_i = d_s$ , which implies  $p_L = p_s$ ,  $\phi = 1$  and  $\gamma_c = \gamma_{sv}$ .

Thus the empirical method of estimating  $\gamma_c$  may result in a value that agrees well with  $\gamma_s^d$  rather than the solid surface tension  $\gamma_{sv}$ .<sup>129</sup> Recent work on plasma copolymerized films with different  $\gamma^d$  and  $\gamma^p$  values<sup>37</sup> shows the relation of these considerations to nematic LC alignment.

### II.1.5.1 Polar interactions of LCs and surfaces

The interactions between the dipoles of LC molecules and the charged surfaces of oxides or ionic surfactants are certainly very important in the formation of the first surface layers, although theoretical understanding of the problem and the experimental data are poor. The effect of surface polarization has been demonstrated in the case of MBBA,<sup>130</sup> for which it was suggested that the MBBA molecules orient with their dipoles towards acid treated glass, but with their butyl chain towards surface cetylammonium bromide monolayers on glass.

In addition, the surface dipoles of sputter etched indium oxide have in some (but unreproducible) cases been observed<sup>131</sup> to align LCs of negative dielectric anisotropy parallel to the substrate, but positive LCs perpendicular to it. The same behavior is observed with surfaces treated with dicarboxylate<sup>78b</sup> chromium complexes, suggesting that only part of the acid group is absorbed onto the substrate. The polar interaction of MBBA with a humid glass substrate,<sup>†</sup> where  $E_s = 4.35 \times 10^9$  V/m, have been shown<sup>132</sup> to be accounted for through the surface electric field,  $E_s$  (Table VIII) as the polar part  $W_a$  of adhesion energy.  $W_a$  is related to the LCs molecular dipole through

$$W_a p = \delta \mu E_s \quad (\delta \text{ effective dipole density}) \\ (\mu \text{ effective dipole moment}).$$

In view of this the existence of a double layer (§ II.1.6) should be considered.

### II.1.5.2 Dispersive interactions of LCs and polymers

As already mentioned, nonpolar surfaces offer an important simplification in the theoretical description of liquid-solid interactions as the polar term becomes negligible regardless of the character of the liquid molecules. Most organic compounds as well as Liquid Crystals and polymers have  $d > p$ .

Denoting  $\gamma_i^d$  as the dispersive component of the surface tension, the

---

<sup>†</sup> This work has been extended to 5CB by these authors in Ref. 133 but the observation of homeotropic alignment of 5CB on glass cast some doubts on their conclusions.

TABLE VIII

Electrostatic field strength  $E_s$  and dispersion energies  $\gamma_s^d$  for some inorganic substrates (from Ref. 132)

Substrate	$E_s^a$	$\gamma_s^d (10^{-3} \text{ J m}^{-2})$
Rutile	$8.1 \times 10^4$	145
Rutile (bare)	$6. \times 10^4$	125
$\text{Al}_2\text{O}_3\text{-SiO}_2$ coated	$9.6 \times 10^4$	135
$\text{CaF}_2$	$7.5 \times 10^4$	105
$\text{SiO}_2$	$3.3 \times 10^4$	75
$\text{Al}_2\text{O}_3$ (40 Å on Al)	$5.7 \times 10^4$	335
Carbon black	$2.1 \times 10^4$	105
Teflon	0	25

<sup>a</sup> Calculated from the heat of adsorption  $E_\mu$  ( $\text{J m}^{-2}$ ) of the powders in solvents of different dipole moment  $\mu$ .  $E_\mu = E_{s\mu}$ .  $E_s$  in  $\text{V m}^{-1}$  per  $\text{cm}^2$  of surface.

Girifalco, Good, Fowkes, Young equation (GGFY) permits the calculation of the interfacial energy  $\gamma_{SL}$ :

$$\gamma_{SL} = \gamma_s + \gamma_L - 2\sqrt{\gamma_s^d \gamma_L^d}$$

For LCs,  $\gamma_L^d$  is of the order of  $10^{-2} \text{ J m}^{-2}$ .<sup>96,99</sup> Polyethylene has  $\gamma_s = \gamma_s^d = 3 \times 10^{-2} \text{ J m}^{-2}$  thus  $\gamma_{SL} 27 \times 10^{-3} \text{ J m}^{-2}$ .

In general the alignment of LCs on polymers is well described by the FCK rule.<sup>34,37</sup>

### II.1.6 The "smecticlike" interfacial layer

The interfacial layer between a solid and a liquid gives rise to a charge separation, which can be well described in terms of a double layer (DL) which consists of a compact ordered monolayer firmly bound to the substrate, followed by a layer of diffuse charges. This DL has not been studied in LCs where the electric charge density is not known, but its existence has been theoretically<sup>134</sup> predicted and is supported by electrical measurements.<sup>135,136</sup> It could be relevant to the higher order parameter of the interface between nematic LCs and solids or gases.

Practical LCs being ionically very pure the compact layer will be the main component.

Many experimental observations imply that the surface layer has a higher order than the bulk. Microscopic observation of nematic layers squeezed between glass slides suggested that there is a thin interfacial layer firmly bound to the glass substrate,<sup>10</sup> which determines the orientation of the adjacent layer.

Infrared spectroscopy indicates that the excess order depends upon the nature of the substrate (glass,  $\text{In}_2\text{O}_3$ , polysiloxane).<sup>137b</sup> Additional evidence for the existence of a DL comes from observations of a film of the LC 5CB, less than 250 Å thick pulled apart in air. Such a layer has the appearance of a smectic layer with an order parameter,  $S_\phi$ , 1.005 times that of the bulk value  $S_\zeta$ .<sup>120</sup>

Also, whereas the surface tension of a normal liquid decreases when the temperature increases, the reverse has frequently been observed with nematic LCs.<sup>113</sup> ‡ This effect could be explained by a higher surface order parameter  $S_\phi$ :  $\gamma_{\text{CL}}^0$  is the surface tension of the isotropic LC, then the surface tension  $\gamma^0(S)$  of the oriented layer is

$$\gamma^0(S_\phi) = \gamma_{\text{CL}}^0 - \alpha S_\zeta \text{ with } \alpha \sim 2 \times 10^{-4} \text{ J m}^{-2}.$$

Optical measurements clearly show the higher birefringence of the interfacial layer, e.g.,  $S_\phi = 0.5$ , and  $S_\zeta = 0.4$  (Ref. 137) for the LC 7CB. Theoretical investigations of surface alignment have to take into account this more ordered surface layer.<sup>111</sup> The structure of this first compact layer, which also determines the surface pressure of the adsorbed LC vapor, influences the orientation of the nematic crystal layers throughout the bulk of the LC, as does a layer of smectic liquid crystal deposited on a substrate.<sup>90</sup>

The dispersive interactions of LCs with solid surfaces are strong. For metals and oxides  $\gamma_s^d$  is about  $0.1 \text{ J m}^{-2}$  and around  $3 \times 10^{-2} \text{ J m}^{-2}$  for polymers. The dispersive component of LC surface tension has been found predominant over polar interactions  $\gamma_{\text{L}}^d \sim 3 \times 10^{-2} \text{ J m}^{-2}$ ; the interfacial energy is for most LCs essentially dispersive leading to the parallel alignment of the alkyl-aromatic part of the LC molecules.<sup>124</sup> The polar contribution of the solid-liquid interactions will favor the parallel alignment of negative  $\Delta\epsilon$  LCs while it will lower the anchorage of positive  $\Delta\epsilon$  LCs.<sup>133</sup> Experimentally it is observed that cyanobiphenyls are more easily oriented homeotropically than negative esters. Silicone layers, for example, orient high positive  $\Delta\epsilon$  LCs homeotropically but not phenyl cyclohexanes.

During the initial contact between the LC and the surface, the smecticlike layer forms. Defects spreading out through the LC film are initiated by some surface irregularities. Often they evolve in time as adsorbed atmospheric components exchange with LC molecules.

The energy confined in the smecticlike layer is higher than can be added to the LC film by mechanical, electrical, or thermal action. Once it is formed, the substrate enclosing the LC film may be twisted without changing the interfa-

---

‡ We have not reviewed the influence of temperature on LC surface tension and alignment as our own work on the subject is insufficient on the one hand and published results too contradictory on the other hand. Some indications may be found in Refs. 3 and 111.

cial layer.<sup>54</sup> Also its orientation at the free surface is not changed by applying a magnetic field.<sup>138</sup> Consequently, the physical properties of LCs are weakly affected by the very first layer (see also § II.3).

### II.1.7 *Nonuniform coverage*

When an aligning layer is deposited nonuniformly on a substrate, both the exposed substrate and the aligning layer will influence the LC alignment. If the substrate and the alignment layer tend to induce different orientations of the LC molecules, tilted alignment will be observed. The theoretical computation of the equilibrium director orientation shows that different tilt angles will be observed, depending on relative values of the LC elastic constants.<sup>139</sup> This situation is likely to occur in the case of absorbed surfactants at low coverage<sup>140</sup> or when hydrolyzed chloro or amino silanes form polymeric nodules on the surface,<sup>141</sup> or when very thin polymeric<sup>91</sup> or evaporated films are deposited on the substrates.<sup>132</sup> In these cases one is dealing with a parallel-orienting substrate presenting patches of homeotropic-aligning layers.

Alternating stripes of surface materials, one giving a homeotropic and the other giving parallel alignment produce a bulk average tilt angle of  $45^\circ$ .<sup>139</sup> When the bend constant,  $K_{33}$ , is larger than the splay constant,  $K_{22}$ , theoretical calculations indicate that the angles will be less than  $45^\circ$ , while it will be greater in the inverse case.

### II.1.8 *Alignment by surfactant*

Almost every known class of surface active agent has been observed to influence LC alignment (see § 3, Part I).

In most cases LCs are aligned homeotropically by long chain surfactants adsorbed on inorganic substrates. Because they lower surface tension, it has often been thought that the FCK rule should apply and explain the observed alignment.

Superficial films of adsorbed molecules are known to exist in four states<sup>121</sup>: the G (gaseous) state corresponds to a weak coverage. Higher coverages lead to an L (liquid) state either expanded ( $L_1$ ) with an average surface of  $50 \text{ \AA}^2$  ( $40\text{--}70 \text{ \AA}^2$ ) covered by each adsorbed molecule as for long chain polar compounds or a condensed ( $L_2$ ) state where the surface covered by each adsorbed molecule is about  $22 \text{ \AA}^2$  (cetyl alcohol).

Dense layers create S (solid) films with an area of  $20.5 \text{ \AA}^2$ . Some surfactants produce both the  $L_1$  and  $L_2$  state with an intermediate (I) phase. The properties of superficial films of phospholipids (e.g., lecithin) have been explained as due to their liquid crystalline organization (Figure 7).

In order to obtain monolayers of known structure, a Langmuir balance is generally used,<sup>124</sup> but the technique is tedious and difficult to apply in industry. The normal practice, therefore, is to adsorb layers from solution and relate



their structure to that of the Langmuir monolayer. The retraction method has been shown to form good monolayers<sup>142</sup> although they present slight differences in their properties compared to the former,<sup>143</sup> probably because of the incorporation of solvent into the layer.

The investigation of the structure of layers adsorbed from solutions is still in progress<sup>144</sup> and there are few cases where it is complete. In Figure 4 we have gathered experimental values of the critical surface tension of glass covered with adsorbed layers of fatty derivatives of increasing chain length. If the results are assumed to indicate the influence of the carbon content of the chain on the substrate interfacial energy, the relation of LC alignment is not so clear, as in every case MBBA is aligned parallel to the substrate in the upper portion of the curves and homeotropically in the lower one. "On the completion of the adsorbed monolayer on the surface of a solid, the orientation of hydrocarbon molecules is parallel to the substrate as shown in Figure 5, whereas polar-nonpolar molecules on a polar solid stand upright as shown in 5b. However, if plenty of area is available, as in a dilute film, the polar-nonpolar molecules also lie down. As the film thickens and becomes multimolecular, the orientation in the first layer of polar-nonpolar molecules preserves the perpendicular type of orientation. If the vapor becomes saturated and the liquid of the film wets the solid, the film is relatively thick (about seven molecules thick for water at 25°C) and the molecules in the surface of the film have approximately the same orientation as in the surface of the liquid itself".<sup>124</sup>

In addition, the packing density of fatty acids depends on their chain length.<sup>142,145</sup> This could be an explanation for the tilted alignment of MBBA on surfaces covered by retracted layers of C<sub>10</sub>-C<sub>6</sub> fatty derivatives.

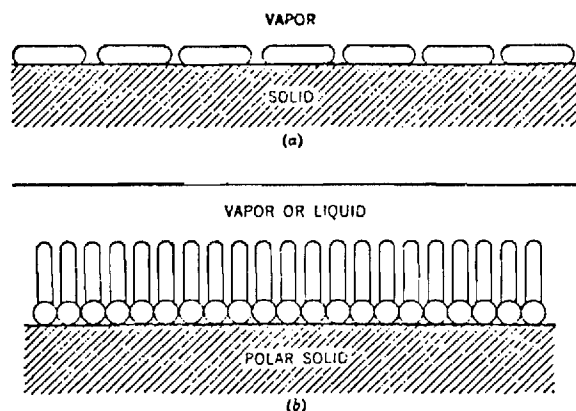


FIGURE 5 Orientation of molecules in complete monolayers. (a) Hydrocarbon molecules. (b) Polar molecules on the surface of a polar substrate. (From Ref. 124).

Liquid crystal alignment may be understood from the surfactant's adsorption isotherms. Cetyl ammonium bromide (CTAB) solutions in water adsorb parallel to the substrate at low concentration while at higher concentration the surfactant molecules orient perpendicular to the substrate.<sup>8</sup> MBBA deposited on these layers takes the surfactant orientation (Figure 6).

Phospholipids (e.g., lecithin) monolayers have different structures (Figure 7) depending on their surface pressure, retraction on glass substrate keeps the layer structure.<sup>147</sup> On tightly packed layers, cyanobiphenyls show a tilted orientation whereas on layers of lower packing density homeotropic orientation is observed. Experimental evidence leads to the conclusion that LC molecules are imbricated in the surfactant layer.<sup>148</sup>

The efficiency of a surfactant to align LCs also depends on its molecular structure: cyanobiphenyls are much more easily aligned homeotropically than phenylcyclohexanes.

As silanes may form covalent bonds with oxide substrates one would expect more permanent effects to result from the adsorption of long chain silane derivatives.

Very little is known about the structure of silane monolayers. Polymeric nodules very often form on the surface<sup>141</sup> but can be avoided by anhydrous conditions.<sup>149</sup>

Octadecyltrichlorosilane (OTS) adsorbed from nonaqueous solutions forms dense monolayers.<sup>144</sup> Carbon-14 counting shows a surface density of  $1.5 \times 10^{14}$  mole/cm<sup>2</sup>, as compared to  $5 \times 10^{14}$  for <sup>14</sup>C arachidic acid, which corresponds to close packing of Si-O bonds associated in three dimensions.<sup>150</sup> All our test LCs aligned homeotropically on oxide substrates covered with OTS. 3-(2-Aminoethyl)aminopropyl TMS, used to facilitate homogeneous alignment (Table V), is also known to be densely adsorbed on tin oxide from a 5% solution in toluene.<sup>149</sup>

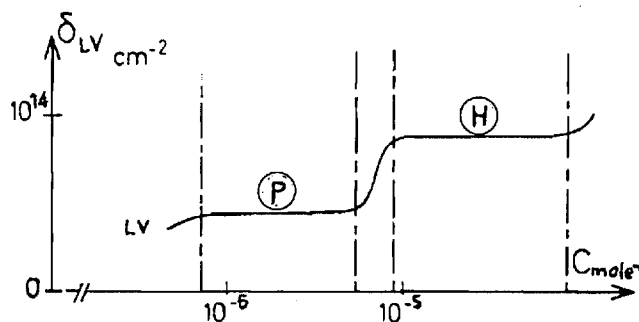


FIGURE 6 Variation of the superficial density ( $\delta_{sv}$ ) of adsorbed cetyl trimethyl ammonium bromide (CTAB) with its concentration in solution. (From Ref. 157).

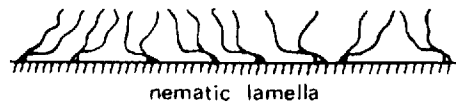
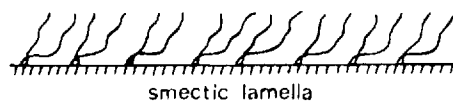
ALIGNMENT OF LIQUID CRYSTALS

51

GASEOUS (G) STATE



LIQUID (L) STATE



SOLID (S) STATE

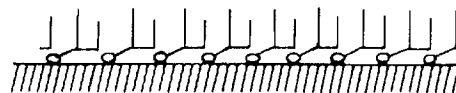
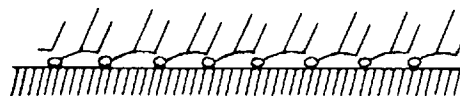


FIGURE 7 Schematic representation of phospholipid (e.g., lecithin) monolayers. (From Ref. 146).

### II.1.9 *Surface hydrolysis*

Liquid esters have surface tensions of  $28\text{--}30 \times 10^{-3} \text{ J m}^{-2}$  and should spread on high energy surfaces such as metals and oxides. Whereas they do spread on metals they do not always do so on glasses or oxides. This irreproducibility has been related to the ester hydrolysis catalyzed by adsorbed water,<sup>142</sup> the ester being unable to spread on an adsorbed layer of its own hydrolysis products.

The same is believed to be true of the occasionally observed homeotropic alignment of LC esters of Schiff bases (SB) on glasses and some oxides ( $\text{Al}_2\text{O}_3$ ,  $\text{In}_2\text{O}_3$ ). This effect is normally only observed if the surfaces have previously been washed in acid. This alignment disappears when the substrate is fired and is not observed with pure LCs of other molecular structure. On dry substrates, LC esters, as opposed to liquid esters,<sup>142</sup> are flat on the surface due to the carboxylic group interacting strongly with the oxide.<sup>151</sup>

SBs are completely hydrolyzed during HPLC on silica columns<sup>20</sup> and are known to be very sensitive to moisture.<sup>152</sup> Hydrolysis of ester or SB LCs produce alkylbenzoic acid or alkylamine, respectively, both of which are known to induce homeotropic alignment. Surface hydrolysis leads to local concentrations higher than could be adsorbed from solutions; 1% concentrations of these substances in the LC are required to induce the same alignment. An indication that surface hydrolysis has occurred is the formation of defects that remain stuck to the substrate even after a heating cycle or the emptying and refilling of a cell. A related impurity induced homeotropic aligning effect is observed when LC layers are either left in air or submitted to light irradiation. Photooxidation of the LC forms oxyderivatives<sup>45c</sup> that induce homeotropic alignment. In the case of unsealed cells the perpendicular orientation proceeds from the outer edge.

### II.1.10 *Measurement of LC surface tension*

This section is not devoted to a discussion of experimental surface tension measurements that would be found, for instance, in Ref. 121, but to the implications of the choice of one method. Capillary, du Nouy, Wilhemy methods imply the contact of LCs with surfaces.

From the preceding considerations of the LC–solid interaction one can understand the difficulties, generally underestimated, of obtaining reliable values; after long and careful studies it has been concluded that surface tension of MBBA is “impossible to measure”.<sup>113</sup>

As LCs lie generally parallel to solid surfaces the above quoted method should give a value near that of  $\gamma_{\parallel}$ .

Only in the hanging drop method are the solid–LC interactions minimized and the  $\gamma_{LV}$  values should be obtained.<sup>116</sup> As LCs often orient perpendicular to the free surface the value of  $\gamma_{\perp}$  would be obtainable with a precision of about 5%. In fact, even in this method the solid–liquid interactions are predominant.<sup>20</sup>

The wide range of literature values may correspond to different aligning conditions and indicate an anisotropy  $\Delta\gamma$  of about 10 erg, in agreement with theoretical considerations.<sup>119</sup>

### II.1.11 Summary of Section II.1

As the solid surface tension,  $\gamma_s$ , is not measurable, one has sought to use, instead, the experimental  $\gamma_e$  value, which gives a rough expectation of the direction of LC alignment. This can only be exact when the ratio of the polar and dispersive components of both the solid and the LC are equal.

A quantitative description of a LCs alignment requires knowledge of the polar and dispersive parts of surface tension as polar interactions depend on a LCs dielectric anisotropy and may be predominant.

Determination of a LCs surface tension is, currently, not accurate enough to allow a precise comparison of substrate and LC surface tension. The majority of recent work suggests the validity of the FCK rule; much more work has to be done to get reliable values of a LCs surface tension. As long as experimental values of  $\gamma_{MBBA}$  continue to be found between 38 and 28 erg/cm<sup>2</sup>, or  $\gamma_{SCB}$  between 30 and 40, critical evaluation of the FCK rule, which requires a knowledge of  $\gamma$  to better than 1 erg/cm<sup>2</sup>, is meaningless.

In our opinion there are no sound experimental data that invalidate this rule. Discrepancies indicate experimental error and we will suggest its use as a fair estimate of the expected alignment of a LC.

## II.2 Elastic orientation on grooved surfaces

### II.2.1 Geometrical factors

On high energy substrates ( $\gamma_{sv} \geq 4 \times 10^{-2}$  J m<sup>-2</sup>), LCs align parallel to the substrate. Sometimes, the flow of a LC drop will produce a nearly uniform alignment, albeit with many defects. This orientation occurs most easily when the LC is in its isotropic state. Very slow cooling<sup>5</sup> favors uniformity and good alignment is obtained on cooling in a magnetic field.<sup>54</sup>

These methods are impractical and uniformity is more easily obtained on grooved surfaces. Grooves are produced by rubbing (glass plates), unidirectional polishing, tangential evaporation, tangential ion-beam etching of oxides, or the formation of a grating on the substrate.<sup>47,54</sup>

Once the first interfacial layer is formed, the LC layer aligns through the nematic interactions at the shear plane; the LCs anchorage is fairly weak and defines a slippery surface. (see § II.3.1.) In these conditions, theoretical calculations of the elastic energy added to the LC bulk by a periodic surface deformation show<sup>43</sup> that the LC layer has an energy which is greater when the LC director is perpendicular to the groove direction  $\mathbf{d}$  (but parallel to the substrate) than when the director lies in the direction of the groove.

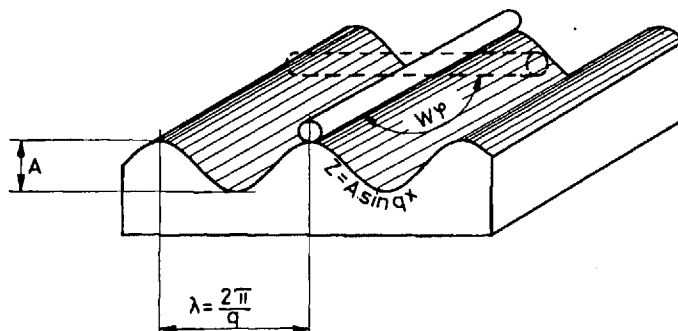


FIGURE 8 The sinusoidal model of a grooved surface. The LC molecules have higher elastic energy in the orientation perpendicular to the plane than parallel to it.

If the surface profile (Figure 8) is defined by the depth,  $A$ , of the grooves and their spacing  $\lambda = 2\pi/q$

$$Z = A \sin qx \quad U = \frac{K}{4} A^2 q^3$$

where  $K$  is the LC elastic constant. Table IX summarizes the profiles obtained by different grooving techniques and the related increases in energy for alignment parallel to the grooves. Photolithographically formed gratings allow the characterization of the periodic profile that influences the alignment. For 250 Å deep grooves uniform alignment of MBBA is obtained for

$$\lambda < 3.4\mu.$$

In general the ratio  $A/\lambda$  is smaller than 1.

TABLE IX

Estimated values of depth and spatial distribution of grooves on various substrates in the sinusoidal approximation

Surf. preparation	Depth $A$ (Å)	Spacing (Å)	Energy <sup>a</sup> $U$ $\text{J m}^{-2}$	Ref.
Rubbed glass	10	200	$8 \times 10^{-5}$	43(a)
Polished glass (diamond paste)	200	1000	$2.4 \times 10^{-4}$	43(b)
Diamond pencil scratches	10000	$< 10 \mu$	$15 \times 10^{-7}$	47
Evaporated $\text{SiO}_2$ 60°	100	200–400	$6 \times 10^{-4}$	44(a)
Gratings	250	3200	$1.2 \times 10^{-4}$	54

<sup>a</sup>  $U$  is the excess energy of the nematic liquid crystal aligned perpendicular to the grooves over its energy when it is aligned parallel to them. Calculated from  $U = (1/4)K A^2 q^3$  assuming a unique elastic constant  $K = 10^{-11}$  N.

If the different elastic constants of the LC are taken into account, calculations<sup>47</sup> indicate that for  $K_{22} > 3K_{33}$  a metastable configuration exists where  $n$  is  $\perp$  to  $d$  which cannot be observed, as  $K_{22} \sim K_{33}/2$  for LCs.

Grooving does not influence homeotropic alignment provided the surface profile is symmetrical (Figure 9a'). Silanes or silicones deposited on grooved surfaces still induce homeotropic alignment.<sup>20,157</sup> Sawtooth profiles may produce an average tilted orientation in the bulk of a LC<sup>44</sup> (Figure 10), as will an unsymmetrical coating of the grooves.<sup>108</sup> Considering that the LC molecules are either lying parallel to the substrate or orthogonal to it<sup>111b</sup> three configurations of the LC may exist.<sup>7</sup> In the case of Figure 9a' the elastic energy of the LC layer is not a minimum and it will not be observed on a sinusoidal profile as described in Figure 8.

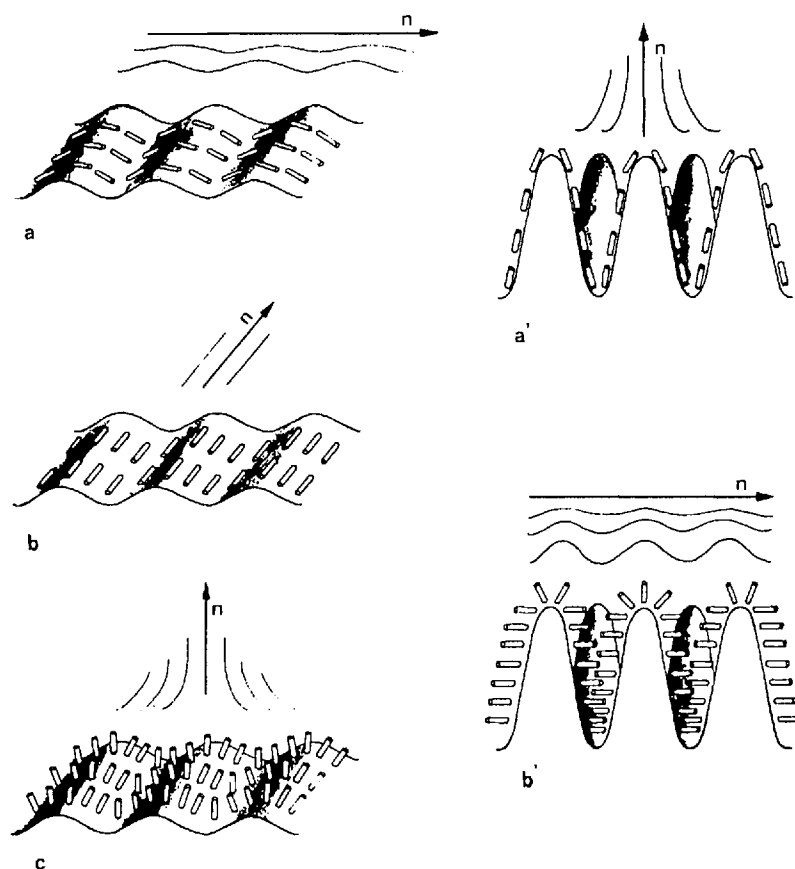


FIGURE 9 On grooved surface, parallel or homeotropic alignment may be observed depending upon the spatial period to amplitude ratio.

A three dimensional profile will create an alternation of peaks and valleys and constrain the LC to take the configuration of Figure 9b.

Depending on the width to depth ratio as compared to the molecular dimension the following situation may occur: if the substrate tension energy is high the molecules will lie flat on the surface but the bulk average will be homeotropic (similar considerations are found in Ref. 57). Lowering the surface tension energy by surfactant adsorption will orient the molecules perpendicular to the surface resulting in an homogeneous alignment.

Experimental evidence will be published later.† It requires that the depth of the hole be bigger than its width and the spacing of two pits is of the order of, at least, three molecular dimensions (i.e., 60 Å as LC molecules typically have length of 20 Å and width of 6 Å).

### II.2.2 Mixed alignment

The alignment of LCs on parallel orienting surfaces with patches of a homeotropic aligning agent has been considered in § I.1.7.

Obliquely ( $\theta > 15^\circ$ ) evaporated  $\text{SiO}_x$  layers align LCs homogeneously. An additional tangential evaporation ( $\theta < 15^\circ$ ), which would otherwise produce a tilt angle of  $25^\circ$ , permits the selection of any orientation ( $\pm 3^\circ$ ) of the LC molecules between  $0^\circ$  and  $25^\circ$ , as the asymmetry of the grooves increases. Deposition of a dense layer of a homeotropic aligning agent (see § II.1.8.) on a symmetrically grooved surface (either rubbed or obliquely evaporated) will not change the homeotropic orientation,<sup>69,17</sup> but as the first monolayer is oriented normal to the surface, a distortion exists in the LC layer. When such a homeotropic aligning layer is deposited on a nonsymmetric layer, producing a tilt angle  $\phi$ , the complementary,  $\phi + \pi/2$ , tilt angle is observed (Figure 3).<sup>5,20,157</sup> ‡

## II.3 Anchoring energies

### II.3.1 Anchoring energies and the interfacial layer

The interactions of the LC molecules with the surface have to be taken into account when considering the LCs static deformation.

The energy of interaction,  $W_s$ , can be expressed phenomenologically as the sum of an isotropic energy term,  $W_0$ , an in-plane (twist or torsion) anchorage and an out-of-plane (azimuthal) anchorage:

$$W_s = W_0 + W_\phi + W_\theta, \quad (3.1)$$

where the angles are as indicated on Figure 11. The angular dependence of  $W_\phi$  and  $W_\theta$  can be described<sup>153</sup> by

† Similar observations have been reported in Appl. Phys. Lett. **36**, 144 (1980) by W. R. Heffner *et al.*

‡ F. Gharadjedaghi, "Liquid crystal alignment techniques producing controllable tilt angles" presented at the 4th Liquid Crystal Conference of Socialist Countries, October, 1981.



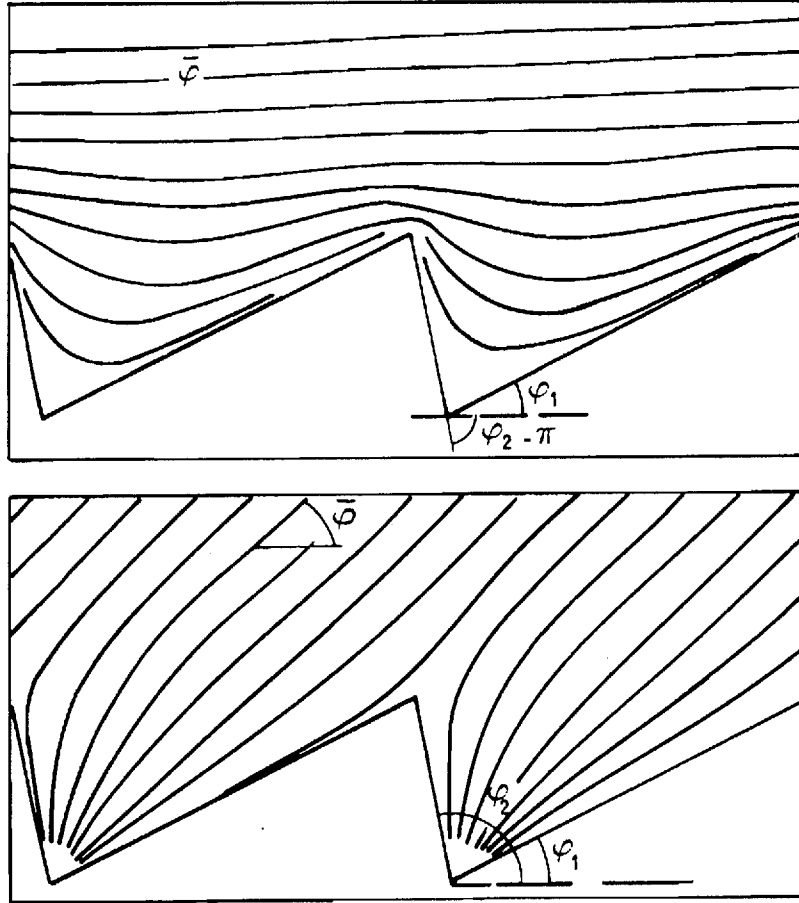


FIGURE 10 Unsymmetrical grooves may induce tilted alignment (case b) as evidenced by a rheographic model. (From Ref. 44). (a)  $\phi = \phi_1$  on surface 1,  $\phi = \phi_2 - \pi$  on surface 2,  $\bar{\phi} = 0$ . (b)  $\phi = \phi_1$  on surface 1,  $\phi = \phi_2$  on surface 2,  $\bar{\phi} = \phi_1[\pi/(\pi - \phi_2 + \phi_1)]$ .

$$W_\phi = B_\phi \sin^2 \phi, \quad (3.2)$$

$$W_\theta = W_0 + B_\theta \sin^2 \theta. \quad (3.3)$$

In the physical chemistry of surfaces, interfacial interactions are usually described by the surface tension of both phases.

When a liquid of surface tension  $\gamma_{LV}$  comes into contact with a solid of surface tension  $\gamma_{SV}$ , and interfacial layer builds up whose energy  $\gamma_{SL}$  (identical to  $W_s$ ) is

$$\gamma_{SL} = \gamma_{SV} + \gamma_{LV} - W_a, \quad (3.4)$$

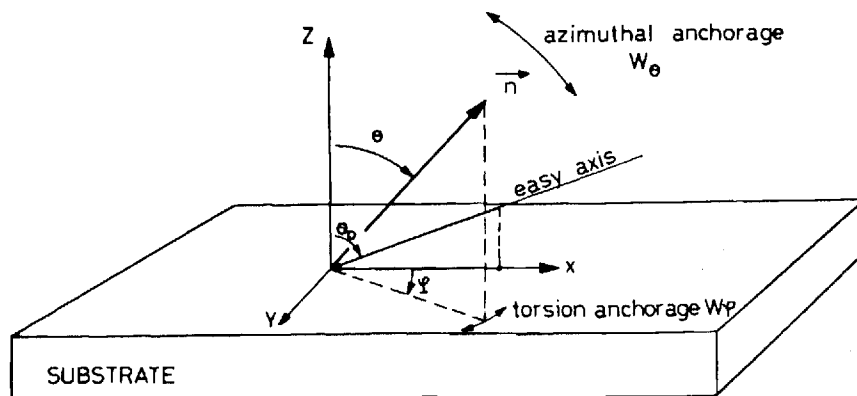


FIGURE 11 Definition of in-plane and azimuthal anchoring energies.

where  $\gamma_{sv}^0$  is the solid surface tension at equilibrium with liquid saturated vapor (which is related to the solid-vacuum interface free energy  $\gamma_s$  and the adsorbed liquid layer surface pressure  $\pi_0$  by  $\gamma_{sv}^0 = \gamma_s - \pi_0$ ) and  $W_a$  is the adhesion energy which may be approximated<sup>159</sup> by

$$W_a = 2\sqrt{\gamma_{sv}^0 \gamma_{LV}}. \quad (3.5)$$

The solid surface energy,  $\gamma_s$ , is not directly measurable and depends on the surface preparation and history, but for inorganic substrates  $\gamma$  is calculated to be  $>0.2 \text{ J m}^{-2}$ , in agreement with values obtained from heat of immersion measurements.<sup>121</sup> For polar liquids the surface pressure  $\pi_0$  exceeds  $0.1 \text{ J m}^{-2}$  leading to  $\gamma_{sv}^0$  values  $>7 \times 10^{-2} \text{ J m}^{-2}$  (Ref. 117) (the surface tension of an inorganic substrate covered with a water layer).

In the case of a liquid of  $\gamma_{LV} = 3 \times 10^{-2} \text{ J m}^{-2}$ , which is typical for LCs, the interfacial layer energy  $\gamma_{SL}$  is obtained from (3.4) and (3.5) giving  $\gamma_{SL} = 8 \times 10^{-3} \text{ J m}^{-2}$ .

The thickness of the interfacial layer is not known precisely but it extends over at least  $100 \text{ \AA}$  in a resistive liquid with LC molecular dimensions.

From the interfacial energy profile as sketched in Figure 12, one sees that the anchoring energy varies with the distance from the surface.

The excess energy of the interfacial layer produces in nematic LCs a higher ordering which creates the smecticlike layer described in § II.1.6. As surface tension exerts a force normal to the substrate, there is no dependence of the interfacial energy on the in-plane orientation of the molecules.

### II.3.2 In-plane anchorage energy

The torsion anchorage,  $W_\phi$ , results from substrate nonuniformity which may be controlled, for instance, by uniform grooving of the surface (Figure 8), in

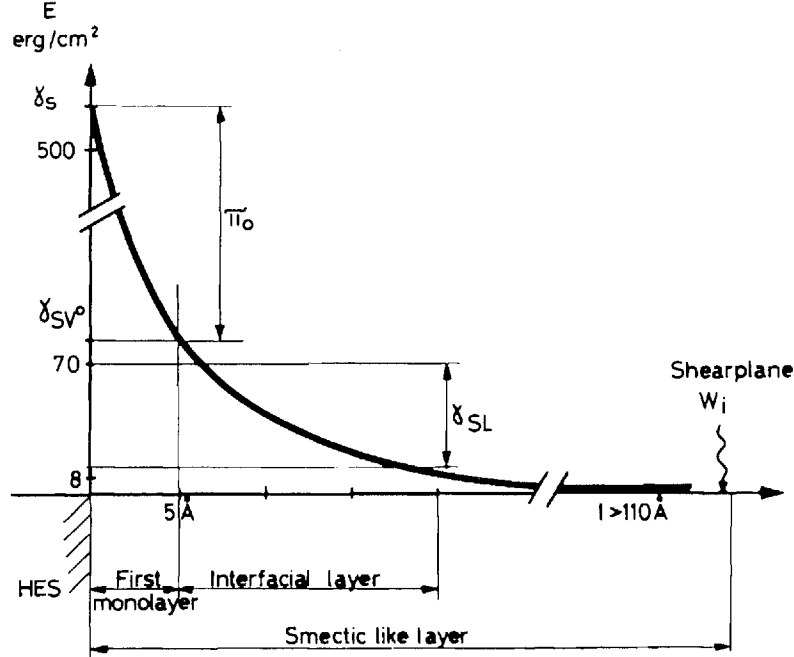


FIGURE 12 The surface-LC interaction energies vary with the distance to the surface. Close to the surface an ordered layer is related to the smectic organization. There exists a shearing plane at a distance where the energy of elastic deformation equals the excess energy due to surface interactions.

which case  $W_\phi$  may be calculated (see § II.2;  $W_\phi \equiv U$ ).  $W_\phi$  may be roughly estimated from the width,  $h$ , of surface disclination lines<sup>153</sup>

$$W_\phi = \frac{\pi^2 K h}{2 d^2}$$

(where  $d$  is the LC layer thickness), or measured from the variation in twist angle of a twisted layer subject to a magnetic field.<sup>155</sup> As both experimental measurements and the elastic alignment theory relate to the alignment beyond the smectic layer, calculated and experimental values, as compared in Table X, show that the orders of magnitude are in fair agreement. In every case the torsion anchoring energy is higher than the bulk twist energy

$$W_{\text{twist}} = K \phi_r^2 / 2d \approx 10^{-6} \text{ J m}^{-2}$$

( $\phi_r$  = twist angle, See Ref. 158).

In a twisted nematic layer, minimizing the bulk free energy leads to the equilibrium condition  $d\phi/dz = \text{constant}$ . In the vicinity of the substrate it is

TABLE X  
Comparison of calculated and experimental values of the in-plane (torsion) anchoring energies

Substrate	$W_\phi$ calc ( $\text{J m}^{-2}$ ) <sup>a</sup>	$W_\phi$ exptl ( $\text{J m}^{-2}$ )
Glass	...	$5 \times 10^{-5}$ (153)
Rubbed glass	$8 \times 10^{-5}$	$7 \times 10^{-6}$ (155) $10^{-4}$ (153)
SiO <sub>2</sub> evap 30°	$5 \times 10^{-4}$	$10^{-3}$ (153)
Heptylamine on glass	...	$\sim 5 \times 10^{-5}$ (5)
Trimethyltrichlorosilane on glass	...	$\leq 5 \times 10^{-6}$ (5)

<sup>a</sup>  $W_\phi \equiv U(\text{Table IX}) = 1/4 K A^2 \phi^3$  ( $1 \text{ erg/cm}^2 = 10^{-3} \text{ J m}^{-2}$ ).

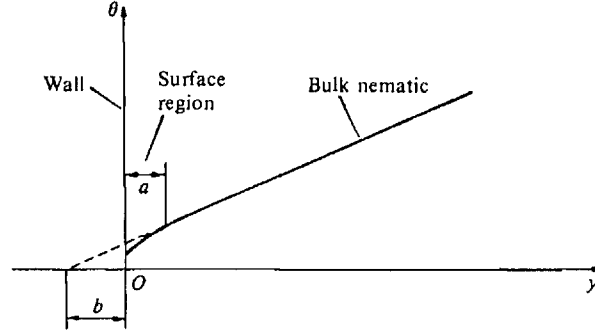


FIGURE 13 Definition of the "extrapolation length." Weak in-plane anchoring corresponds to  $b \ll d$ . (From Ref. 156).

expected that this condition does not hold<sup>156</sup> and extrapolation of the linear variation of  $\phi_{(z)}$ , to  $\phi = 0$  occurs at  $z = -b$  (Figure 13). The "extrapolation length"  $b = K/B\phi$  would in this case define the condition of strong anchoring. The twisted nematic layer behaves as if it had a thickness  $d + 2b$ ; thus the anchoring is strong if  $2b \ll d$ .

The threshold voltage under applied electric field is given<sup>157</sup> by

$$V_{th} = \frac{\pi}{d + 2b} \sqrt{\frac{4\pi K}{\Delta\epsilon}} \left( 1 - \frac{2K}{B_\phi d} \right). \quad (3.6)$$

As the torsion anchoring energy on grooved surfaces may vary from  $5 \times 10^{-6}$  to  $10^{-4} \text{ J m}^{-2}$  (Table IX) the extrapolation length may reach  $2\mu$  for a typical LC cell ( $d = 10^{-5} \text{ m}$ ) ( $K = 10^{-11} \text{ N}$ ). In fact we have not found experimental evidence for the extrapolation length.

### II.3.3 Azimuthal anchorage

As  $W_\phi$  is independent of the interfacial interactions on uniform surfaces, the anchoring energy reverts to the energy of the azimuthal anchorage, which is equal to the difference between the interfacial energy when the LC is aligned parallel or perpendicular. Let  $\xi(0)$  and  $\xi(\pi/2)$  be the values of the physical property  $\xi$  in both orientations

$$W_\theta = W_0 + B_\theta \sin^2 \theta = \gamma_{SL}(0) + \left[ \gamma_{SL}\left(\frac{\pi}{2}\right) - \gamma_{SL}(0) \sin^2 \theta \right]. \quad (3.7)$$

In Eqs. (3.4) and (3.5),  $\pi_0$ ,  $\gamma_{SL}$  and  $W_a$  are  $\theta$  dependent, and

$$B_\theta = \gamma_{SL}\left(\frac{\pi}{2}\right) - \gamma_{SL}(0) \\ = \left[ \pi_0(0) - \pi_0\left(\frac{\pi}{2}\right) \right] + \left[ \gamma_{LV}\left(\frac{\pi}{2}\right) - \gamma_{LV}(0) \right] + \left[ W_a(0) - W_a\left(\frac{\pi}{2}\right) \right]. \quad (3.8)$$

There is no reliable data on these values for LCs. No account has been taken of the surface pressure in the literature. As on inorganic substrates LCs prefer to be parallel to the substrate,  $\pi_0(0) > \pi_0(\pi/2)$  and the anisotropy is not expected to be large. The LC surface tension anisotropy,  $\gamma = \gamma_{LV(0)} - \gamma_{LV(\pi/2)}$  is estimated to be  $+4.5 \times 10^{-5} \text{ J m}^{-2}$  for MBBA<sup>66</sup> and  $5 \times 10^{-6} \text{ J m}^{-2}$  for 5 CB (102 a). The difference in adhesion energy  $W_a$  between the parallel and perpendicular orientation has been deduced from experimental data at the glass/MBBA interface to be  $6.2 \times 10^{-3} \text{ J m}^{-2}$  (8 c) and is calculated to be  $7.16 \times 10^{-3} \text{ J m}^{-2}$  for PAA on glass (102).

Thus the energy in the interfacial layer is mainly determined by the adhesion energy. From (3.8) one gets:

$$B_\theta = \gamma_{SL(\pi/2)} - \gamma_{SL(0)} \sim W_a(0) - W_a\left(\frac{\pi}{2}\right) = 6 \times 10^{-3} \text{ J m}^{-2}.$$

This large difference in the surface energy means that the orientation of the interfacial layer cannot be modified by elastic deformation of the LC where the energy is at most  $10^{-5} \text{ J m}^{-2}$ . In this case,<sup>138</sup> one should not minimize the bulk plus surface energy, but minimize the bulk energy and require the boundary conditions to be satisfied at the surface.

Writing the LC layer energy as

$$F = \frac{1}{2} W_a \theta^2_{(0)} + \int_0^d \frac{1}{2} K \left( \frac{d\theta}{dz} \right)^2 dz$$

is tantamount to putting a flea on an elephant and minimizing the weight of the flea to lower the weight of the combined system. A LC layer of thickness  $d$ , homeotropically oriented and subject to a magnetic field directed parallel to the substrate will change its orientation beyond a distance  $d_c$ :

$$d_c = \frac{3K}{2(\gamma_\perp - \gamma_\parallel)} \quad (3.9)$$

as observed<sup>138</sup> on a homogeneously aligned drop of PAA deposited in a hole drilled in a crystal sheet, and subjected to a magnetic field perpendicular to the substrate. Azimuthal anchoring energies are either estimated from surface disclination lines<sup>153</sup> or measured by magnetic deformation of homeotropically

TABLE XI

Experimental values of the angular coefficient  $B_\theta$  of azimuthal anchoring energy  $W_\theta$   
 $(W_\theta = W_0 + B_\theta \sin^2 \theta)$

Substrate	LC	$B_\theta$ ( $10^{-6} \text{ J m}^{-2}$ )	Method <sup>a</sup>	Ref.
Air	5CB	4	DA	120(a)
SiO <sub>2</sub> (30° + 5°)	6CB	2.1	$\Delta n$	109
Glass + R <sub>n</sub> N <sup>+</sup> Me <sub>3</sub> X <sup>-</sup>	MBBA	3	MD	75
Glass + NH <sub>2</sub> C <sub>n</sub> H <sub>2n+1</sub>	MBBA	2	MD	155
Glass + NH <sub>2</sub> -C <sub>7</sub> H <sub>15</sub>	MBBA	2.6	SD	5(a)
Glass + lecithin	MBBA	3	MD	75
Glass + DMOAP	MBBA	6	MD	75
In <sub>2</sub> O <sub>3</sub> + DMOAP	MBBA	10	MD	75
In <sub>2</sub> O <sub>3</sub> + lecithin	MBBA	6	MD	75
In <sub>2</sub> O <sub>3</sub> + NH <sub>2</sub> C <sub>16</sub> H <sub>33</sub>	MBBA	3.5	MD	75

<sup>a</sup> Method: DA, differential anchoring;  $\Delta n$ , birefringence; MD, magnetic deformation; SD, surface disclination. The order of magnitudes of  $B_\theta$  compared to the experimental surface tension anisotropy. MBBA:  $\gamma_{||} - \gamma_{\perp} \sim 4.5 \times 10^{-5} \text{ J m}^{-2}$  [Ref. 75(b)]; 5CB:  $\gamma_{||} - \gamma_{\perp} \sim 5 \times 10^{-6} \text{ J m}^{-2}$  [Ref. 120(a)].

oriented layers where (3.9) should apply. The  $B_\theta$  values obtained are weak and comparable to the LC surface tension anisotropy (Table XI). This difference between calculated and experimental values would correspond to a deformation of the LC layer where the LC is not affected by the surface potential and  $B_\theta \sim \gamma(0) - \gamma(\pi/2)$ .

On inorganic layers where a LC would normally align parallel to the substrate, even though the anchorage is strong, weak interactions are observed as the perturbed part of the nematic layer interacts with its smecticlike interfacial layer. The same situation is probably observed on most adsorbed surfactant layers. With  $B_\theta \approx 5 \times 10^{-6} \text{ J m}^{-2}$  the anchorage parameter of Ref. 158

$$\lambda = \pi \frac{K}{B_\theta d}$$

is about 1 for a LC with  $K \approx 10^{-11} \text{ N}$  and a cell thickness of  $d = 10\mu$ .

Thus one may wonder whether it would be possible to observe weaker anchorage than now known. On polymeric films surface interactions are strongly reduced and the interfacial layer may disappear, but very often homeotropic alignment is observed on these surfaces.

#### II.1.4 Conclusions

As prophesized sixty years ago<sup>23</sup>:

"Les actions auxquelles obéissent les liquides anisotropes, qui se révèlent par des structures si variées, pourront sans doute plus tard se résumer en quelques lois très simples.

Bien que ces dernières ne soient pas connues, on est en droit de penser, d'après les observations très nombreuses recueillies jusqu'à ce jour, qu'elles feront jouer un rôle très important aux actions superficielles qui règlent l'orientation du liquide au voisinage de la surface, dans la couche capillaire, et les distingueront nettement des actions intérieures qui fixent l'orientation du liquide par rapport à lui-même dans toute l'étude de sa masse. Aux premières se rattachent par exemple les plages orientées à la surface du verre: aux secondes les coniques focales, les fils."

Mastering the alignment of LCs requires the control of the smecticlike interfacial layer. In addition to the difficulties of obtaining uniform and clean substrates, pure LC and well defined aligning layers free of solvents and ionic contamination, LC molecular structure gives rise to complicated interactions. Constituted of an aromatic core having strong dispersive interactions with the substrate, an alkyl chain tending to orient perpendicularly to the surface as the chain length increases, and a polar group which may counteract the other part of the molecules minimum energy, LC molecules open wide fields to speculation.

Theoretical expectations are summarized in Table (XII). Nevertheless, even if all aspects of LC orientation are not under control, as is also the case for the physical chemistry of surfaces, reproducible and well defined alignment can be obtained, as described in the last paragraph.

In general, inorganic substrates lead to nonuniform parallel alignment, the conditions that lead to homeotropically aligned LCs on these surfaces have not been defined. Rubbing will provide uniformity; it is best achieved on soft polymeric layers. Homeotropic alignment is observed in the absence of interaction with the surface as in suspended films, on low energy polymers and on adsorbed surfactant layers. The very first organized layer reaches its equilibrium slowly and determines the final nematic crystal structure.

### III RECOMMENDED PROCEDURES

Alignment problems arise frequently in laboratory experiments where LCs and temperatures vary. It is therefore desirable to use procedures which have been well tested. The use of good alignment layers allows experiments involving a LCs physical properties to be performed without the use of cumbersome magnets.




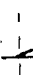
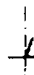
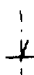
The success of any aligning process depends upon the substrate and the cleaning procedures employed. The alignment of a LC may be studied on metal or crystal surfaces, but it is more usual to employ transparent substrates.

Glass, quartz, silicon coated glass, or transparent conducting coatings ( $\text{SnO}_2$ ,  $\text{In}_2\text{O}_3$ )—patterned or otherwise—are most frequently employed. One should be aware of the many varieties of glass compositions available and the various manufacturing methods (pulled, floated, fire polished) which lead to



TABLE XII

Alignment expected from substrate/LC interaction characterized by the dispersive and polar components of the solid and LC surface tension



Liquid crystal		$\gamma_{cl} < \gamma_s$		$\gamma_{cl} > \gamma_s$	
Surface	Surf. state	$\Delta\epsilon > 0^a$	$\Delta\epsilon < 0$	$\Delta\epsilon > 0$	$\Delta\epsilon < 0$
$\gamma_s = \gamma_s^p + \gamma_s^d$					
	Smooth	$\perp^b$	$\times^b$	No cases	
$\gamma_s^p \gg \gamma_s^d$				polar surfaces ( $\gamma_s^p \gg \gamma_s^d$ )	
Activated oxides diacids	Sym grooves	$\perp$	$\parallel$	have	$\gamma_s > \gamma_{cl}$
	Unsym grooves				
	Tridimensional <sup>c</sup> pit array	$\parallel$	$\perp$		
$\gamma_s^p \gg \gamma_s^d$	Smooth	$\times$	$\times$	$\perp^d$	$\perp^d$
Humid oxides polymers fatty deriv.	Sym grooves	$\parallel$	$\parallel$	$\perp$	$\perp$
	Unsym grooves				
	Tridimensional <sup>c</sup> pit array	$\perp^d$	$\perp^d$	$\parallel$	$\parallel$

<sup>a</sup>  $\Delta\epsilon$  gives an indication of the LC polarity.

<sup>b</sup> This case is not experimentally very well documented.

<sup>c</sup> Regularly repeating tridimensional array of peaks and valleys.

<sup>d</sup> Homeotropy due to tridimensional array does not depend upon LCs nature while that due to absence of interaction does.

<sup>e</sup>  and  = tilted alignment.

different interactions with the LC to be aligned. The use of an acid bath to clean the substrate changes its properties towards certain classes of LCs. These considerations are not too important if the substrate is to be coated with a polymeric or oxide layer, but they are essential when silanes or surfactants are to be employed as aligning agents. More reproducible results are always obtained on an underlying coating.

The following methods have been widely used with success and give good results with most combinations of substrate and LC.

### III.1 Cleaning

Cleaning of solid substrates is still an art despite the considerable amount of work done on it.<sup>160</sup> Our studies use either a detergent bath or dipping in boiling sulfuric acid followed by thorough 18 M $\Omega$  water rinse and centrifuge drying.

Other methods may be found in the literature, as for instance in Ref. 159.

A very important step in any cleaning procedure is the drying, which has to be effected rapidly, i.e., under a high pressure stream of gas.

### III.2 Parallel alignment

Alignment by the rubbing of a substrate has been reviewed. In the laboratory, uniform alignment will be difficult to obtain reproducibly on every substrate. Industrial processing employs sophisticated machines. Rubbing by hand with a woven material or a polishing paste can only be expected to give uniform and reproducible results on soft substrates (glass or polymers).

#### III.2.1 Rubbed PVA

Thin polymeric films are best deposited by spin coating. A spinner may easily be constructed for laboratory uses. Polyvinyl alcohol (PVA) is commercially available in different grades (Wacker Polyviol®), but it appears that its aligning properties are not related to the grade used. We currently use the M 13/140 grade, which is very soluble and produces uniform films.

An aqueous solution (3%) is filtered on 0.5 $\mu$  millipore filters and deposited on a spinning (4000 rpm) substrate at room temperature. The deposited film ( $d \sim 1000$  Å) is dried at 80°C for 30 min and subsequently rubbed with a textile cloth. Uniform alignment with a very low tilt angle is obtained on all substrates and with most LCs.

#### III.2.2 Rubbed polyimide

Although PVA forms good aligning layers it is water and temperature sensitive. Polyimide is a very stable polymer. Films may be formed on a solid substrate from a monomer solution of an acid anhydride and a polyamine. Such solutions in *N*-methylpyrrolidone are commercially available (Rhône Pou-

lenc, Nolimide 32). The deposition of a uniform film is more difficult than with PVA.

Spin coating is effected as described above from a 1/10 diluted solution and the resulting deposit dried at 80°C for 30 min. The soft prepolymer is then rubbed. Polymerization is achieved by curing in two steps, 130°C, 30 min, followed by 200°C, 30 min.

### III.2.3 *SiO<sub>x</sub> evaporation*

If an evaporator is available, SiO<sub>x</sub> evaporation is the easiest way to obtain stable, uniform, reproducible alignment in the laboratory, provided that the substrate is flat and homogeneous. Uniform alignment with varying tilt angles may be obtained by variation of the angle between the substrate plane and the direction of the incident beam. Parallel alignment is obtain for a 30° angle.

Pure silicon monoxide (Balzers 99.99) is evaporated by techniques which are well known<sup>161</sup>: boat temperature 1300–1400°C,  $p \cong 10^{-4}$  mm Hg, air bleeding. Typical thicknesses are 200–300 Å. (MgF<sub>2</sub> may also be used.)

## III.3 Homeotropic alignment

There are at present no entirely satisfactory methods to obtain easy, reproducible homeotropic alignment free of complications (short lifetime, conductivity increase, etc.); for experimental evaluation the following methods give good results.

### III.3.1 *Lecithin (DMOAP)*

The easiest way to obtain a homeotropically aligned LC layer is to sandwich it between lecithin coated layers. A solution of natural egg lecithin (Merck 5331) in a volatile solvent (e.g., alcohol) is used and the substrates are either spin-coated or dipped in the solution. The concentration is unimportant but the use of a dilute (1%) solution avoids the formation of spots. The coating is rinsed with the solvent and dried at 80°C for 30 min.

Alignment of most LCs is obtained in a direction orthogonal to the substrate plane without any tilt. There is no variation of the orientation with temperature, but the LC conductivity is increased. With the same technique DMOAP [dimethyloctadecyl-3-(trimethoxysilyl)propylammonium chloride, Petrarch 09745] gives similar results and drawbacks but is somewhat more substrate sensitive.

### III.3.2 *DMCS*

For the alignment of positive LCs (the technique fails in the case of many negative  $\Delta\epsilon$  LCs) a polymethylsiloxane, insulating, homeotropically aligning layer may easily be formed on the substrate from a Dimethyldichlorosilane

(Fluka 40140) solution 10% in toluene) by dipping the plate for 15 min at room temperature. The coating is rinsed with isopropyl alcohol and cured at 100°C for 30 min.

### III.4 Tilted alignment

#### III.4.1 *Tangentially evaporated SiO<sub>x</sub>*

As previously stressed, tilt angle is a bulk average, depending on both the surface state and the LCs elastic constants. It is thus difficult to know with precision the tilt angle one will obtain with different LCs sandwiched between the same plates. A tilt angle of 15° to 30° will be obtained on tangentially evaporated SiO<sub>x</sub>. The evaporating conditions are the same as in § III.2.3.

#### III.4.2 *Crossed evaporation*

To obtain angles between 0° and 30° it is possible to deposit a thin layer of tangentially evaporated SiO<sub>x</sub> on top of a 30° evaporated layer (low angles) or the reverse (high angles). Care must be taken to rotate the substrate by 90° between each evaporation as the nematic director is oriented perpendicular to the evaporation direction for tangentially evaporated layers.

#### III.4.3 *"Tilted homeotropic" alignment*

To obtain a slight tilt angle from the direction normal to the substrate a homeotropic aligning agent (e.g., Lecithin or DMOAP) is combined with one of the above methods (4.1., 4.2.). The procedure is as outlined in § III.3.

### Acknowledgments

Thanks are due "Direction Technique of Ebauches S.A." which supported this work. The participation of the LC group allowed the evaluation of many processes, particularly appreciated being the evaluation of silanes treatment by Dr. J. P. Ehrbar. Authorization of publication and typing assistance by ASULAB S.A. is gratefully acknowledged. We thank the Laboratoire Suisse de Recherches horlogères for providing us with glasses covered with photopolymerized PTFE.

### References

1. F. J. Kahn, G. N. Taylor and H. Schonhorn, "Surface-Produced Alignment of Liquid Crystals," *Proc. IEE*, **61**, 823 (1973).
2. L. A. Goodman, "Liquid-Crystal Displays-Packaging and Surface Treatments," *RCA Review*, **35**, 477 (1974).
3. I. Haller, "Thermodynamic and static properties of LCs," *Prog. Solid State Chem.*, **10**, 103 (1975).
4. (a) R. S. Porter, E. M. Barral and J. F. Johnson, "Some flow characteristics of mesophase types," *J. Chem. Phys.*, **45**, 1452 (1966). (b) Ch. Gänwiller, "Temperature Dependence of Flow Alignment in Nematic LCs," *Phys. Rev. Lett.*, **28**, 1554 (1972).
5. (a) G. Porte, "Tilted Alignment of MBBA Induced by Short-Chain surfactant," *J. Phys. (Paris)*, **37**, 1245 (1976). (b) G. Porte, "Contribution à l'étude de l'orientation des cristaux liquides Nematiques par les surfaces solides," These 3° cycle Grenoble (1977).

6. L. T. Creagh and A. R. Kmetz, "Mechanism of surface Alignment in Nematic LCs," *Mol. Cryst. Liq. Cryst.*, **24**, 59 (1973).
7. T. Uchida, H. Watanabe and M. Wada, "Molecular Arrangement of Nematic LCs," *Jap. J. App. Phys.*, **11**, 1559 (1972).
8. (a) J. E. Proust, L. Ter-Minassian-Saraga and E. Guyon, "Orientation of a Nematic liquid crystal by suitable boundary surfaces," *Solid State Commun.*, **11**, 1227 (1972). (b) J. E. Proust and L. T. Saraga, "Ancrage physicochimique d'un cristal liquide nématique aux interfaces solide-liquide et énergie libre d'adhésion. Hystérésis de mouillage en phase nématique et isotrope," *CR Acad. Sci. Paris*, **279**, C-165 (1974). (c) J. E. Proust and L. Ter-Minassian-Saraga, "Orientation d'un cristal liquide par les surfaces et énergie libre d'adhésion," *J. Phys. (Paris)*, **36**, C1-77 (1975).
9. M. Ohgawara, T. Uchida and M. Wada, "Liquid Crystal Orientation on Various Surfaces," *8th LC Conf.*, J-6 P (Kyoto 1980).
10. M. G. Friedel, "Les états mésomorphes de la matière," *Ann. Phys. IX Ser.*, **18**, 273 (1922).
11. Jap. Pat. 51-105 127 (1976)-Pat. Abst. of Jap. Kokai No 53.29750. Liquid Crystal display device.
12. G. A. Dir, I. P. Gates and K. F. Nelson, "A Vacuum Deposition Alignment Technique for Tilt Control in LCs," *SID Digest*, **66** (1978).
13. German Pat. DT 23 30 909 (1977). Verfahren zur Erzeugung einer Schicht zur homoötrophen Orientierung von Flüssigkristallen.
14. German Pat. 26 25 864 (1978). Flüssigkristall Anzeige Vorrichtung Mit Einer Fluoreszenz Platte.
15. US Pat. 385,339,1 (1974). Fabrication of LC devices.
16. CH 616 005 (1980). Flüssigkristall anzeige vorrichtung.
17. (a) J. L. Janning, "Thin film surface orientation for liquid crystals," *Appl. Phys. Lett.*, **41**, 73 (1972). (b) US Pat. 3,834,792 (1974). Alignment film for a LC display cell. (c) US Pat. 3,964,158 (1961). Method of making a liquid crystal display cell.
18. DT 225 6317 (1977). Verfahren zur Erzeugung einer homogenen Orientierung von Flüssigkristallmolekülen in einer Flüssigkristallanordnung.
19. (a) Germ. Pat. D.E. 253 8331 (1974). Flüssigkristallanzeigeelement. (b) Germ. Pat. D.O. 241 8364 (1973). Nematisches flüssiges Kristallsystem für elektro Anzeigeelemente.
20. This work.
21. Eng. Pat. 146 6438 (1977). Fabrication of LC devices.
22. French Pat. 753 6984 (1975). Dispositif d'affichage à cristaux liquides et son procédé de réalisation.
23. (a) F. Grandjean, "L'orientation des liquides anisotropes sur les cristaux," *Bull. Soc. Fr. Min.*, **39**, 164 (1916), 4069 (1917). (b) C. Mauguin, *Bull. Soc. Fr. Min.*, **34**, 71 (1911).
24. A. Derzhanski, L. Komitov and M. Mikailov, "Oriented action of some solid substrates to liquid crystal layer," *Krist. und Techn.*, **14**, 213 (1979).
25. G. Sprokel and R. M. Gibson, "LC Alignment Produced by RF Plasma Deposited Films," *J. Electrochem. Soc.*, **124**, 557 (1977).
26. A. G. Dewey *et al.*, "Laser-Addressed LC projection displays," *Proc. SID*, **19/1**, 1 (1978).
27. F 743 4708 (1974); F. 74 39 744. Dispositif d'affichage à cristaux liquides.
28. Jap. Pat.-Kokai No 54-128357; No 54-162552 (Jap. Pat. Abst. 1978). Liquid Crystal Display Cell.
29. D.O.S. 253 5674 (1976). Wiedergabevorrichtung mit Flüssigkristall.
30. CH 597 607 (1977). Cellules électro-optiques pour affichage par cristaux liquides à effet de champ.
31. CH 610 667 (1979). Cellule électro-optique.
32. US 410 5298 (1978). Electro-optic devices.
33. (a) CH 586 401 (1977) T. B. Harsch. Verfahren zur Herstellung von Flüssigkristallzellen. (b) F 750 0856 (1975). Procédé d'alignement en surface pour cellules de cristaux liquides, et procédé de fabrication de polariseurs à partir de ces cellules.
34. (a) J. C. Dubois, M. Gazard and A. Zann, "Plasma-polymerized films as orientating layers for LCs," *Appl. Phys. Lett.*, **24**, 297 (1974). (b) F 743 6489 (1974) also D.O.S. 254 8125. Pro-

- cédé d'alignement de cristaux liquides et son application aux cellules de visualisation du type "nématique en hélice." (c) J. C. Dubois, M. Gazard and A. Zann, "Liquid-crystal orientation induced by polymeric surfaces," *J. Appl. Phys.*, **47**, 1270 (1976).
35. J.A. 131 287 to 131 297 LC Abst. 1976 3.2-01646. Orientation of LCs by organic coating of substrate.
  36. CH 583 916 (1977). Dispositif électro-optique à cristal liquide nématique.
  37. P. Datta, A. W. Levine and G. Kaganowicz, "Alignment of Liquid Crystals on Plasma Synthesized Polymer Films: Effects of Composition," 150th Electrochem. Soc. Meeting, Las Vegas, Conference No. 215 (1976).
  38. I. Haller, "Alignment and wetting properties of nematic liquids," *Appl. Phys. Lett.*, **24**, 349 (1974).
  39. H. Zocher and Z. Coper, "Ueber die Erzeugung des Anisotropie von Oberflächen," *Phys. Chem.*, **132**, 295 (1928).
  40. (a) P. Chatelain (these), *Bull. Soc. Fr. Min.*, **60**, 300 (1937). (b) P. Chatelain, "Sur l'orientation des cristaux liquides par les surfaces frottées," *Bull. Soc. Fr. Min.*, **66**, 105 (1943).
  41. L. A. Goodman, D. Meyerhofer and S. Digiovanni, "The Effect of Surface Orientation on the Operation of Multiplexed Twisted-Nematic Devices," *IEEE*, ED-23, 1176 (1976).
  42. W. A. Weyl, "Structure of Subsurface layers and their role in Glass Technology," *J. Non-Cryst. Solids*, **19**, 1 (1975).
  43. (a) D. W. Berreman, "Solid surface Shape and the Alignment of an Adjacent Nematic LC," *Phys. Rev. Letters*, **28**, 1683 (1972). (b) D. W. Berreman, "Alignment of LCs by Grooved Surface," *Mol. Cryst. Liq. Cryst.*, **23**, 215 (1973).
  44. (a) E. Guyon, P. Pieranski and M. Boix, "On different boundary conditions of nematic film deposited on obliquely evaporated plates," *Appl. Eng. Sci. Lett.*, 119 (1973). (b) W. Urbach, M. Boix and E. Guyon, "Alignment of nematics and smectics on evaporated films," *Appl. Phys. Lett.*, **25**, 479 (1974).
  45. (a) M. L. Little, H. L. Garrin and L. J. Miller, "New method for inducing homeotropic and tilted alignments of nematic liquid crystals on silica surfaces," *LC and ordered Fluids*, Vol. 3, edited by J. F. Johnson and R. S. Porter (1977), p. 497. (b) L. J. Miller *et al.*, "A new method for inducing homeotropic and tilted alignments of nematic liquid crystals on silica surfaces," *ibid.*, p. 513 (also F 761 6366 1976).
  46. CH 585 912. Procédé de fabrication d'un dispositif d'affichage à cristal liquide et dispositif d'affichage résultant du procédé.
  47. U. Wolf, W. Greubel and H. Krüger, "The homogeneous alignment of liquid crystals layers," *Mol. Cryst. Liq. Cryst.*, **23**, 187 (1977).
  48. M. Yamashita and Y. Amemiya, "Effect of substrate surface on alignment of LC molecules," *Jpn. J. Appl. Phys.*, **15**, 2087 (1976).
  49. L. A. Goodman, J. T. McGinn, Ch. Anderson and F. Digeronimo, IEE ED 24 795 (1977). "Topography of Obliquely Evaporated Silicon Oxide Films and Its Effect on Liquid-Crystal Orientation.
  50. D. C. Flanders, D. C. Shaver and H. I. Smith, "Alignment of LCs using submicrometer periodicity gratings," *Appl. Phys. Lett.*, **32**, 597 (1978).
  51. G. D. Dixon, T. P. Brody and W. A. Hester, "Alignment mechanism in twisted nematic layers," *Appl. Phys. Lett.*, **24**, 47 (1974).
  52. W. A. Crossland, "Birefringence in silicon monoxide films used for aligning liquid crystal layers," *Appl. Phys. Lett.*, **26**, 598 (1975).
  53. J. M. Pollack, W. E. Haas and J. E. Adams, "Topology of obliquely coated silicon monoxides layers," *J. Appl. Phys.*, **48**, 831 (1977).
  54. J. Cheng and G. D. Boyd, "The LC alignment properties of photolithographic gratings," *Appl. Phys. Lett.*, **35**, 44 (1979).
  55. CH 590 490 (1974). Flüssigkristallzelle.
  56. F. J. Haas, J. Adams and J. B. Flannery, "New Electro-Optic Effect in a Room-Temperature Nematic LC," *Phys. Rev. Lett.*, **25**, 1326 (1970).
  57. F. Kuschel and D. Demus, "Homeotropic Layers of Nematic LCs Induced by Carboxylic Acids," *Krist. Technik*, **15**, K28 (1980).

58. US 369,405,3 (1972). F. J. Kahn. Nematic Liquid Crystal Device.
59. (a) US 365 6834 (1972). Haller *et al.* Additive for Liquid Crystal Material. (b) F. 7144308. A. Vekemans (1971). Additif pour matériau cristallin liquide.
60. F. 743 9744 (1974). G. J. Sproxel. Dispositif d'affichage à cristaux liquides.
61. US 397,258,9. D. W. Skelly and G. J. Sewell (1976). Nematic LC Mixtures with Stable Homeotropic Boundary Conditions and Methods of Making the Same.
62. CH 585 256 (1977). Flüssigkristallgemisch mit nematischer Phase.
63. (a) US 397,931,9 (1976). LC composition. (b) D 231 6864 (1979). Flüssigkristallzusammensetzung.
64. US 384,896,6 (1974). Homeotropic Alignment Additive for LCs.
65. (a) K. Hiltrop and H. Stegenmeyer, "Three-Phase Contact Line Motion in the Disposition of Spread Monolayers," *Ber. Bunsenges. Phys. Chem.*, **82**, 884 (1978). (b) K. Hiltrop and Stegenmeyer, "Contact angles and alignment of LCs on lecithin monolayers," *Mol. Cryst. Liq. Cryst.*, **49**, 61-65 (1978).
66. US 380,945,6 (1974). Liquid Crystal Device.
67. (a) US 380,305,0 (1974). Liquid Crystalline Compositions and Imaging Systems. (b) US 387,190,4 (1975). Method for Providing a Liquid Crystalline Film.
68. US 406,491,9 (1977). Method of Filling Dynamic Scattering LC devices.
69. US 390,479,7 (1975). Homeotropic Alignment of LCs in a Display Cell by Baked on Ionic Surfactants.
70. D 264 6485 (1977). Flüssigkristallzusammensetzung.
71. I. G. Chistyakov, I. I. Gorina and L. K. Vistin, "Method of growing homeotropic LCs," *Sov. Phys. Cryst.*, **22**, 341 (1977).
72. (a) US 389,479,4 (1975). LC Imaging System Using Tributyltin Oxide. (b) US 389,479,3 (1975). LC Imaging System Using Tributyltin Oxide or Tributyltin Chloride.
73. (a) G. B. 152 0901 (1978). Liquid Crystal Device. (b) S. Matsumoto, M. Kawamoto and N. Kaneko, "Surface-induced molecular orientation of LCs by carboxylatochromium complexes," *Appl. Phys. Lett.*, **27**, 263 (1975).
74. F. 753 5384 (1975). Procédé et dispositifs d'orientation oblique des molécules d'un crystal liquide.
75. (a) S. Naemura, "Measurement of anisotropic interfacial between a nematic LC and various substrates," *Appl. Phys. Lett.*, **33**, 1 (1978). (b) S. Naemura, "Anisotropic interactions between MBBA and surface-treated substrates," *J. Phys. Appl.*, **40**, C3-514 (1979).
76. J. A. 117961 (1976) from L.C. Abstract No 2.3-04546 (1978). LC Composition.
77. F. J. Kahn, "Orientation of LCs by surface coupling agents," *Appl. Phys. Lett.*, **22**, 386 (1973).
78. S. Matsumoto *et al.*, "Molecular orientation of LCs by organic metal complexes," *J. Phys. Paris*, **40**, C3 510 (1979). (b) S. Matsumoto *et al.*, "Surface produced alignment of nematic LCs by polynuclear dicarboxylatochromium complexes," *Appl. Phys. Lett.*, **29**, 67 (1976).
79. W. Helfrich, "A simple method to observe the piezoelectricity of LCs," *Phys. Lett.*, **35A**, 393 (1971).
80. L. Pohl and J. Feldman, "Stabilized homogeneous, twisted and tilted liquid crystals layers," *Electrochim. Soc. Meet. Ext. Abst.* No. 212 (1976).
81. DDR 110/399 (1974). Verfahren zur Herstellung homogen orientierter Schichten von Kristallinen Flüssigkeiten.
82. (a) H. Lee and C. Coll., "Wettability and Conformation of Reactive Polysiloxanes," *Int. Sc.*, **27**, 751 (1968). (b) E. Grushka and E. J. Kikta, Jr., "Chemically Bonded Stationary Phases in Chromatography," *An. Chem.*, **49**, 10045 A (1977).
83. US 372,800,8 (1973) Liquid Crystal Display.
84. T. Uchida, K. Ishikawa and M. Wada, "LC Alignments and Surface Energy," *Mol. Cryst. Liq. Cryst.*, **60**, 37 (1980).
85. US Pat. 397,305,7 (1976). Method of Preparing a LC Display.
86. US Pat. 394,718,4 (1976). Imaging Method.
87. T. Uchida, C. Shishido and M. Wada, "Molecular Alignment of Nematic LCs Silane-Treated Glass Surfaces," *Electron. Commun. Jpn.*, **58C**, 224 (1975).

88. K. L. Mittal and D. F. O'Kane, "Vapor deposited silanes and other coupling agents," *J. Adhesion*, **8**, 98 (1976).
89. F 771 3348 (1971). Cellule de cristaux liquides à l'état nématique.
90. (a) US Pat. 393,071,6. Method of Collective Orientation of the Molecules of a Liquid Crystal. (b) H. Warenghem and J. Billard. Orientation mutuelle de Mesophases Nématiques et Smectique B.
91. F. Nakano and M. Sato, "Alignment Deterioration of Homeotropically Aligned LC Cells under d.c. Electric Field. I. Effect of LC Composition and Surface Treatment," *Jpn. J. Appl. Phys.*, **15**, 1937 (1976).
92. DE 232 5998 (1979). Flüssigkristallzelle.
93. R. W. Gurtler and J. W. Casey, "Surface tilt distributions of homogeneously aligned LCs," *Mol. Cryst. Liq. Cryst.*, **35**, 275 (1976).
94. T. J. Scheffer and J. Nehring, "Accurate determination of LC tilt bias angles," *J. Appl. Phys.*, **48**, 1783 (1977).
95. F. Müller, "Déposition oblique de couches minces de SiO et orientation des molécules dans des affichages à cristaux liquides," *Helv. Phys. Acta*, **51**, 59 (1978).
96. W. A. Crossland *et al.*, "Tilt angle measurements of nematic phases of cyanobiphenyls aligned by obliquely evaporated films," *J. Phys. D.*, **9**, 2001 (1976).
97. CH 611 042 (1979). Procédé de fabrication d'un dispositif d'affichage à cristal liquide.
98. CH 611 043 (1979). Procédé de fabrication d'une cellule d'affichage électro-optique passif à cristal liquide nématique en hélice.
99. CH 619 052 (1979). Procédé de fabrication d'une cellule d'affichage électro-optique passif.
100. J. H. Morissy, B. Needham and W. A. Crossland, Bordeaux Conf. (1978), Abstr. HP 60.
101. E. P. Raynes, "Improved contrast uniformity in twisted nematic liquid-crystal electro-optic display devices," *Electronic Lett.*, **10**, 141 (1974).
102. (a) D. M. Buzcek, "A Thin Film Process to Improve Off Axis Viewing of LC Displays," *Mol. Cryst. Liq. Cryst.*, **47**, 145 (1978). (b) K. Odawara, T. Ishiboshi and Kanazahi. LC displays for calculators cited by D. M. Buzcek (Ref. 102(a)) (1975).
103. D. Meyerhofer, "New technique of aligning liquid crystals of surfaces," *Appl. Phys. Lett.*, **29**, 691 (1976).
104. M. R. Johnson and R. A. Penz, "Low-Tilt-Angle Nematic Alignment Compatible with Frit Sealing," *IEEE ED*, **24**, 805 (1977).
105. E. P. Raynes, D. K. Rowel and I. A. Shanks, "LC surface alignment treatment giving controlled low angle tilt," *Mol. Cryst. Liq. Cryst. Lett.*, **34**, 105 (1976).
106. L. Roussille and J. Robert, "Liquid crystal quasihomeotropic orientation induced by a polymer deposited on a SiO surface," *J. Appl. Phys.*, **50**, (6) 3975 (1979).
107. G.B. 2007 865 (1978). Liquid Crystal Displays.
108. (a) R. Chabicovsky and G. Kocmann, "LC Cells with Special Electrodes for the Generation of Uniform Colors by Optical Birefringence," *IEEE ED*, **24**, 807, No. 7 (1977). (b) R. Chabicovsky, "Thin film Electrodes for LC Cells," Proc. 7th Intern. Vac. Congr. Vienna (1977).
109. D. Rivière, Y. Lévy and C. Guyon, "Determination of anchoring energies from surface tilt angle measurements in a nematic liquid crystal," *J. Phys. Lett.*, **40**, 215 (1979).
110. Y. Lévy, D. Rivière, C. Imbert and M. Boix, "Détermination des angles d'obliquité d'un cristal liquide en phase nématique au voisinage d'une surface," *Opt. Commun.*, **26**, 225 (1978).
111. (a) H. Mada, A. Toda and S. Kobayashi, "Temperature dependence of Pretilt Angle for Nematic LCs," *Jpn. J. Appl. Phys.*, **17**, 261 (1978). (b) H. Mada, "Study on the Surface Alignment of Nematic LCs: Temperature dependence of pretilt angles," *Mol. Cryst. Liq. Cryst.*, **51**, 43 (1979); **53**, 127 (1979).
112. K. Suzuki, K. Toriyama and A. Fukuhara, "A method of measuring the low tilt bias angle of LCs," *Appl. Phys. Lett.*, **33**, 561 (1978).
113. M. J. Gannon and T. E. Faber, "The surface tension of nematic LC's," *Phil. Mag.*, **37**, 117 (1978).
114. (a) M. A. Bouchiat and D. Langevin-Cruchon, "Molecular order at the free surface of a nematic LC from light reflectivity measurements," *Phys. Lett.*, **34**, A 331 (1971). (b) D. Lan-



- gevin, "Analyse spectrale de la lumière diffusée par la surface libre d'un cristal liquide nématique," *J. Phys. (Paris)*, **33**, 249 (1972).
115. A. Fergusson and S. J. Kennedy, "On the surface tension of LCs," *Phil. Mag.*, **264** (1938).
  116. S. Krishnawawy and R. Shashidar, "Experimental studies of the surface tension of nematic LCs," *Mol. Cryst. Liq. Cryst.*, **35**, 253 (1976).
  117. (a) W. M. Schwartz and H. W. Moseley, "The surface tension of liquid crystals," *J. Phys. Coll. Chem.*, **51**, 826 (1947). (b) F. M. Jaeger, "Temperatur Abhängigkeit der Mol. Freien Oberflächenenergie," *Z. Anorg. Chem.*, **101**, 1-214, (1917). (c) F. K. Gorskii and N. M. Sakevich, "Determination of the interfacial energy at the boundary between the solid and LC phases of PAA and chol. caprinat," *Sov. Phys.-Crystallogr.*, **12**, 586 (1968).
  118. K. Okano and Murakami, "Van der Waals dispersion force contribution to the interfacial free energy of nematic LCs," *J. Phys. C*, **40**, C3 525 (1979).
  119. (a) J. D. Parsons, "Ordering and Distorsion at the Nematic-Isotropic Fluid Interface," *Mol. Cryst. Liq. Cryst.*, **31**, 79 (1975). (b) J. D. Parsons, "A molecular theory of surface tension in nematic LCs," *J. Phys. C*, **37**, 1187 (1976).
  120. (a) J. E. Proust, E. Perez and L. T. Saraga, "Thin films of nematic LCs on liquid substrate. Bulk and surface structures, surface and line tensions," *Colloid Polym. Sci.*, **254**, 672 (1976). (b) E. Perez, J. E. Proust, L. T. Saraga and E. Manev, "Structural disjoining pressure in thin film of LCs," *Colloid Polym. Sci.*, **225**, 1003 (1977). (c) E. Manev, J. E. Proust and L. T. Saraga, "Structural disjoining in thin films of LCs," *Colloid Polym. Sci.*, **255**, 1133 (1977).
  121. A. W. Adamson, *Physical Chemistry of Surfaces*, 3rd ed. (Wiley, New York, 1976).
  122. G. J. Young, "Interactions of water vapor with silica," *Colloid Sci.*, 1367 (1958).
  123. A. V. Kiselev, in *Hydrophobic Surfaces*, edited by F. M. Fowkes (Academic, New York, 1969).
  124. W. D. Harkins, *Physical Methods in Organic Chemistry*, edited by A. Weissberger, Vol. I, Part I (Interscience, New York, 1949), Chap. X: "Determination of properties of monolayers and duplex films."
  125. B. Ackles, "Tailoring surfaces with silanes," *Chem. Technol.*, 766 (1977).
  126. M. Yamashita and Y. Amemiya, "Critical Surface Tension of Silicon Films and Aligning Properties of Nematic MBBA Molecules," *Jpn. J. Appl. Phys.*, **18**, 1249 (1979).
  127. S. Hirako, H. Mada and S. Kobayashi, "Anisotropy of the Critical Surface Tension of a Treated Solid Surface and the LC Alignment," *Jpn. J. Appl. Phys.*, **18** (1979).
  128. E. G. Shafrin and W. A. Zisman, "Constitutive relations in the wetting of low energy surfaces and the theory of the retraction method of preparing monolayers," *J. Am. Chem. Soc.*, **64**, 519 (1960).
  129. D. H. Kaelble, *Physical Chemistry of Adhesion* (Wiley-Interscience, New York, 1971).
  130. A. I. Derzhanski and A. G. Petrov, "Flexoelectricity in Nematic LCs," *Acta Phys. Pol. A*, **55**, 747 (1979).
  131. G. D. Myers, presentation at "Cristaux Liquides" Congrès Int. Bordeaux (1978), Abstr. HPK 61: Alignment of nematic LCs by surface dipoles.
  132. A. C. Zettlemoyer and J. Chessick, "Wettability by Heats of Immersion," *Adv. Chem.*, 4388 (1964).
  133. (a) F. Perez, "Orientation interfaciale des cristaux liquides," Thesis (1977). (b) J. E. Proust, F. Perez and L. T. Saraga, *Adhesion 2* (Applied Science Publishers Ltd., England), Chap. 2, p. 23-34: "Wetting of Solids by Organized liquids."
  134. V. A. Kir'yanov, "Electric Double Layer at the Metal/LC Interface," *Sov. Electrochem.*, **15**, 382 (1979).
  135. G. J. Sprokel, "Resistivity, Permittivity and the Electrode Space Charge of Nematic LCs," *Mol. Cryst. Liq. Cryst.*, **24**, 9 (1973).
  136. A. Sussman, "Transport of Residual Ions and Rectification in LC Displays," *J. Appl. Phys.*, **49**, 113 (1978).
  137. (a) M. Mada and S. Kobayashi, "Surface and bulk order parameter of a nematic LC," *Appl. Phys. Lett.*, **35**, 4 (1979). (b) A. Hatta, "Application of Infra-red ATR Spectroscopy to Liquid Crystals," *Bull. Chem. Soc. Jpn.*, **50**, 2522 (1977).
  138. (a) V. Naggiar, "Orientation dans le champ magnétique d'une goutte de liquide anisotrope

- suspendue," *C. R. Acad. Sci. Paris*, **208**, 1916 (1939). (b) V. Naggiar, "Phénomènes d'orientation dans les liquides nématiques," *Ann. Phys. (Paris)*, **18**, 5 (1943). (c) D. Meyerhofer, A. Sussman and R. Williams, "Electrooptic and hydrodynamic properties of nematic liquid crystals films with free surfaces," *J. Appl. Phys.*, **43**, 3685 (1972).
139. D. W. Berreman, "Anomalous stiffness and tilt angle in nematic from non-uniform attachment angle," *J. Phys. C*, **40**, C3-58 (1979).
  140. L. D. Brockway and R. L. Jones, "Electron microscopic investigation of the adsorption of long-chain fatty acids monolayers on glass," *Adv. Chem. Ser.*, **43**, 275 (1964).
  141. I. Haller, "Covalently attached organic monolayers on semi-conductor surfaces," *J. Am. Chem. Soc.*, **100**, 8050 (1978).
  142. W. C. Bigelow, D. C. Pickett and W. A. Zisman, "Films adsorbed from solutions in non polar liquids," *J. Colloid Sci.*, 1513 (1946).
  143. E. E. Polymeropoulos and J. Sagiv, "Electrical conduction through adsorbed monolayers," *J. Chem. Phys.*, **69**, 1836 (1978).
  144. J. Sagiv, "Organized Monolayers by Adsorption. 1. Formation and Structure of Oleophobic Mixed Monolayers on the Solid Surfaces," *J. Am. Chem. Soc.*, **102**, 92 (1980).
  145. O. Levine and W. A. Zisman, "Physical properties of monolayers adsorbed at the solid-air interface. I. Friction and wettability of aliphatic polar compounds and effect of halogenation," *J. Am. Chem. Soc.*, **61**, 1068 (1957).
  146. F. Sackmann, "Dynamic Molecular Organization in Vesicles and Membranes," *Phys. Chem.*, **82**, 891-909 (1978).
  147. R. Steiger, private communication.
  148. K. Hiltrop, Thesis. Presented at Meeting on LCs of one and two dimensional order, Garmisch, 1980.
  149. D. F. Untereker *et al.*, "Evidence for formation of monolayers of bonded organosilanes reagents," *J. Electroanal. Chem.*, **81**, 309 (1977).
  150. A. F. Diaz and K. K. Kanazawa, "Electrodes with Covalently Attached Monolayers," *IBM J. Res. Dev.*, **23**, 316 (1979).
  151. H. Winde and P. Steiger, "Interaction of 4-nitrophenyl-4-n-octyloxybenzoate with SiO<sub>2</sub>," LC Abstr. No. 2.5.04125.
  152. A. Denat, B. Gosse and J. P. Gosse, "Étude du cristal liquide MBBA: I. Stabilité chimique et conductibilité ionique," *J. Chim. Phys. (Paris)*, **2**, 319 (1973).
  153. (a) G. Ryschenkow and M. Kleman, "Surface defects and structural transitions in very low anchoring energy nematic thin films," *J. Chem. Phys.*, **64**, 404 (1976). (b) M. Kleman and C. Williams, "Anchoring energies and nucleation of surface disclination lines in nematics," *Phil. Mag.*, **28**, 725 (1973).
  154. L. A. Girifalco and R. J. Good, "A theory for the estimation of surface and interfacial energy," *J. Phys. Chem.*, **61**, 904 (1957).
  155. J. Sicart, "Méthode de mesure de l'énergie d'ancrage d'un nématique. Application à l'ancrage sur une paroi non traitée," *J. Phys. Lett.*, **37**, 25 (1976).
  156. P. G. de Gennes, *The Physics of Liquid Crystals* (Oxford Univ. Press, London, 1974).
  157. F. Guyon and W. Urbach, in "Anchoring properties and alignment of LCs," *Non-Emissive Electrooptic Displays*, edited by A. R. Kmetz and F. K. von Willisen (Plenum, New York, 1976).
  158. J. Nehring, A. R. Kmetz and T. J. Scheffer, "Analysis of weak-boundary-coupling effects in LC displays," *J. Appl. Phys.*, **47**, 850 (1976).
  159. W. H. de Jeu, *Physical Properties of Liquid Crystalline Materials* (Gordon and Breach, New York, 1980).
  160. K. L. Mittal, *Surface Contamination* (Plenum, New York, 1979).
  161. L. Holland *Vacuum Deposition of Thin films* (Chapman and Hall, London, 1961).

# INDEX

- Adsorbed layers 21, 48, 49
  - of CTAB 50
  - packing density 21
  - of silanes 50
  - structure 48
- Alignment
  - of azoxy LC 6, 37, 62
  - of cyanobiphenyls 23, 32, 33, 47
  - expected from substrate LC interaction 65
  - by heating to isotropic phase 5
  - homeotropic see homeotropic alignment
  - homogeneous see homogeneous alignment
  - on indium oxide see indium oxide
  - on inorganic substrates 6, 7, 8, 14
  - mechanism 4, 8
  - on inorganic polymers 6, 9
  - parallel to the surface see parallel alignment
  - and homogeneous alignment
  - perpendicular to the surface see homeotropic alignment
  - on phenylcyclohexane LC 8, 47, 50
  - on polyimide see polyimide
  - on polymers 6, 9-13, 15
  - on polyvinyl alcohol see polyvinyl alcohol
  - rule for prediction 37
  - of Schiff's bases LC 6, 23
  - on smooth layers 8
  - by surfactants see surfactants
  - tilted see tilt
  - on tin oxide 6
- Anchoring energies 56
  - from disclination lines 59
  - in plane (twist) 56, 58-60
  - out of plane (azimuthal) 56, 61, 63
  - "weak" 63
- Azimuthal anchorage 56, 61
- Azoxys
  - alignment of 6, 37, 62
  - surface tension 41
- Binding of surfactants 22
  - see also silanes
- Biphenyls 33, 47, 50
  - see also cyanobiphenyls
- Calcium fluoride 14
  - alignment on tangentially evaporated 15
  - evaporated 15
- Carboxylic acids 16, 21
  - monolayers 50
  - see also fatty derivatives
- Cetyl trimethyl ammonium bromide (CTAB) 20, 21, 50
  - isotherm of adsorption 50
  - solution in LC 21
  - superficial density 50
- Chromium carboxylate 22
- Cleaning 66
  - in boiling sulfuric acid 6
  - influence on alignment 6
  - procedures 66
- Cyanobiphenyls
  - alignment of 23, 32, 33, 47
  - orientation on phospholipids monolayers 50
  - surface tension 41
- Dimethyl dichlorsilane 67
- DMOAP (*dimethyl-N-octadecyl-3-aminopropyl trimethoxysilyl chloride*)
  - aligning layer 22
  - on grooved surface 22
- Esters (Liquid crystalline)
  - surface hydrolysis 52
- Evaporated layers
  - homeotropic alignment on 6
  - ion beam etching of 14
- Evaporation 35
  - crossed evaporation 35
  - double evaporation 68
  - influence of angle of incidence on LC direction 35

- oblique 33, 34
- tangential 1, 14, 34
- Extrapolation length 61
  
- Fatty acids and derivatives 21, 22, 43, 50
  - reaction with silica layers 22
  
- Glass
  - cleaning 66
  - quality 64
  - rubbing see rubbing
- Gratings (alignment on) 15
- Grooves produced by
  - Shallow angle ion beam etching 14, 43
  - tangential evaporation 2, 14
- Grooved surfaces 14, 53-55, 57, 58
  - homeotropic alignment on 15, 55
  
- Homeotropic alignment
  - on acid washed glasses 6
  - on calcium fluoride 15
  - on DMOAP see DMOAP
  - on fluorinated polymers 8
  - on grooved surfaces 15, 55
  - by impurities 6
  - on inorganic surfaces 6, 55
  - on lecithin see lecithin
  - by polar compounds 21
  - on polymers 9-13
  - on polysiloxane 23, 47
  - relation with surface tension 37
  - by silanes see silanes
  - on surface giving a tilted orientation 35
  - by surface hydrolysis 52
- Homogeneous alignment
  - action of surfactants 22, 66
  - on rubbed polymers 14, 66
  - on rubbed surfaces 14, 53
  
- Impurities
  - influence on alignment 6
- Indium oxide
  - alignment on 6, 64
- Interfacial layer 58, 59
  - smecticlike 46, 64
  - thickness 58
  
- Lecithin 20, 21, 48, 50, 51, 68
  - structure of monolayers 67
- Liquid crystals
  - commercial mixtures 3
  
- of current industrial use 4
  - surface pressure 62
  - surface tension anisotropy 53, 62
  
- Magnesium fluoride 14
  - evaporated layers 14, 34
- Mixed alignment 22, 48, 56
- Monolayers
  - of 3(2-aminoethyl)aminopropyl trimethoxysilane 50
  - of fatty acids 49
  - Langmuir 48
  - of lecithin 50-51
  - of octadecyl trichlorosilane 50
  - of surfactants 48
  
- Nonuniform coverage 48
  
- Octadecyl dimethyl (3-trimethoxysilylpropyl) ammonium chloride
  - see DMOAP
- Octadecyl trichlorosilane (OTS) 27, 50
  - monolayers 50
- Organic acids 16, 21
  
- Parallel alignment 66
  - on inorganic surfaces 6, 7
  - on polymers 6, 9
  - relation to surface tension 37
  - see also homogeneous alignment
- Perpendicular orientation
  - see homeotropic alignment
- Phenyl cyclohexane LCs (alignment of) 8, 47, 50
- Plasma
  - heating oxides in oxygen plasma 6
  - polymerization 8, 45
- Polyimide
  - (alignment of LCs on) 8, 10, 32
- Polymers (alignment of LCs on) 6, 9-13, 15, 46
  - dispersive interactions 45
  - preparation of films of 8
- Polytetrafluoroethylene 8, 13, 43
  - sputtered 39
- Polyvinyl alcohol (alignment of LCs on) 9, 15
- Pyridinium salts 19, 20
  
- Quaternary ammonium deriv. 18, 23
  - see also CTAB

- Rubbing 14, 15, 53, 66
  - of glass 14, 66
  - of polyimide 66
  - of polyvinyl alcohol 66
- SAIBE (Shallow angle ion beam etching) 14, 43
- Schiff's base LC
  - alignment of 6, 23
  - discomposition 6
  - surface hydrolysis 52
- Sealing (of displays) 4, 8, 32
- Silanes 22, 23-31, 67
  - monolayers 50
  - reaction with surfaces 23, 24
- Silicones 8, 23
- Silicon oxide
  - evaporated  $\text{SiO}_x$  14, 67, 68
  - influence of thermal treatment 39
  - sputtered  $\text{SiO}_2$  14
  - surface properties 43
- Siloxanes (poly-) 23, 47
- $\text{SiO}_2$ 
  - surface modification by heating 39
  - surface tension 43
- Smectic phases (alignment of) 20
- Stearyl trichlorosilane
  - see Octadecyl trichlorosilane
- Surface tension 37, 40
  - critical 42
  - of LC (anisotropy) 38, 53
  - of MBBA 52
  - measurement 52
  - of solids (influence on alignment) 37, 38
- Surfactants (alignment by) 15, 16-20
  - anionics 16
  - cationics 15, 18
  - (homeotropic alignment by) 15, 22
  - (homogeneous alignment by) 22
  - influence on conductivity of LCs 15, 21, 22
  - mechanism 48
  - nonionics 15, 19
- Tangential evaporation 2, 14
  - effect on tilt angle 34
  - of  $\text{SiO}_x$  68
- Tilt angle 32, 34, 36, 56, 68
  - control by alignment layers 36
  - on inorganic surfaces compared to organic ones 32
  - modification by surfactants 35
  - values 33
- Tilted alignment 69
  - from homeotropic 35, 68
- Tin oxide
  - alignment on 6
  - CVD films 39
  - reaction with long chain alcohol 22
- Tolans 8
- Twist
  - anchorage 56, 58
  - energy 59